

**The interaction between tyrosine protein kinase  
receptor B (TrkB) and neural cell adhesion  
molecule NCAM in *Mus musculus***

Dissertation  
zur Erlangung des Doktorgrades am Department Biologie  
der Fakultät für Mathematik, Informatik und Naturwissenschaften  
an der Universität Hamburg

vorgelegt von Claudia Friedrich

Hamburg, 2006

Genehmigt vom Department Biologie  
der Fakultät für Mathematik, Informatik und Naturwissenschaften  
an der Universität Hamburg  
auf Antrag von Frau Professor Dr. M. SCHACHNER  
Weiterer Gutachter der Dissertation:  
Herr Professor Dr. K. WIESE  
Tag der Disputation: 09. Dezember 2005

Hamburg, den 23. November 2005



A handwritten signature in black ink, appearing to read "Arno Frühwald".

Professor Dr. Arno Frühwald  
Dekan



Universität Hamburg

Hamburg, den 27.10.2005

Dr. Heather P. Ostendorff  
ZMNH  
AG Bach  
Martinistr.52  
D-20246 Hamburg

Hiermit erkläre ich mich bereit als „native speaker“ die sprachliche Korrektheit der Doktorarbeit von Frau Claudia Friedrich zu bestätigen.

Mit freundlichen Grüßen

Dr. Heather P. Ostendorff

## Table of Contents

<b>Figures</b> .....	<b>VI</b>
<b>1 Introduction</b> .....	<b>1</b>
1.1 The neural cell adhesion molecule (NCAM).....	2
1.1.1 NCAM-deficient mice .....	4
1.1.2 Intracellular NCAM signaling .....	5
1.2 The receptor tyrosine kinase TrkB .....	6
1.2.1 TrkB-deficient mice .....	11
1.2.2 Trk-mediated signaling .....	12
1.3 Proteolysis.....	14
1.3.1 Ubiquitination and ubiquitin-dependent proteolysis .....	16
1.3.2 NCAM-dependent proteolysis.....	17
1.3.3 Neurotrophin receptor-dependent proteolysis.....	18
<b>2 Aim of the study</b> .....	<b>20</b>
<b>3 Materials</b> .....	<b>21</b>
3.1 Chemicals.....	21
3.2 Solutions and buffers.....	21
3.3 Synthesized peptides .....	26
3.3.1 NCAM peptides.....	26
3.3.2 TrkB peptides .....	26
3.4 Bacterial media.....	27
3.5 Bacterial strains and cell lines .....	27
3.6 Cell culture media.....	28
3.7 Inhibitors and activators .....	29
3.8 Molecular weight standards .....	30

---

3.9	Plasmids.....	31
3.10	Mouse model ( <i>Mus musculus domesticus</i> , Linneaus, 1758) ...	31
3.11	Antibodies.....	32
3.11.1	Primary antibodies.....	32
3.11.2	Secondary antibodies.....	33
<b>4</b>	<b>Methods.....</b>	<b>35</b>
4.1	Molecular biology.....	35
4.1.1	Bacterial strains.....	35
4.1.2	Plasmid isolation of <i>Escherichia coli</i> .....	36
4.1.3	DNA Gel-electrophoresis.....	36
4.1.4	Determination of DNA concentrations.....	37
4.1.5	DNA Sequencing.....	37
4.1.6	Phage display.....	37
4.2	Protein-biochemistry.....	38
4.2.1	SDS-polyacrylamide gel electrophoresis.....	38
4.2.2	Western Blot-analysis.....	40
4.2.3	Recombinant expression of proteins in <i>Escherichia coli</i> using the pQE-system.....	41
4.2.4	Lysis of bacteria.....	42
4.2.5	Determination of protein concentration (BCA).....	42
4.2.6	Preparation of phosphorylated intracellular domain of TrkB (pTrkB-ID).....	43
4.2.7	ELISA (Enzyme-linked immunosorbent assay).....	43
4.2.8	Epitope mapping.....	44
4.2.9	Brain homogenization.....	44
4.2.10	Isolation of brain subfractions enriched with synaptosomes, synaptosomes from mossy fibers, myelin and nuclei.....	45

---

4.2.11	Preparation of a nuclear extract.....	47
4.2.12	Biochemical cross-linking with Sulfo-SBED .....	47
4.2.13	Biochemical cross-linking using TrkB peptides for coupling .	48
4.2.14	Biochemical cross-linking using NCAM-ID for coupling .....	48
4.2.15	Immunoprecipitation .....	50
4.2.16	Proteolysis assay using isolated brain membranes .....	51
4.3	Cell culture .....	52
4.3.1	LMTK-/LMTK-PST cell culture .....	52
4.3.2	Transfection of CHO cells, N2a cells and LM-TK cells .....	53
4.3.3	Primary hippocampal cell culture .....	53
4.3.4	Primary cerebellar cell culture .....	54
4.3.5	Cerebellar microexplant culture .....	55
4.4	Immunocytochemistry .....	56
4.4.1	Immunocytochemistry of living cells.....	56
4.4.2	Immunocytochemistry of fixed cells .....	56
4.4.3	Confocal laser-scanning microscopy .....	57
4.5	Computer-based sequence analysis.....	57
<b>5</b>	<b>Results.....</b>	<b>58</b>
5.1	Phage display analysis revealed a TrkB peptide showing selective binding towards NCAM180-ID.....	58
5.2	Epitope mapping .....	59
5.3	Binding study of recombinant NCAM180-ID to TrkB-ID and a TrkB peptide using an ELISA approach .....	61
5.4	Cross-linked TrkB peptide did not interact with NCAM180-ID .	63
5.5	Binding of a Trk fragment to NCAM180-ID under P+ lysis conditions in a modified cross-linking approach.....	65

---

5.6	NCAM180-ID interacts with full-length TrkB under P+ lysis conditions and in the presence of specific protease inhibitors in an optimized cross-linking approach.....	66
5.7	Verification of the NCAM180-Trk interaction by co-immunoprecipitation.....	68
5.8	No spatial relationship between NCAM and TrkB shown in co-localization and co-capping experiments.....	72
5.9	Isolation of the Trk and NCAM fragments for protein sequencing.....	76
5.10	Proteolysis of Trk and NCAM in addition to ectodomain shedding of TrkB.....	77
5.11	Ubiquitin/proteasome-dependent proteolysis of Trk and NCAM.....	82
5.12	Ubiquitination of full-length NCAM.....	85
5.13	Potential nuclear localization of the intracellular NCAM fragment.....	87
5.14	The effect of BDNF stimulation on NCAM-induced neurite outgrowth.....	88
	5.14.1 Using dissociated cerebellar cell culture.....	88
	5.14.2 Using cerebellar microexplant culture.....	89
<b>6</b>	<b>Discussion.....</b>	<b>91</b>
6.1	Characterization of the NCAM180–TrkB interaction.....	91
6.2	Functional analysis of the NCAM180–TrkB interaction.....	98
<b>7</b>	<b>Summary.....</b>	<b>101</b>
<b>8</b>	<b>Literature.....</b>	<b>104</b>
<b>9</b>	<b>Appendix.....</b>	<b>123</b>
9.1	Abbreviations.....	123

---

9.2	Accession numbers .....	125
9.3	Plasmids .....	126
9.3.1	CHL1ICpQE30 construct .....	126
9.3.2	NCAM140IC and NCAM180ICpQE30 constructs .....	126

## Figures

Figure 1. Examples of members of the Ig superfamily in the nervous system.....	3
Figure 2. Intracellular signaling pathways in NCAM-dependent neurite outgrowth. ....	6
Figure 3. Members of the neurotrophin receptor family including the Trk family of receptor tyrosine kinases and the p75 <sup>NTR</sup> receptor.....	8
Figure 4. The main functions of the Trk receptors. ....	9
Figure 5. Trk receptor signaling pathways. ....	14
Figure 6. Isolation of brain subfractions enriched with synaptosomes, synaptosomes from mossy fibers, myelin, mitochondria and nuclei using a discontinuous sucrose gradient. ....	46
Figure 7. Principle of optimized cross linking protocol using Sulfo-SBED. ....	49
Figure 8. Schematic representation of the ID of mouse TrkB (TrkB ID).....	58
Figure 9. Epitope mapping.....	59
Figure 10. Comparison of the IDs of mouse NCAM180 and NCAM140.....	60
Figure 11. Binding of NCAM180 ID to a TrkB peptide and to TrkB ID.....	63
Figure 12. No specific binding between cross-linked TrkB peptide and NCAM180.....	64
Figure 13. Binding of the intracellular TrkB fragment to NCAM180 ID. ....	66
Figure 14. An interaction between NCAM180 ID and full-length TrkB. ....	67
Figure 15. Immunoprecipitation of NCAM180 and NCAM140, but no co- immunoprecipitation of Trk.....	70
Figure 16. Co-immunoprecipitation of Trk and NCAM180.....	71
Figure 17. Co-immunoprecipitation of NCAM180 and Trk.....	72
Figure 18. Clustering of NCAM did not induce a re-distribution of TrkB in co-transfected LMTK-PST cells.....	74
Figure 19. Clustering of NCAM did not induce a re-distribution of TrkB in primary hippocampal neurons. ....	75
Figure 20. Clustering of PSA-NCAM did not induce a re-distribution of TrkB in primary hippocampal neurons. ....	76
Figure 21. Silver staining for subsequent protein sequencing of the Trk and NCAM fragments discovered in the cross-linking experiments.....	77
Figure 22. Proteolysis of Trk and NCAM. ....	80
Figure 23. Ectodomain shedding of TrkB. ....	81
Figure 24. Proteolysis of Trk and ectodomain shedding of TrkB. ....	82
Figure 25. Densitometric quantification of proteasome-dependent proteolysis of Trk and NCAM under P- lysis conditions. ....	84
Figure 26. Ubiquitination of full-length NCAM180. ....	86
Figure 27. Immunoprecipitation of intracellular NCAM180 fragment in nuclear extract. .....	88
Figure 28. Effect of BDNF on NCAM-incuded neurite outgrowth.....	89
Figure 29. Effect of BDNF with or without Endo-N and K252a on NCAM-incuded neurite outgrowth. ....	90

## 1 Introduction

The human nervous system consists of hundreds of billions of neurons, and each neuron receives and creates tens of thousands of connections. To guarantee an appropriate development and maintenance of such a complex structure, a precisely regulated net of cellular processes and functional pathways is essential. Neurogenesis, neuronal migration, neurite outgrowth, neuritogenesis, and synaptogenesis begin at an early embryonic stage and most processes are completed during young adulthood. However, some cellular contacts can still be altered, to a certain extent, during adulthood to enable pivotal processes such as neuronal regeneration and synaptic plasticity, including learning and memory consolidation (Williams and Herrup, 1988; for review see Amaral, 2000).

Cell adhesion molecules (CAMs) and neurotrophic factors with their respective receptors are involved in these processes by establishing various neuron–neuron and neuron–glial cell interactions from the embryonic age until adulthood (Kaplan and Miller, 2000; Diestel *et al.*, 2004; Williams *et al.*, 2005). Over the past decade, neurotrophic factors have been considered as potential therapeutics as they improve neuronal degeneration in many model systems for neurological disorders, including multiple sclerosis, schizophrenia, Parkinson’s disease, Alzheimer’s disease, and amyotrophic lateral sclerosis. However, poor stability and penetration of neurotrophins in the central nervous system (CNS) are currently the limiting factors during therapeutic application. Recently, mimetics of neurotrophins were developed to overcome these limitations (Massa *et al.*, 2003). So far, a causal role for mutations in neurotrophins or neurotrophin receptors in human neurodegenerative diseases has been mostly missing (Kruttgen *et al.*, 2003). Neurotrophins and their respective receptors have been implicated as key modulators of neuronal survival, neurite outgrowth, and synaptic connectivity, from development to adulthood (for review see Huang and Reichardt, 2003).

CAMs are also well known for their involvement in various neurological disorders, including hydrocephalus, schizophrenia and Alzheimer’s disease (Rentzos *et al.*, 2005). Similar to the neurotrophins and their receptors, CAMs influence neurogenesis, neuronal migration, neurite outgrowth, neuritogenesis, axon pathfinding, axon fasciculation, synaptogenesis, and myelination (Cotman *et al.*, 1998; Diestel *et al.*, 2004; Williams *et al.*, 2005). CAMs not only act as attractive or repellent modulators of recognition and adhesion functions between cells, but also activate multiple signaling cascades. CAMs undergo homophilic and heterophilic cell–cell and cell–extracellular matrix (ECM) interactions (Crossin und Krushel, 2000). They can be divided into four groups: (1) integrins (Hynes, 1992; Reichardt and

Tomaselli, 1991), (2) cadherins (Takeichi, 1991), (3) molecules of the ECM (Reichardt and Tomaselli, 1991), and (4) cell surface glycoproteins of the immunoglobulin (Ig) superfamily (Williams and Barclay, 1988; Crossin and Krushel, 2000).

## 1.1 The neural cell adhesion molecule (NCAM)

NCAM is the best-characterized member of the Ig superfamily of cell recognition molecules, typically containing several Ig-like domains (Brummendorf and Lemmon, 2001). NCAM was the first member of this family to be isolated and completely characterized (Brackenbury *et al.*, 1977). It was first described by Jørgensen and Bock (1974). However, antibodies (Edelman *et al.*, 1969) and MHC molecules (Orr *et al.*, 1979) have been described as the prototypical members of this superfamily. The majority of CAMs are characterized by repetitive Ig-like domains followed by other repetitive motifs such as the fibronectin subtype III repeat (FNIII domain), as shown in Fig. 1. FNIII domains have been shown to participate in cell–ECM interactions. Typical members of the Ig superfamily present in the nervous system are depicted in Fig. 1. Originally, NCAM was characterized as a mediator of cell–cell adhesion, but now it is also considered as a signaling receptor (Fig. 2) responding to both homophilic and heterophilic cues (Paratcha *et al.*, 2003; Hinsby *et al.*, 2004). The extracellular domain (ED) of NCAM is well known to be a modulator of various cell–cell and cell–ECM interactions. Its intracellular domain (ID) is mainly involved in multiple signaling cascades, including pathways of receptor tyrosine kinases and non-receptor kinases (Williams *et al.*, 1994a; Williams *et al.*, 1994b; Williams *et al.*, 1995; Beggs *et al.*, 1997; Kolkova *et al.*, 2000; Paratcha *et al.*, 2003; Diestel *et al.*, 2004; Hinsby *et al.*, 2004). NCAM is also involved in the activation of voltage-dependent  $\text{Ca}^{2+}$  channels (Povlsen *et al.*, 2003) and in the regulation of inwardly rectifying  $\text{K}^+$  channels of the Kir3 family (Rogalski *et al.*, 2000; Delling *et al.*, 2002). It plays a pivotal role in neurogenesis, neuronal migration, neurite outgrowth, axon fasciculation, and synaptic remodeling (Doherty *et al.*, 1990; Schachner, 1991; Doherty *et al.*, 1992; Doherty and Walsh, 1992; Jørgensen, 1995; Fields and Itoh, 1996; Cremer *et al.*, 1997; Ronn *et al.*, 1998; Paratcha *et al.*, 2003). NCAM is not only involved in homophilic interactions in “cis” (*i.e.* on the same cell membrane) and in “trans” configuration (*i.e.* on different cell membranes) (Hoffman and Edelman, 1983; Walmod *et al.*, 2004) but also in heterophilic binding, like all members of the Ig superfamily. Homophilic binding takes place between NCAM molecules (Walmod *et al.*, 2004), whereas the CAM L1 (Horstkorte *et al.*, 1993), heparin a major component of the ECM (Cole *et al.*, 1986a; Cole and Glaser, 1986) and collagen (Probstmeier *et al.*,

1989) are examples for heterophilic binding partners of NCAM. For cell recognition functions, individual domains of NCAM or the unglycosylated protein are sufficient. NCAM proteins undergo transcriptional and posttranslational modifications. Additionally, a single gene encodes for several NCAM isoforms. Alternative splicing results in the expression of three major isoforms, the 180- and 140-kDa transmembrane isoforms and a 120-kDa isoform that is linked to the plasma membrane by a glycosylphosphatidylinositol (GPI) anchor (Cunningham *et al.*, 1987).

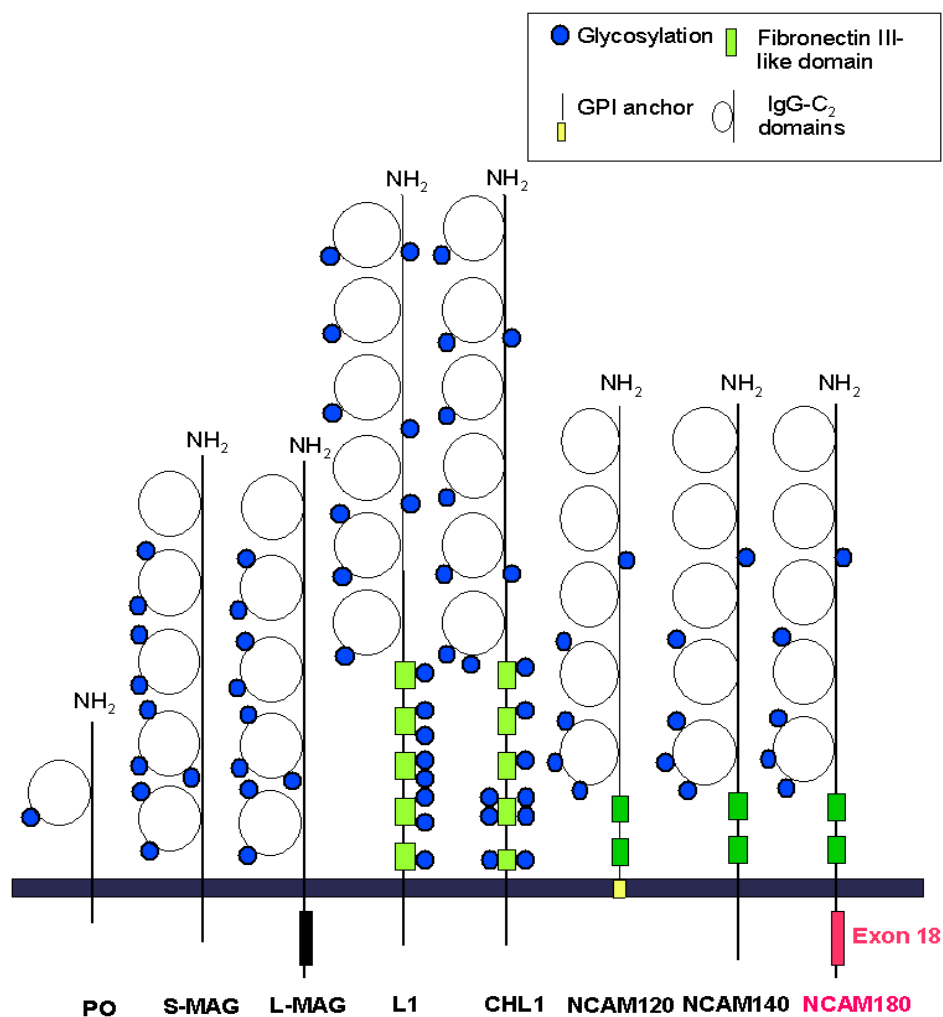


**Figure 1. Examples of members of the Ig superfamily in the nervous system.**

CAMs belong to the Ig superfamily. They consist of an ED with IgG-C<sub>2</sub> domains, fibronectin type III repeats, a single-spanning transmembrane region or a GPI anchor, and, in most cases, an ID (Cunningham *et al.*, 1987).

The difference between the IDs of NCAM140 and NCAM180 only consists in the presence of an additional 261-amino acid insert in the cytoplasmic region of NCAM180, encoded by exon 18. All three NCAM isoforms are characterized by an ED containing five Ig domains

and two FNIII-domains, a single-spanning transmembrane region or a GPI anchor, and, in most cases, an ID (see Fig. 1). NCAM120 is mainly expressed in glial cells, while the 180- and 140-kDa isoforms are primarily expressed in neurons (Keilhauer *et al.*, 1985; Nybroe *et al.*, 1985). NCAM140 is mainly expressed in growth cones of immature neurons, distributed on pre- and postsynaptic membranes, and promotes neurite outgrowth. In contrast, NCAM180 is particularly found in the postsynaptic densities of synapses of mature neurons and is responsible for the stabilization of cell–cell contacts (Pollerberg *et al.*, 1985; Persohn *et al.*, 1989; Dityatev *et al.*, 2000). Examples for posttranslational modifications are glycosylation of asparagines in the ED and palmitoylation of cysteine residues in the ID (Little *et al.*, 1998; Niethammer *et al.*, 2002). According to a recent publication, not only serine and threonine residues in the cytoplasmic domain (Mackie *et al.*, 1989) but also the only cytoplasmic tyrosine at position 734 of human NCAM180 is posttranslationally phosphorylated. The physiological relevance of the intracellular modifications, for instance the tyrosine phosphorylation, has not yet been entirely elucidated (Diestel *et al.*, 2004). One has to emphasize that all isoforms of NCAM can carry high amounts of the developmentally regulated carbohydrate  $\alpha$ -2,8-linked polysialic acid (PSA). The embryonic brain contains 30% PSA relative to the NCAM moiety, which gradually decreases to 10% in the adult brain (Hoffman *et al.*, 1982; Rothbard *et al.*, 1982; Schachner and Martini, 1995). The negatively charged PSA moiety on NCAM not only prevents homophilic NCAM–NCAM adhesion, but also serves generally as a negative regulator of cell–cell interactions. Promotion of neurite outgrowth seems to be increased by PSA. If PSA is removed from NCAM by endoneuraminidase N (Endo-N), myelination is increased four- to fivefold (Rutishauser, 1990; Charles *et al.*, 2000). PSA is likely to participate in synaptic plasticity and regeneration (Regan and Fox, 1995; Muller *et al.*, 1996; Becker *et al.*, 1996; Kiss and Muller, 2001). Beyond this, PSA was hypothesized to be involved in the recruitment of brain-derived neurotrophic factor (BDNF) to the neurotrophin receptor TrkB (Muller *et al.*, 2000; Vutskits *et al.*, 2001).

### 1.1.1 NCAM-deficient mice

NCAM-deficient (NCAM<sup>-/-</sup>) mice present only mild morphological changes in the adult nervous system (Cremer *et al.*, 1994; Cremer *et al.*, 1997). A smaller olfactory bulb has been reported in NCAM<sup>-/-</sup> mice (Cremer *et al.*, 1994) and in adult mice deficient for NCAM180 (Tomasiewicz *et al.*, 1993) compared to wild-type (NCAM<sup>+/+</sup>) mice. The following morphological changes of the hippocampus have been observed in NCAM<sup>-/-</sup> mice: disarray of the hippocampus including reduced fasciculation and a decreased number of

mossy fibers and their terminals, in addition to impaired long-term plasticity (LTP) (Cremer *et al.*, 1994; Stork *et al.*, 1997). Deficient LTP found in brain slices prepared from NCAM<sup>-/-</sup> mice and in organotypic slice cultures treated with Endo-N (an enzyme that cleaves the PSA moiety of NCAM) can be rescued by BDNF. Exogenous application of PSA residues or recombinant PSA-modified NCAM (PSA-NCAM) also prevents LTP. Furthermore, TrkB phosphorylation, and thus BDNF signaling, is reduced in both NCAM<sup>-/-</sup> mice and Endo-N-treated slice cultures. This suggests that one action of PSA-NCAM could be to sensitize neurons to BDNF, thereby modulating activity-dependent synaptic plasticity (Muller, 2000; Vutskits *et al.*, 2001). Behavioral studies on NCAM<sup>-/-</sup> mice showed altered exploratory activity, deficits in spatial learning, increased anxiety-like behavior (Stork *et al.*, 1999), and an increased intermale aggression (Jørgensen, 1995).

### 1.1.2 Intracellular NCAM signaling

Beyond cell–cell adhesion through homophilic NCAM binding, NCAM is also considered as a signaling receptor based on the response to heterophilic cues (Paratcha *et al.*, 2003; Hinsby *et al.*, 2004). NCAM-mediated adhesion leads to the activation of second-messenger cascades (Schuch *et al.*, 1989) and of various intracellular signal transduction pathways. One pathway is dependent on the fibroblast growth factor receptor (FGFR). After homophilic NCAM interaction, FGFR is activated, resulting again in an activation of phospholipase C $\gamma$  (PLC $\gamma$ ) and diacyl glycerol (DAG) lipase in order to release arachidonic acid (AA) and inositol trisphosphate (IP<sub>3</sub>). Activated voltage-dependent Ca<sup>2+</sup> channels are responsible for Ca<sup>2+</sup> entry into cells, and IP<sub>3</sub> releases Ca<sup>2+</sup> from intracellular stores. The receptor tyrosine kinase FGFR is one of the main initiators in NCAM-dependent signal transduction resulting in neurite outgrowth (Williams *et al.*, 1995; Crossin and Krushel, 2000; Niethammer *et al.*, 2002). Another intracellular signal transduction pathway includes the Ras–mitogen-activated protein kinase (MAPK) cascade leading to the phosphorylation of the cAMP response element-binding (CREB) protein in the nucleus (Schmid *et al.*, 1999). Particularly, the activation of the non-receptor tyrosine kinase Fyn and the focal adhesion kinase (FAK)-dependent MAPK pathway is only achieved by NCAM140, in contrast to the above-described pathway that can be initiated by NCAM180 and NCAM140. Furthermore, NCAM also initiates the PI3K/Akt pathway (Ditlevsen *et al.*, 2003). In addition, NCAM stimulation has been shown to activate the transcription factor NF- $\kappa$ B (Krushel *et al.*, 1999). These signal transduction pathways, illustrated in Fig. 2, determine the NCAM-mediated neurite outgrowth. An intense interplay among the said pathways and cross-talk between the individual mediators take place (Doherty *et al.*, 2000;

Povlsen *et al.*, 2003). Neurite outgrowth is one of the essential events in neural development and it is mediated by multiple CAMs of the Ig superfamily, as for example NCAM (Doherty *et al.*, 2000). Receptor tyrosine kinases use signaling pathways similar to those utilized by NCAM (Figs. 2 and 4), including common interaction partners such as the non-receptor tyrosine kinase Fyn (Beggs *et al.*, 1997; Iwasaki *et al.*, 1998). In order to fully understand the complexity of the NCAM signaling pathways, other potential intracellular interaction partners have to be identified.

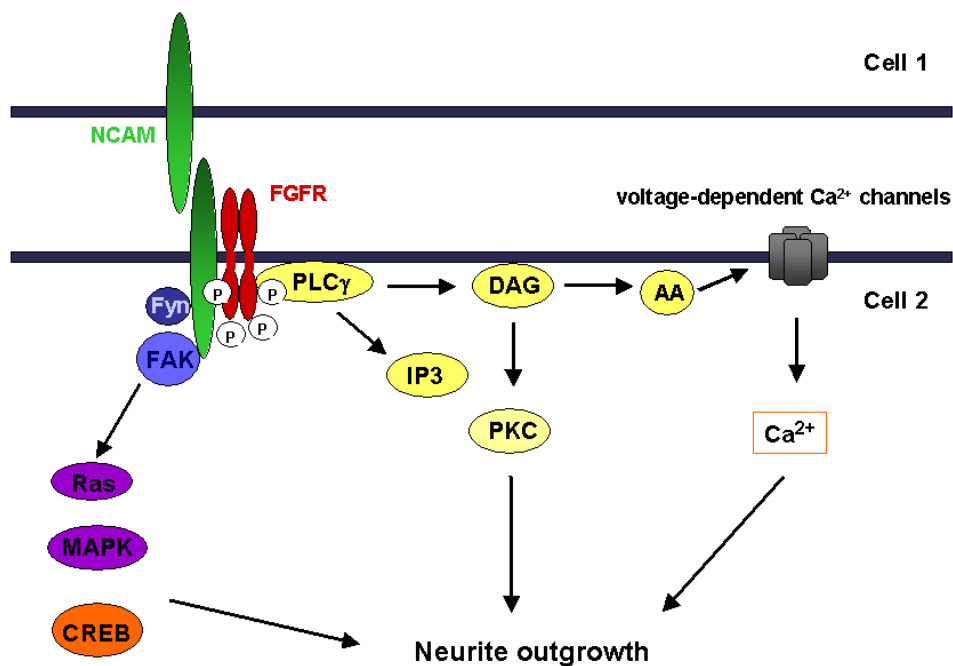


**Figure 2. Intracellular signaling pathways in NCAM-dependent neurite outgrowth.**

Homophilic interaction of NCAM results, beyond Ca<sup>2+</sup> release, in heterophilic interaction and activation of FGFR. Consequently, the Ras–MAPK pathway is initiated leading to phosphorylation of CREB and PLCγ modulates voltage-dependent Ca<sup>2+</sup> channels *via* DAG and AA. These signal transduction pathways determine the NCAM-mediated neurite outgrowth (Povlsen *et al.*, 2003).

## 1.2 The receptor tyrosine kinase TrkB

TrkB was discovered as the second member of the receptor tyrosine kinase family that also includes TrkA and TrkC (Klein *et al.*, 1989; Middlemas *et al.*, 1991). The name of the Trk family originates from the oncogene that led to its discovery (Martin-Zanca *et al.*, 1986; Barbacid *et al.*, 1991). This oncogene was isolated in gene transfer assays from a carcinoma and, when cloned, was found to consist of the first seven of the eight exons of nonmuscle tropomyosin fused to the transmembrane and cytoplasmic domains of a novel tyrosine kinase. Therefore, the kinase proto-oncogene was called tropomyosin-related kinase (trk) and

is referred to as *trkA*. The *trkB* and *trkC* genes were identified because of their high homology to *trkA*. The three Trk receptor tyrosine kinases are glycoproteins and form the Trk family of neurotrophin receptors. This family is characterized by strong similarities in both the extracellular region, with 37% amino acid sequence identity, and the intracellular region, with 75% sequence identity (Klein *et al.*, 1989, Klein *et al.*, 1990; Martin-Zanca *et al.*, 1990; Middlemas *et al.*, 1991; Lamballe *et al.*, 1991). All members of this family share a rather uniform array of structural motifs (Fig. 3). They possess a highly conserved ED, a single-spanning transmembrane domain (TMD), and an ID containing a catalytic tyrosine kinase domain as well as regulatory sequences frequently located near the C terminus. The ED exhibits a complex subdomain organization consisting of a signal peptide, two cysteine-rich clusters framing a tandem array of three leucine-rich motifs, and two Ig-like domains adjacent to the membrane (Schneider and Schweiger, 1991; Windisch *et al.*, 1995). The ED has structural homology with the CAMs of the Ig superfamily and is therefore capable of homophilic adhesion, and it is involved in ligand recognition. In early studies, two distinct domains of TrkB have been identified as functional neurotrophin-binding sites; one corresponds to the second leucine-rich motif and the other is located in the vicinity of the second Ig-like domain (Windisch *et al.*, 1995; Haniu, 1997). After gaining structural information on all Trk receptors, the location of the neurotrophin-binding site of the Trk receptors was narrowed down to the C-terminal part of the second Ig-like domain (Ultsch *et al.*, 1999; Banfield *et al.*, 2001). A distinguishing characteristic of the Trk receptors is that they have an ID which contains a catalytic tyrosine kinase domain with several potential sites for tyrosine phosphorylation – for instance TrkB has 13 (Segal *et al.*, 1996) – and regulatory sequences frequently located near the C terminus. In response to receptor activation, the phosphorylation state of the Trk catalytic domain changes. Neurotrophins can interact independently (Chao, 1992; Chao and Hempstead, 1995) or simultaneously (Bibel and Barde, 2000) with two transmembrane glycoproteins, the above-mentioned Trk receptors and the p75 neurotrophin receptor (p75<sup>NTR</sup>). In addition, neurotrophin receptors can interact with each other (Bibel and Barde, 2000). p75<sup>NTR</sup> belongs to the tumor necrosis factor (TNF) receptor family (Mallett and Barclay, 1991) and to the neurotrophin receptor family.

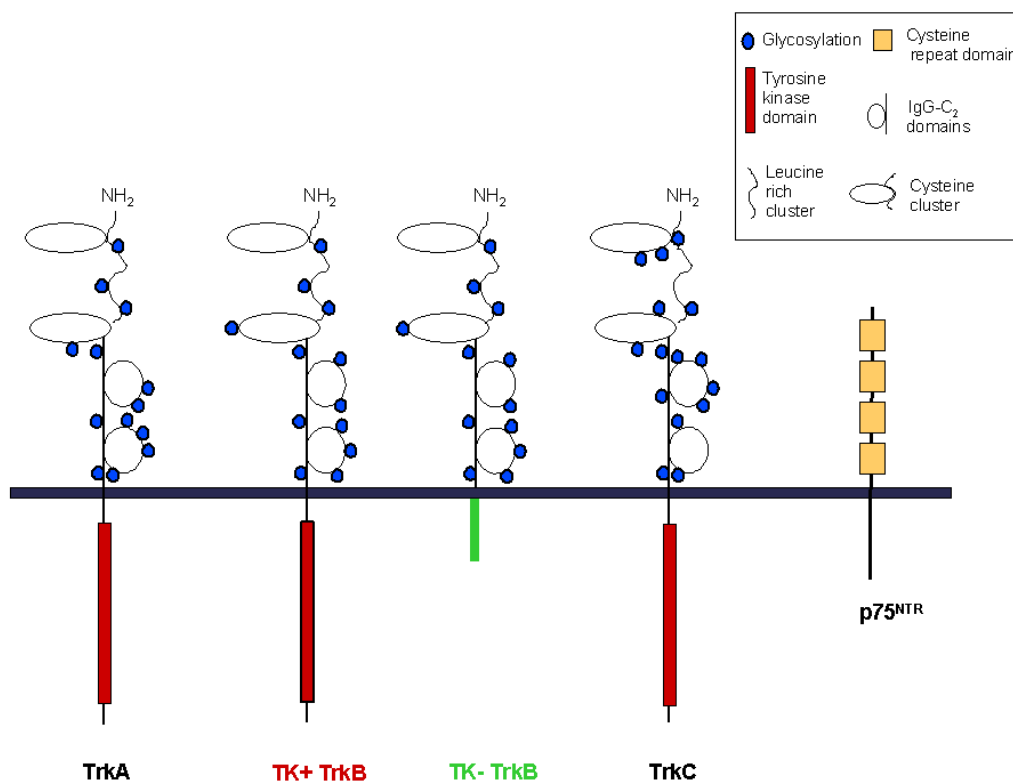


**Figure 3. Members of the neurotrophin receptor family including the Trk family of receptor tyrosine kinases and the p75<sup>NTR</sup> receptor.**

Trk receptors belong to the neurotrophin receptor family and the Ig superfamily. Extracellular motifs found in the Trk family are two cysteine-rich clusters, three repeats rich in leucine and two IgG-like domains, followed by a single-spanning TMD and an ID containing the tyrosine kinase domain (shown in red). The ID of the truncated isoform of TrkB (TK– TrkB; depicted in green) lacks the catalytic tyrosine kinase domain, in contrast to full-length TrkB (TK+ TrkB). The p75<sup>NTR</sup> receptor, which belongs to the TNF receptor family and to the neurotrophin receptor family, is characterized by four cysteine-rich repeats with six conserved cysteine residues (Allendoerfer *et al.*, 1994; Segal *et al.*, 1996).

Neurotrophic factors were originally identified based on their ability to support the survival of neuronal cells (Levi-Montalcini and Angeletti, 1968), but nowadays it is known that they have various effects on developing neurons *in vivo* and *in vitro* (Lewin and Barde, 1996). Beyond the “classical” effects of neurotrophins, like promotion of cell survival and prevention of apoptosis, they also influence the commitment to a specific lineage (Knusel *et al.*, 1991) and stimulate neurite elongation (Davies *et al.*, 1986; Cohen *et al.*, 1994). For example, BDNF as prototypical neurotrophin plays a pivotal role in neuronal survival and differentiation (Lewin and Barde, 1996; Huang and Reichardt, 2001), regulates neuronal activity and neurotransmitter release and participates in synapse development and plasticity (Thoenen, 1995; Poo, 2001; McAllister *et al.*, 1999). Moreover, neurotrophins are also involved in rapid signaling by changing multiple cellular functions such as synaptic

transmission and activity-dependent synaptic plasticity. Prerequisite for these fast modulations is the interaction of Trk receptors with ion channels in the plasma membrane (Blum and Konnerth, 2005). In particular, TrkB binds to various ion channels such as the non-voltage-gated cation channel TRPC3 (Li *et al.*, 1999) and the sodium channel  $\text{Na}_v1.9$  (Balkowiec *et al.*, 2000). Furthermore, the inwardly rectifying  $\text{K}^+$  channel Kir3.4 is tyrosine-phosphorylated by TrkB (Wischmeyer *et al.*, 1998; Rogalski *et al.*, 2000; Ippolito *et al.*, 2002).

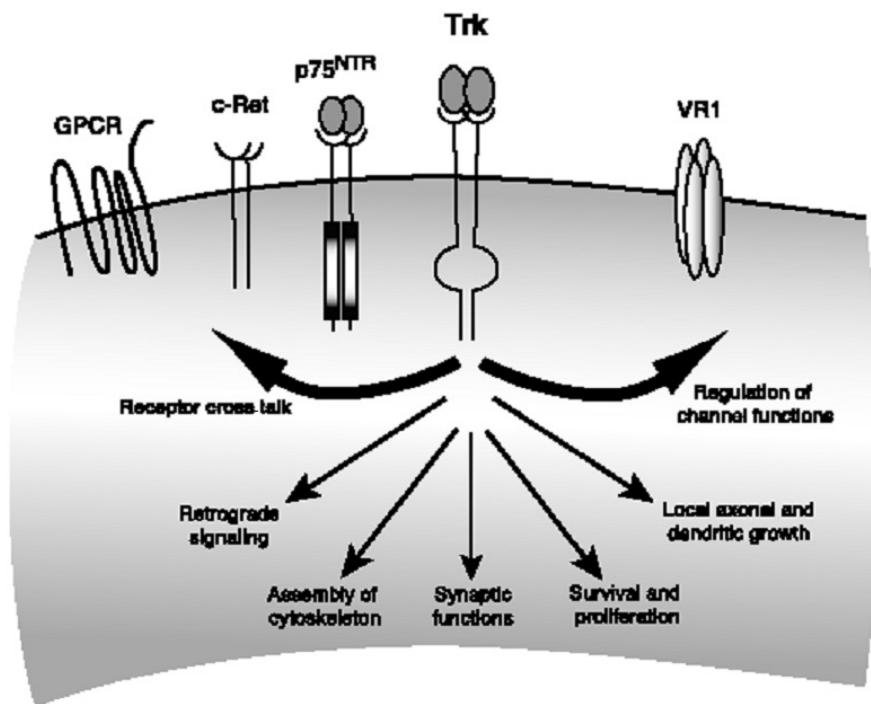


**Figure 4. The main functions of the Trk receptors.**

Activation of Trk receptors by neurotrophins mediates neuronal survival, proliferation, neurite outgrowth, synaptic connectivity, assembly and remodeling of the cytoskeleton, membrane trafficking, and receptor cross-talk. A number of receptors, *i.e.* p75<sup>NTR</sup>, GPCR, VR1 and c-Ret, communicate with the Trk receptors (Huang and Reichardt, 2003).

Beyond the regulation of ion channels, the main functions of the Trk receptors include modulation of neuronal survival, proliferation, neurite outgrowth, synaptic connectivity, assembly and remodeling of the cytoskeleton, membrane trafficking, and receptor cross-talk (Fig. 4). The co-receptor p75<sup>NTR</sup>, G protein-coupled receptors (GPCRs), the vanilloid receptor (VR1), the receptor tyrosine kinase c-Ret, and the N-methyl-D-aspartate (NMDA) receptor are representative examples for cross-talk partners of Trk receptors (Marini *et al.*, 1998; Chao, 2003; Huang and Reichardt, 2003). Trk receptors can, alternatively, be activated in the absence of neurotrophin binding *via* a GPCR mechanism. Two GPCR ligands,

adenosine and pituitary adenylate cyclase-activating polypeptide (PACAP), can activate Trk receptors to guarantee the survival of neural cells and thereby compensate the lack of neurotrophins (Lee and Chao, 2001; Rajagopal *et al.*, 2004).

TrkB undergoes transcriptional and posttranslational modifications. TrkB is highly glycosylated and contains 33.3% carbohydrate moieties. The 12 potential N-glycosylation sites of TrkB account for the fact that although the unglycosylated full-length and truncated TrkB isoforms have predicted molecular weights of only 93 and 57 kDa, respectively, they have apparent molecular weights of 145 and 95 kDa, respectively (Klein *et al.*, 1990; Haniu *et al.*, 1995). Early in development, TrkB possesses high-mannose oligosaccharides, which lack sialic acid or N-acetyl-D-glucosamine. However, later in development, a switch occurs so that the full-length receptor is synthesized with complex oligosaccharide side chains possessing sialic acid and/or N-acetyl-D-glucosamine in at least some of the terminal positions (Fryer *et al.*, 1996). The truncated isoforms, which arise from alternative splicing, have the complete extracellular region and the TMD, but differ in their short cytoplasmic domain which is characterized by the lack of the catalytic tyrosine kinase domain (Fig. 3). The truncated isoform T2TrkB (TK– TrkB), which has the same splice site as T1TrkB but has a unique cytoplasmic tail region, has been described in rodent brain and is absent in human brain. The IDs of T1TrkB and T2TrkB consist of 23 and 21 amino acids, respectively. The first 12 amino acids of the cytoplasmic tail are identical to the full-length isoform, whereas the following 11 and 9 amino acids are specific for T1TrkB and T2TrkB, respectively (Klein *et al.*, 1990; Middlemas *et al.*, 1991). The T–Shc isoform is the only one of the truncated isoforms that contains, additionally, a Src homology domain-containing transforming protein (Shc)-binding site in the juxtamembrane domain, similar to TK+ TrkB (Chao, 1992).

TrkB is expressed in lung, the CNS, and in multiple structures of the PNS such as dorsal root ganglia and sympathetic plexus (Klein *et al.*, 1989). TrkB and TrkC occur as the major Trk receptors in the mammalian CNS (Allendoerfer *et al.*, 1994; Fryer *et al.*, 1996; Minichiello and Klein, 1996). TrkB and BDNF are highly expressed in the cerebellum (Kaplan *et al.*, 1991; Segal *et al.*, 1995; Lindholm *et al.*, 1997; Ohira *et al.*, 1999; Rico *et al.*, 2002), the cerebral cortex (Klein *et al.* 1990), and the hippocampus (Minichiello and Klein, 1996; Yan *et al.*, 1997; Shimada *et al.*, 1998; Rabacchi *et al.*, 1999). TrkB is expressed in both pre- and postsynapses (for review see Chao, 2003). The two truncated receptors T1TrkB and T2TrkB (TK– TrkB) are characterized by differential distribution in the rodent nervous system; however, both are co-expressed with the signal-transducing TK+ TrkB. The ex-

pression of T2TrkB parallels that of TK+ TrkB and seems to be exclusively neuronal, whereas T1TrkB is found mainly in non-neuronal cells such as the ependymal linings of the cerebral ventricles, the choroid plexus, astrocytes and, to a lesser extent, in a subpopulation of hippocampal neurons (Klein *et al.*, 1990; Armanini *et al.*, 1995; Fryer *et al.*, 1996). So far, it is known that T–Shc is the only isoform that is neuron specific. This isoform is highly conserved between humans and mice, which indicates that T–Shc plays an important role in TrkB signal transduction. Neurotrophins as well as their receptors are developmentally regulated (Klein *et al.*, 1989; reviewed by Davies *et al.*, 1994; Jungbluth *et al.*, 1997). TK– TrkB becomes more prevalent with increasing age whereas TK+ TrkB is the predominant form during development. In the rat brain, TK+ TrkB and TK– TrkB are present at equal levels by embryonic day 15 (E15). Rat TK+ TrkB reaches adult expression levels between E18 and E20, while TK– TrkB increases immensely between postnatal day 10 (P10) and P15 in order to represent the most abundant adult form of TrkB (Klein *et al.*, 1989; Allendorfer *et al.*, 1994; Escandón *et al.*, 1994; Armanini *et al.*, 1995; Eide *et al.*, 1996). So far, the functional role of the truncated, non-catalytic TK– TrkB is poorly understood. Some evidence indicates that the truncated isoforms of TrkB could either trap the catalytic TK+ TrkB by homophilic interaction or act as dominant-negative receptors by sequestering ligands (Fryer *et al.*, 1997).

### 1.2.1 TrkB-deficient mice

Although both the TrkB receptor and the ligand BDNF are required for cell survival and differentiation in the developing and adult CNS (for review see Korsching, 1993; Reichardt and Fariñas, 1997), only subtle morphological changes in the adult nervous system were caused in mice with a targeted disruption of the *trkB* gene. Transgenic mice with null mutations of the *trkB* gene show a relatively normal cytoarchitecture in the CNS (Liu *et al.*, 1995; Fryer *et al.*, 1996). However, minor neuronal deficiencies in the CNS and PNS, neuronal loss due to increased apoptosis especially in the hippocampus (Minichiello and Klein, 1996), and a reduced number of motor neurons in addition to several nervous system lesions have been described (Klein *et al.*, 1993; Piñón *et al.*, 1996; Schober *et al.* 1998). Admittedly, homozygous mutant ( $TrkB^{-/-}$ ) mice show a high mortality during the early postnatal period and barely survive one week (Klein *et al.*, 1993; Rico *et al.*, 2002) in contrast to heterozygous ( $TrkB^{+/-}$ ) mice which survive normally. Adult mice with haploinsufficiencies of the *trkB* and/or *trkC* genes can be characterized by obvious morphological deficits in hippocampus and amygdala (von Bohlen and Halbach, 2003). Conditional mutant mice without TrkB expression in the cerebellum ( $Wnt1Cre/trkB$  mice)

survive to adulthood with a normal cerebellar cytoarchitecture. The absence of TrkB evoked significant deficits in GABAergic enzymes and led to a quantitative reduction of GABAergic boutons and synaptic specializations. These results underline the important role that TrkB plays in synapse formation and the development of GABAergic neurons and axon terminals (Rico *et al.*, 2002). In *trkB* conditional mutant mice, short-term synaptic functions and long-term potentiation in the CA3–CA1 hippocampal region are impaired (Patterson *et al.*, 1996; Xu *et al.*, 2000). Behavioral studies on mutant mice deficient for the TrkB receptor in the forebrain (*trkB/CaMKII-CRE* mice) revealed behavioral impairments such as cognitive deficits, indicating a dysfunction of the hippocampus and the connected forebrain structures (Minichiello *et al.*, 1999). In summary, TrkB regulates both short-term synaptic functions and long-term potentiation of brain synapses (Vyssotski *et al.*, 2002).

### 1.2.2 Trk-mediated signaling

The discovery of neurotrophins and the Trk receptors gave enormous insights into neural function and was a huge step forwards for the understanding of essential mechanisms of intracellular communication in the nervous system. Consequently, multiple tyrosine kinase-regulated signal transduction pathways initiated by neurotrophins were identified in the nervous system (for review see Shooter, 2001). First, neurotrophin-mediated activation of Trk receptors includes pivotal positive biological functions (Fig. 4) such as cell proliferation and cell survival, but also axonal and dendritic growth and remodeling, assembly and remodeling of the cytoskeleton, membrane trafficking and fusion, and synapse formation, function and plasticity. Second, neurotrophins can bind to  $p75^{\text{NTR}}$  and mediate neuronal cell survival, differentiation, growth, and apoptosis. Trk and  $p75^{\text{NTR}}$  influence each other. Signals that are generated by these receptors can be enhanced or suppressed by the others. The Trk receptors are well known for promoting neuronal survival, whereas  $p75^{\text{NTR}}$  mainly triggers apoptosis and cell death (Bibel and Barde, 2000).  $p75^{\text{NTR}}$  can potentiate the NF- $\kappa$ B activation by Trk (Kaplan and Miller, 2000). Previous studies have demonstrated that level and duration of Trk phosphorylation vary as a function of receptor number (Hempstead *et al.*, 1992) and the presence of  $p75^{\text{NTR}}$  (Barker *et al.*, 1994; Hantzopoulos *et al.*, 1994; Verdi *et al.*, 1994). Up to this point, there are three known intracellular signaling cascades that mediate TrkB–BDNF signaling: the PLC $\gamma$ –CaM kinase pathway, the PI3K–AKT pathway and the Ras–MAPK pathway (Fig. 5). The Ras and PI3K–AKT pathways induce suppression of apoptotic proteins and MEK/MAPK activation of anti-apoptotic proteins, to stimulate cell survival. The selective activation of these cascades is initiated by the recruitment of adapter proteins that specifically bind to certain tyrosines within the TrkB receptor.

The neurotrophin BDNF is released in an activity-dependent manner (Balkowiec *et al.*, 2000; Hartmann *et al.*, 2001) and is capable of binding two TrkB molecules with high affinity, resulting in receptor dimerization. As a consequence, a series of tyrosine phosphorylation events follows, starting with the autophosphorylation of tyrosines in “trans” of the dimerized receptors (Klein *et al.*, 1991a, Klein *et al.*, 1991b; Jing *et al.*, 1992; Philo *et al.*, 1994). Phosphorylation of tyrosine 675 (Y-675) in the TrkB ID, which is located in the activation loop of the active site, proceeds to completion *in vivo* before other sites are fully phosphorylated. Other tyrosines within the TrkB ID have been identified as autophosphorylation sites as well: Y-701, Y-705 and Y-706. The phosphorylation state of Y-705 is considered to be especially important (Segal *et al.*, 1996). Two other tyrosine phosphorylation sites outside the catalytic domain create docking sites for proteins such as Shc, FGF receptor substrate 2 (FRS2), and PLC $\gamma$ , which activate second messengers and other downstream effectors (Middlemas *et al.*, 1991; Schneider and Schweiger, 1991). These include the transcription factor CREB which activates the transcriptional machinery in the nucleus and thereby regulates a wide range of genes (Finkenbeiner *et al.*, 1997; Bibel and Barde, 2000; Minichiello *et al.*, 2002). One of these phosphorylation sites outside the catalytic domain, Y-515 in the juxtamembrane domain of TrkB, is critical for Shc and FRS2 binding and hence for activation of the Ras–MAPK signaling cascade (Postigo *et al.*, 2002; Stephens *et al.*, 1994). Another site in the C terminus of TrkB, Y-816, has been shown to play a functional role in binding PLC $\gamma$  to TrkB (Postigo *et al.*, 2002; Stephens *et al.*, 1994; Llovera *et al.*, 2004). Phosphorylation at the Shc site (Y-515) positively regulates the autophosphorylation of TrkB (Postigo *et al.*, 2002). Tyrosine autophosphorylation is required for both the catalytic and the signaling activities of the Trk receptors (Obermeier *et al.*, 1993, Obermeier *et al.*, 1994; Stephens *et al.*, 1994; Kaplan and Stephens, 1994).

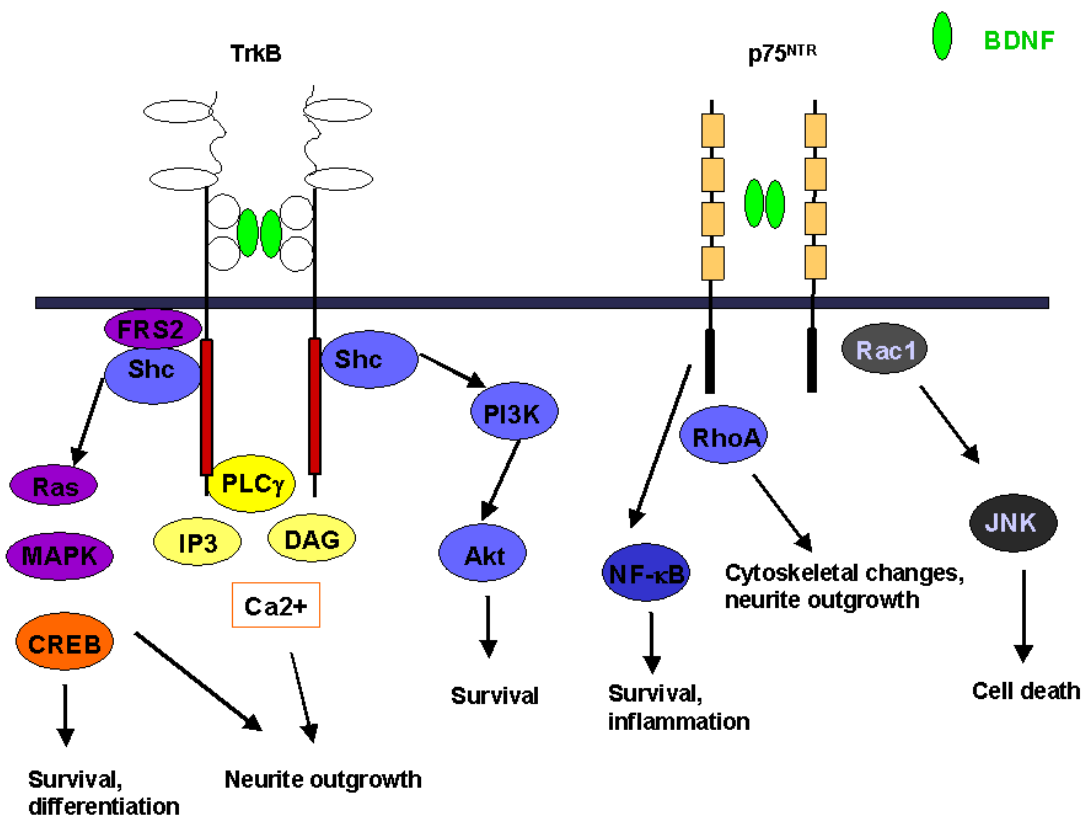


**Figure 5. Trk receptor signaling pathways.**

Neurotrophin binding (*e.g.* BDNF, indicated as green ellipse) to Trk receptors (*e.g.* TrkB) causes dimerization and autophosphorylation of the receptors; then, a battery of signaling proteins is recruited to the docking sites of the receptors. Trk-mediated signaling triggers three pathways: the PLC $\gamma$ , the PI3K–AKT and the Ras–MAPK pathways. The Trks initiate the phosphorylation of PLC $\gamma$ , Shc and FRS2. This leads to activation of gene expression (*e.g.* via induction of the transcription factor CREB), neuronal survival, and neurite outgrowth. The p75<sup>NTR</sup> receptor particularly activates NF- $\kappa$ B and Jun N-terminal kinase (JNK), and mediates RhoA activity. The biological responses of p75<sup>NTR</sup> consist of the activation of cell survival, neurite outgrowth, growth arrest and cell death (for review see Chao, 2003).

### 1.3 Proteolysis

Proteolysis is a process in which certain enzymes, the proteases, specifically cleave proteins into fragments of various sizes. The protease family consists of serine, cysteine and aspartate proteases and metalloproteases (Bode *et al.*, 1999). Nowadays the accepted functional role of the proteases is not restricted to the activation of inactive precursor molecules such as pro-neurotrophins (Mowla *et al.*, 2001). Through proteolysis, an important kind of post-translational modification, proteases act as key players in a wide range of biological processes. Adequately positioned at the plasma membrane, they regulate many aspects of protein function, including tissue remodeling and regulation of activation, modification, localization and liberation of biological factors. In addition to remodeling of ECM compo-

nents and regulating cell migration and adhesion, proteases have also been implicated in the activation of signaling pathways of receptors, growth factors, and cytokines (Werb and Yan, 1998; Rifkin *et al.*, 1999; Egeblad and Werb, 2002; McQuibban *et al.*, 2002; Hoege, 2003). Membrane-anchored proteins are subjected to proteolytic processing, thereby releasing, partially or completely, the ED as soluble protein, with the rest of the protein being left behind as membrane-associated part. This process is termed ectodomain shedding (Peschon *et al.*, 1997; Blobel, 2000). When transmembrane proteins undergo regulated proteolysis, metalloproteinases are involved that either belong to the ADAM (a disintegrin and a metalloprotease) family, to the family of matrixmetalloproteinases (MMPs) or to the family of prohormone convertases (PCs). The ADAM family has been implicated in physiological processes such as neurogenesis, but also in pathological processes including arteriosclerosis and Alzheimer's disease (Werb und Yan, 1998; Schlondorff and Blobel, 1999; Primakoff and Myles, 2000). The family of MMPs are responsible for the degradation of ECM components such as Tenascin C and laminin, with some members of this family being involved in regulated processing. MMPs play an important role in the nervous system by mediating neurite outgrowth and participating in cell survival, migration or cell death (Schlondorff and Blobel, 1999; Yong *et al.*, 2001; for review see Kalus, 2005). The PCs are serine proteases and include neuronal peptide hormones, growth factors, receptors, and enzymes. They are generated as inactive pro-proteins, *e.g.*, the pro-neurotrophins such as pro-BDNF (Seidah and Chretien, 1997; Mowla *et al.*, 2001). Furthermore, pro-neurotrophins bind with a higher selectivity to p75<sup>NTR</sup> as compared to the mature forms. Thereby pro-neurotrophins activate apoptosis more efficiently than the mature proteins (Lee *et al.*, 2001). PCs, in general, are involved in synaptic plasticity and LTP (for review see Kalus, 2005). Recently, a new mode of processing has been described: the 'regulated intramembrane proteolysis' (RIP). It involves site-specific, membrane-localized proteases and is the proteolytic processing of membrane-bound precursors of multiple regulatory proteins. Examples for these events are Notch signaling, amyloid precursor protein processing and sterole regulation. In principle, the first of the sequential steps of RIP involves the cleavage of the ED, which seems to be a prerequisite for the second proteolytic event which occurs at the TMD. The initial shedding step is necessary for a better accessibility of the TMD to the second protease, in order to prepare the substrate for RIP. The released intracellular fragment often migrates to the nucleus as a transcriptional regulator. Intramembrane cleaving proteases are the responsible proteases for RIP, which is considered as a precisely regulated mechanism that guarantees controlled proteolysis in the plane of the membrane (Brown *et al.*, 2000; Hoppe *et al.*, 2001; Urban and Freeman, 2002).

Since the cell membrane is under constant reconstruction, proteolytic processing seems to represent an ideal mechanism or tool to ensure dynamic changes in its protein composition. The activity of proteases is controlled by a complex system of physiological inhibitors. However, when protease expression and substrate proteolysis are altered or out of regular control, pathological events follow, leading to several diseases such as Alzheimer's disease or multiple sclerosis. Therefore, proteases and their substrates are more and more recognized as precious drug targets in disease treatment (Werb und Yan, 1998; Blobel, 2000; Yong *et al.*, 2001).

### 1.3.1 Ubiquitination and ubiquitin-dependent proteolysis

The ubiquitin-proteasome system (UPS), one of the posttranslational modification systems, is known to be classically responsible for targeted protein degradation by the proteasome (Hershko und Ciechanover, 1998; Laney and Hochstrasser, 1999). Recent observations have shown that ubiquitination of proteins within the proteasome is the major proteolytic processing mechanism used by mammalian cells to regulate cytosolic and nuclear protein levels (Klimschewski, 2003). UPS has also been implicated as a component of the mechanism that regulates endosomal trafficking of membrane receptors (Levkowitz *et al.*, 1998; Kerkhof *et al.*, 2001). Moreover, UPS is involved in the formation of long-term memory (Lopez-Salon *et al.*, 2001) and in regulation of protein activation, immune responses, signal transduction, DNA repair, and transcription (Pickart, 2001; Hoege, 2002). Furthermore, ubiquitin-like modifier systems (UBLs) have recently been discovered (Jentsch and Pyrowolakis, 2000). Ubiquitin, an 8.5-kDa protein, can be covalently attached to cellular proteins *via* an isopeptide linkage between the C-terminal groups of two glycines of ubiquitin and lysine amino groups on the acceptor protein. This conjugation of ubiquitin (or ubiquitin-like proteins) *via* an isopeptide linkage to target proteins is defined as **ubiquitination** or **ubiquitylation** (Hoege, 2002). This process often leads to the formation of ubiquitin chains which are recognized and degraded by a multicatalytic protease, namely the 26S proteasome, which is located in the cytosol or in the nucleus. The 26S proteasome is a cylindrical organelle that recognizes ubiquitinated proteins, often degrades the proteins and recycles ubiquitin (Enenkel *et al.*, 1999; Russell *et al.*, 1999). Certain proteins are only monoubiquitinated, others are polyubiquitinated without any later contact with the proteasome (Pickart, 1997). Ubiquitin-like proteins such as small ubiquitin-related modifier (SUMO) are conjugated to their substrates in analogy to ubiquitin. Both, the UPS and the UBLs seem to influence each other, but how exactly is poorly understood (Jentsch und Pyrowolakis, 2000). For instance, SUMO seems to act as an antagonist to ubiquitin or

functions as regulator in protein–protein interactions. It is very likely that SUMO enhances the stability or mediates the subcellular location of proteins (for review see Melchior, 2000; Müller *et al.*, 2001). The regulatory function of both systems not only includes ubiquitination but also deconjugation of ubiquitin from the target proteins. As soon as ubiquitin is removed from proteins, they have different functions (Hoegge, 2002). The UPS provides a clue for understanding the molecular mechanisms underlying cancer and various neurodegenerative diseases such as Parkinson's disease and Huntington's disease (Doherty *et al.*, 2002; Ross and Pickart, 2004).

A new ubiquitin processing pathway termed 'regulated ubiquitin/proteasome-dependent processing' (RUP) has been recognized for transcriptional control. The first description of RUP was the processing of the soluble protein p105, the precursor of the p50 NF- $\kappa$ B transcription factor. Processing of p105 by the proteasome proceeds by a mechanism in which the C-terminal half of the molecule is quickly degraded, whereas the N-terminal portion (p50) is left intact (Palombella *et al.*, 1994). The transcription factors SPT23 and MGA2, relatives of the mammalian NF- $\kappa$ B, are attached to the membrane *via* their C-terminal tails and the N-terminal domains are 'saved from' degradation. In most cases, however, proteasome action leads to complete degradation of the protein into small peptides (Hoppe *et al.*, 2000; Rape and Jentsch, 2004). Another example for RUP is the *Drosophila* protein Cubitus interruptus (Ci), a component of the Hedgehog signaling pathway (Noureddine *et al.*, 2002). However, not much is known about other substrates that undergo RUP.

### 1.3.2 NCAM-dependent proteolysis

Several studies have shown the involvement of NCAM in proteolytic processing. Beyond the various soluble NCAM isoforms that have been detected so far, the 110-kDa fragment is the most prevalent one (Gennarini *et al.*, 1984; Nybroe *et al.*, 1989; Olsen *et al.*, 1993). This NCAM fragment interacts with ECM molecules and can be produced in a calmodulin (CaM)-regulated manner when brain membranes are incubated at 37 °C (Probstmeier *et al.*, 1989). TNF $\alpha$ -converting enzyme (TACE), a metalloprotease and member of the ADAM family, is probably one of the responsible enzymes for the shedding of NCAM140 and -180 EDs. NCAM120 seems to be cleaved by a different mechanism. The matrix metalloprotease inhibitor GM 6001 has an inhibitory effect on the generation of soluble NCAM fragments and on NCAM-dependent neurite outgrowth (Kalus, 2005). The tissue-type plasminogen activator (tPA), a serine protease, has been shown to proteolytically cleave the NCAM-ED. The identified NCAM isoforms had a molecular weight of 65 kDa and 90 kDa

(Endo *et al.*, 1999). Soluble NCAM disturbs cell adhesion whereas substrate-coated NCAM mediates this process (Olsen *et al.*, 1993). After activation of NMDA receptors, the generation of 65- and 75-kDa soluble NCAM fragments was increased and caused induction of LTP (Hoffman *et al.*, 1998a; Hoffman *et al.*, 1998b). NCAM processing seems to play an essential role in certain neurological diseases such as schizophrenia and Alzheimer's disease (Poltorak *et al.*, 1995; Vawter *et al.*, 1998).

### 1.3.3 Neurotrophin receptor-dependent proteolysis

The neurotrophin receptor p75<sup>NTR</sup> was the first member of this family to be found involved in proteolysis and ectodomain shedding (DiStefano and Johnson, 1988; Schlondorff und Blobel, 1999). It has been shown that p75<sup>NTR</sup> undergoes RIP. The cleavage of p75<sup>NTR</sup> is modulated by the sequential action of  $\alpha$ - and  $\gamma$ -secretase leading to the release of intracellular fragments into the cytosol. This reveals a new mechanism for transmitting neurotrophin signals from the cell surface to intracellular sites. NRH1 and NRH2, two p75<sup>NTR</sup> homologues, also undergo proteolytic processing, mediated by a different protease, whereby soluble ID fragments are released. Soluble IDs of p75<sup>NTR</sup> and NRH2 are involved in the activation of NF- $\kappa$ B, which implicates intracellular and nuclear signaling functions through distinct proteases (Chao, 2003; Kanning *et al.*, 2003). TrkA and TrkB have been recognized as mediators of p75<sup>NTR</sup> processing whereas neurotrophins do not regulate this process. p75<sup>NTR</sup> acts as a co-receptor for neurotrophins by creating a high-affinity heteromeric receptor complex with Trk receptors (Esposito *et al.*, 2001). In the absence of Trks p75<sup>NTR</sup> signals cell death, but potentiates survival in the presence of Trks (for review see Roux and Barker, 2002). In the absence of Trks, truncated and intracellular forms of p75<sup>NTR</sup> more effectively induce neuronal cell death (Coulson *et al.*, 2000; Roux *et al.*, 2001). Therefore, the regulation of p75<sup>NTR</sup> cleavage by TrkA and TrkB may be one mechanism by which Trks affect p75<sup>NTR</sup> cell death signaling (Kanning *et al.*, 2003). TrkA forms a molecular complex together with either full-length p75<sup>NTR</sup> or membrane-bound cytosolic fragments (Jung *et al.*, 2003).

Beyond p75<sup>NTR</sup>, ectodomain shedding has also been described for TrkA, resulting in two fragments which contain the TMD and ID (Cabrera *et al.*, 1996; Diaz-Rodriguez *et al.*, 1999; Diaz-Rodriguez *et al.*, 2000; Diaz-Rodriguez *et al.*, 2002). Cleavage of TrkA was induced by a calmodulin (CaM) inhibitor and was highly sensitive to metalloprotease inhibitors (Diaz-Rodriguez *et al.*, 2000; Llovera *et al.*, 2004).

---

The p75<sup>NTR</sup> is a marker for cholinergic neurons in the degenerated forebrain of Alzheimer's disease patients (Auld *et al.*, 2002), and it is speculated that the proteolysis of p75<sup>NTR</sup> might be linked to Alzheimer's disease or the chronic inflammatory reaction in an autosomal dominant disease (Chao, 2003).

## 2 Aim of the study

Multiple interactions of cell adhesion molecules (CAMs) (Cunningham *et al.*, 1987; Doherty *et al.*, 1990; Diestel *et al.*, 2003), and neurotrophic factors (Cohen *et al.*, 1994; Williams *et al.*, 2005) influence the development and maintenance of the nervous system. Various neuronal functions are impaired in NCAM-deficient (NCAM<sup>-/-</sup>) mice such as reduced hippocampal fasciculation in addition to impaired long-term plasticity (LTP) (Cremer *et al.*, 1994; Stork *et al.*, 1997). For example, it has been shown that the phosphorylation of the receptor tyrosine kinase B TrkB was reduced in neural CAM deficient mice NCAM<sup>-/-</sup>. When  $\alpha$ -2,8-linked polysialic acid was removed from the NCAM, brain-derived neurotrophic factor (BDNF) function was reduced. Earlier studies have implicated a putative extracellular interaction between TrkB and NCAM *via* a binding between PSA-modified NCAM (PSA-NCAM) and BDNF (Mueller *et al.*, 1999; Vutskits *et al.*, 2001).

This study, however, addressed the question whether the 180-kDa isoform of NCAM (NCAM180) and TrkB interact intracellularly. Results from the phage display analysis revealed a peptide in the intracellular domain of NCAM180 (NCAM180-ID) that bound to a peptide in the TrkB-ID. The major aim of this work was to characterize the potential binding between NCAM180-ID and TrkB-ID. For this purpose, biochemical cross-linking, co-immunoprecipitation assays and binding studies were performed. Beyond that, the functional role of the interaction between these two proteins was scrutinized by investigating the effect of BDNF on NCAM-dependent neurite outgrowth. The main focus of this study was based on the hypothesis that a cross-talk exists between TrkB and NCAM with the potential of causing convergence and divergence of downstream signaling cascades in various ways.

## 3 Materials

### 3.1 Chemicals

All chemicals were obtained from the following companies in p.a. quality: GibcoBRL (Life technologies, Karlsruhe, Germany), Qiagen (Hilden, Germany), Calbiochem (La Jolla, California, USA), Dynal (Hamburg, Germany), Perbio Science (Bonn, Germany), and Sigma-Aldrich (Deisenhofen, Germany).

### 3.2 Solutions and buffers

(in alphabetical order)

ABTS staining solution ( <i>ELISA</i> )	2% (w/v) ABTS in 100 mM sodium acetate buffer, pH 4.2 0.001% (v/v) H <sub>2</sub> O <sub>2</sub> freshly prepared
Antibody buffer ( <i>Immunocytochemistry</i> )	0.3% (w/v) BSA in PBS, pH 7.4 0.02% (w/v) Triton X-100
BCA-Reagent A ( <i>BCA kit</i> )	1% (w/v) Bicinchoninacid disodium salt 1.7% (w/v) Na <sub>2</sub> CO <sub>3</sub> x H <sub>2</sub> O 0.16% (w/v) Sodiumtartrat 0.4% (w/v) NaOH 0.95% (w/v) NaHCO <sub>3</sub> , pH 11.25
BCA-Reagent B ( <i>BCA kit</i> )	4% (w/v) CuSO <sub>4</sub> x 5 H <sub>2</sub> O
Blocking buffer ( <i>ELISA-TrkB-ID</i> )	3% (w/v) BSA in 50 mM Tris buffer, pH 7.5 0.2% (w/v) Tween 20
Blocking buffer ( <i>ELISA-TrkB pepides</i> )	1% (w/v) BSA in PBS or TBS, pH 7.4
Blocking buffer ( <i>Immunocytochemistry</i> )	3% (w/v) BSA in PBS, pH 7.4 0.2% (w/v) Triton X-100
Blocking buffer ( <i>Western Blot</i> )	3-4% (w/v) instant milk powder in TBS
Blotting buffer ( <i>Western Blot</i> )	25 mM Tris 192 mM Glycin

---

Boston buffer ( <i>Bacterial lysis</i> )	50 mM Tris, pH 8.0 1% (w/v) Triton X-100 50 mM KCl 2.5 mM EDTA
Coomasie Blue Solution	0.1% Coomassie Blue Solution 250 ml Ethanol 50 ml Acetic acid (ad to 500 ml H <sub>2</sub> O)
Coupling solution ( <i>Covalent coupling of antibody to beads</i> )	20 mM dimethylpimelimidate in 200 mM sodium tetraborate, pH 9.0
Destaining solution	350 ml Ethanol 50 ml Acetic acid (ad to 1l H <sub>2</sub> O)
Developing solution ( <i>Silver stain</i> )	0.04% Formaldehyde in 2% Na <sub>2</sub> CO <sub>3</sub> 7.5 g Na <sub>2</sub> CO <sub>3</sub> 30 µl Formaldehyde up to 250 ml H <sub>2</sub> O (freshly added)
Elution buffer ( <i>Protein expression</i> )	50 mM NaH <sub>2</sub> PO <sub>4</sub> , pH 8.0 300 mM NaCl 250 mM Imidazole
Ethidiumbromide- staining solution ( <i>DNA-gels</i> )	10 µg/ml Ethidiumbromide in 1x TAE
Fixation solution ( <i>Silver stain</i> )	50% (v/v) Methanol 5% (v/v) Acetic acid 45% (v/v) H <sub>2</sub> O
Homogenization buffer ( <i>Isolation of subfractions from brains</i> )	0.32 M Sucrose 1 mM CaCl <sub>2</sub> 1 mM MgCl <sub>2</sub> 50 mM Tris-HCl, pH 7.4
Hypotonic lysis buffer ( <i>Cell lysis</i> )	10 mM HEPES, pH 7.4 0.5 mM EDTA
IPTG ( <i>Protein expression</i> )	resuspending 238 mg/ml results in a 1 M stock solution
Lysis buffer 1 ( <i>Cell lysis for cross- linking-TrkB peptides</i> )	20 mM Na <sub>3</sub> PO <sub>4</sub> , pH 7.4 150 mM NaCl 1 mM CaCl <sub>2</sub> 1 mM MgCl <sub>2</sub> 1x Complete <sup>TM</sup> EDTA-free protease inhibitor mixture

---

Lysis buffer P+ ( <i>Conditions inhibiting dephosphorylation</i> )	1x PBS, pH 7.4 1mM MgCl <sub>2</sub> 1mM Mn Cl <sub>2</sub> 1mM EGTA 1mM NaF 0.5 mM Pervanadate solution freshly prepared 20 μM GM 6001 1 μM DAPT 1x Complete <sup>TM</sup> EDTA-free protease inhibitor mixture
Lysis buffer P- ( <i>Conditions inhibiting tyrosine kinase phosphorylation</i> )	1x PBS, pH 7.4 5 μM Trk inhibitor K252a 1x Complete <sup>TM</sup> EDTA-free protease inhibitor mixture
Native lysis buffer ( <i>Bacterial lysis</i> )	50 mM NaH <sub>2</sub> PO <sub>4</sub> , pH 8.0 300 mM NaCl 10 mM Imidazole
Pervanadate solution ( <i>Lysis buffer P+</i> )	1 mM Na <sub>3</sub> VO <sub>4</sub> 1 mM H <sub>2</sub> O <sub>2</sub> freshly prepared
Phosphate Buffered Saline (PBS)	150 mM NaCl 20 mM Na <sub>3</sub> PO <sub>4</sub> , pH 7.4
Phosphorylation buffer ( <i>Preparation of phosphorylated TrkB-ID</i> )	50 mM HEPES 1 mM ATP 10 mM MgCl <sub>2</sub> 10 mM MnCl <sub>2</sub> 0.1% (w/v) Tween 20, pH 7.0
Protease-inhibitors	Complete <sup>TM</sup> EDTA-free pills resuspending 1 tablet in 1 ml solution results in a 50x stock solution (Roche Diagnostics, Mannheim, Germany)
RIPA-buffer ( <i>Cell lysis</i> )	50 mM Tris-HCl, pH 7.4 1% (w/v) Triton X-100 or NP-40 150 mM NaCl 1 mM EGTA 1 mM Na <sub>3</sub> VO <sub>4</sub>
Roeder C buffer ( <i>Nuclear fractions</i> )	10 mM Tris, pH 8.0 10% (v/v) Glycerol 300 mM NaCl 2 mM MgCl <sub>2</sub> 0.5 mM EDTA

---

Running Gel 8% ( <i>Protein gels</i> )	4.89 ml deionized water 5.26 ml 1 M Tris, pH 8.8 0.14 ml 10% SDS 3.73 ml 30% Acrylamide-Bis 29:1 70 $\mu$ l 10% APS 7 $\mu$ l TEMED
Sample buffer (5x) ( <i>Protein gels</i> )	0.312 M Tris-HCl, pH 6.8 10% (w/v) SDS 5% (w/v) $\beta$ -Mercaptoethanol 50% (v/v) Glycerol 0.13% (w/v) Bromphenol blue
Sensitising solution ( <i>Silver stain</i> )	0.02% Sodium thiosulfate in water
SDS running buffer (10x) ( <i>Protein gels</i> )	0.25 M Tris-HCl, pH 8.3 1.92 M Glycine 1 M SDS
Stacking Gel 5% ( <i>Protein gels</i> )	3.77 ml Deionized water 0.32 ml 1 M Tris, pH 6.8 0.05 ml 10% (w/v) SDS 0.83 ml 30% Acrylamide-Bis 29:1 25.0 $\mu$ l 10% APS 7 $\mu$ l TEMED
Staining solution ( <i>Protein gels</i> )	40% (v/v) Ethanol 10% (v/v) Acetic acid 0.1% (w/v) Serva Blue R250
Stripping buffer ( <i>Western blots</i> )	0.5 M NaCl 0.5 M Acetic acid
Sucrose buffered solutions ( <i>Sucrose gradient</i> )	1.0 M/1.2 M/2.27 M/2.3 M 1 mM CaCl <sub>2</sub> 1 mM MgCl <sub>2</sub> 5 mM Tris-HCl, pH 7.4
TAE (50x) ( <i>DNA gels</i> )	2 M Tris-Acetate, pH 8.0 100 mM EDTA TE (10x) 0.1 M Tris-HCl, pH 7.5 10 mM EDTA
TBF1 ( <i>Competent E.coli</i> )	100 mM RbCl 50 mM MnCl <sub>2</sub> 30 mM Potassium acetate 10 mM CaCl <sub>2</sub> 15% (v/v) Glycerol (pH 5.8, sterile-filter)

---

TBF2 ( <i>Competent E.coli</i> )	10 mM MOPS 10 mM RbCl 75 mM CaCl <sub>2</sub> 15% (v/v) Glycerol (pH 8.0, sterile-filter)
Tris Buffered Saline (TBS)	10 mM Tris-HCl, pH 8.0 150 mM NaCl
TBST ( <i>ELISA</i> )	0.2% Tween 20 in TBS, pH 7.4
TBST ( <i>Western Blot</i> )	0.05% Tween 20 in TBS, pH 7.4
Tris plus buffer ( <i>Isolation of nuclear fraction</i> )	5 mM Tris-HCl, pH 7.4 1 mM CaCl <sub>2</sub> 1 mM MgCl <sub>2</sub> 1 mM NaHCO <sub>3</sub>
Wash buffer A ( <i>Protein expression</i> )	50 mM NaH <sub>2</sub> PO <sub>4</sub> , pH 8.0 600 mM NaCl 10 mM Imidazole
Wash buffer B ( <i>Protein expression</i> )	50 mM NaH <sub>2</sub> PO <sub>4</sub> , pH 8.0 300 mM NaCl 20 mM Imidazole
Wash buffer C ( <i>Protein expression</i> )	50 mM NaH <sub>2</sub> PO <sub>4</sub> , pH 8.0 300 mM NaCl 40 mM Imidazole
Wash buffer D ( <i>Protein expression</i> )	50 mM NaH <sub>2</sub> PO <sub>4</sub> , pH 8.0 300 mM NaCl 60 mM Imidazole
Washing buffer 1 ( <i>Co-IP with H28 antibody</i> )	0.5% (w/v) NP-40 50 mM Tris-HCl, pH 8.0 500 mM NaCl
Washing buffer 2 ( <i>Co-IP with H28 antibody</i> )	0.5% (w/v) NP-40 50 mM Tris-HCl, pH 8.0
Washing buffer 3 ( <i>Co-IP with D3 antibody</i> )	10 mM Tris, pH 7.5 750 mM NaCl 0.5% Triton X-100

Washing buffer 0.2% (w/v) Tween 20 in TBS, pH 7.4 (TBST)  
(*ELISA-TrkB-ID*) 0.1% BSA

Washing buffer 0.05% (w/v) Tween 20 in PBS or TBS, pH 7.4  
(*ELISA-TrkB peptides*) (PBST or TBST)

### 3.3 Synthesized peptides

#### 3.3.1 NCAM peptides

(Synthesis by Dr. Jochen Heukeshoven, Hamburg, Germany)

Peptide	Sequence
1	H-DITCYFLNKCGLLMCIAVNLCGKAGPGAKGKDMEEG-OH
2	H-KAAFSKDESKEPIVEVRTEEERTPNHDGGKHTEPNETTPLTEPE-OH
3	H-KGPVETKSEPQESEAKPAPTEVKTVPNEATQTKENESKA-OH

#### 3.3.2 TrkB peptides

(Synthesis by Dr. Jochen Heukeshoven, Hamburg, Germany)

Peptide	Sequence
1	H-Q <b>HFVHKHP</b> GLSAC-OH
2	H-CGMVYLAS <b>QHFVHR</b> DLATRNC <b>LVGC</b> -OH

(Synthesis by Dr. Christian Schafer, Copenhagen, Denmark)

Peptide	Sequence
3	H-CS <b>QHFVHR</b> D-OH
4	H-S <b>QHFVHR</b> DLATRNC-OH

The putative binding site from the page display analysis is depicted in bold letters.

### 3.4 Bacterial media

(Media were autoclaved and antibiotics were supplemented prior to use)

LB-medium	10 g/l Bacto-tryptone, pH 7.4 10 g/l NaCl 5 g/l Yeast extract
LB/Amp-medium	100 mg/l Ampicillin in LB-Medium
Ampicillin stock solution	100 mg/ml in H <sub>2</sub> O
IPTG/XGAL stock solution ( <i>LB/IPTG/XGAL plates</i> )	1.25 g IPTG 1 g XGAL in 25 ml Dimethyl formamide
Kanamycin stock solution	25 mg/ml in H <sub>2</sub> O
LB/Amp-plates	20 g/l Agar in LB-Medium 100 mg/l Ampicillin
LB/Kan-plates	20 g/l Agar in LB-Medium 25 mg/l Kanamycin
LB/IPTG/XGAL plates	15 g/l Agar in LB-Medium 1 ml IPTG/XGAL stock solution
Psi broth	4 mM MgSO <sub>4</sub> 10 mM KCl in LB-Medium

### 3.5 Bacterial strains and cell lines

CHO-K1	Chinese Hamster Ovary
N2a	Mouse neuroblastoma cell line Origin: Established from the spontaneous tumor of a strain A albino
Escherichia coli DH5 $\alpha$	Clontech
Escherichia coli M15pREP4	QIAGEN

### 3.6 Cell culture media

Media were prepared from a 10x stock solution purchased from Gibco GBL

CHO-cell Medium	Glasgow MEM (GMEM) (with nucleotides, L-Glutamine) supplemented with 10% (v/v) Fetal calf serum (FCS) 50 U/ml Penicilline/Streptomycine 4 mM L-Glutamine
N2a-cell Medium / LMTK/LMTK-PST Medium	Dulbecco MEM (DMEM) supplemented with 10% (v/v) Fetal calf serum (FCS) 50 U/ml Penicilline/Streptomycine 1 mM Pyruvate
Cerebellar microexplant culture medium	Minimum Eagle's medium (MEM) supplemented with 10% (v/v) Horse serum (HS) 10% (v/v) Fetal calf serum (FCS) 6 mM Glucose 200 µM L-Glutamine, 50 units/ml Penicilline/Streptomycine 10 µg/ml Transferrin 10 µg/ml Insulin 10 ng/ml Selenium
Cerebellar culture medium (Medium X-1)	Basal Eagle's medium (BEM) 50 units/ml Penicilline/Streptomycine 0.1% BSA 10 µg/ml Insulin 4 nM L-Thyroxin 100 µg/ml Transferrin 0.027 TIU/ml Aprotinin 30 nM Sodium selenit optional: 1 x Sodium pyruvat 1 x L-Glutamine
RPMI medium	PAA Laboratories, Pasching, Austria
Versene	Gibco GBL
Hanks' balanced salt solution (HBSS)	PAA Laboratories, Cölbe, Germany

### 3.7 Inhibitors and activators

All inhibitors were ordered from Calbiochem (LaJolla, CA, USA), recombinant expressed brain-derived neurotrophic factor (BDNF) from Sigma-Aldrich (St Louis, MO, USA), and the Calmodulin inhibitor CGS9343B from Novartis Pharma (Basel, Switzerland).

<b>K-252a</b> ( <i>Norcardiopsis sp.</i> in solution, a tyrosine kinase inhibitor)	5 $\mu$ M in DMSO for lysis buffer and 100 nM in cell culture
<b>GM 6001</b> (Broad-spectrum inhibitor of matrix metalloproteinases)	20 $\mu$ M in DMSO for homogenization buffer and 100 nM in cell culture, 50 $\mu$ M in proteolysis assay
<b>DAPT</b> ( $\gamma$ -Secretase inhibitor IX)	1 $\mu$ M in DMSO for homogenization buffer and 100 nM in cell culture
<b>CGS9343B</b> (Calmodulin inhibitor)	50 $\mu$ M for proteolysis assay
<b>1,10-Phenantroline</b>	10 mM in proteolysis assay
<b>ALLN</b> (MG-101; inhibitor of neutral cysteine proteases, calpain and proteasome)	50 $\mu$ M in DMSO for proteolysis assay and 100 nM in cell culture
<b>BDNF</b> (brain-derived neurotrophic factor; human, recombinantly expressed in <i>E. coli</i> )	50 ng/ml (50 $\mu$ M stock solution dissolved in ddH <sub>2</sub> O)

### 3.8 Molecular weight standards

6  $\mu$ l of the *BenchMark Prestained Protein Ladder* (Life Technologies) (2) or *Precision Plus Protein Standards Dual Color* (Biorad, Hercules, CA, USA) (1) were loaded on the SDS-PAGE gel.

(1)

Band No.	apparent molecular weight (kDa)
----------	---------------------------------

---

1	250
2	150
3	100
4	75*
5	50
6	37
7	25*
8	20
9	15
10	10

\*Orientation bands (pink in color)

---

(2)

---

Band No.	apparent molecular weight (kDa)
----------	---------------------------------

---

1	220
2	160
3	120
4	100
5	90
6	80
7	70
8	60
9	50*
10	40
11	30
12	25*
13	20
14	15
15	10

\*Orientation bands (50 kDa and 25 kDa are more prominent)

---

### 3.9 Plasmids

pQE30 prokaryotic expression plasmid for recombinant expression of proteins carrying a polyhistidine-domain (6xHis) at the 5' end of the multiple cloning site for purification. Amp-resistance (Qiagen).

pcDNA3 mammalian expression vector for transfection. Amp-resistance (Invitrogen).

### 3.10 Mouse model (*Mus musculus domesticus*, Linnaeus, 1758)

Developing (postnatal) and adult (> 2 months) C57BL/6J mice, *Mus musculus*, were taken from our breeding colony and raised according to standard protocols. NCAM knockout mice (NCAM<sup>-/-</sup>) (Cremer *et al.*, 1994) were generated either by breeding heterozygous mutant mice kept on a mixed C57BL/6 background or by a homozygous breeding. TrkB knock-out mice (TrkB<sup>-/-</sup>) (Klein *et al.*, 1993) were generated by breeding heterozygous

mutant mice kept on a mixed C57BL/6 background. Standard procedures (Laird *et al.*, 1991) were used for the genomic DNA extraction from tail biopsies of mice. All mice were kept in our animal facility. Mice were kept under standard conditions with food and water ad libitum and a light:dark cycle of 12:12 h. The animals were sacrificed in a CO<sub>2</sub>-chamber prior to removal of the brain. All animal experiments were approved by the University and State of Hamburg animal care committees and were conformed to NIH guidelines.

### 3.11 Antibodies

#### 3.11.1 Primary antibodies

- Kir3.3 rabbit polyclonal Kir3.3 antibody derived from a peptide encoding for the C-terminus of Kir3.3 (kindly provided by Dr. Rüdiger Veh, Universitätsklinikum der Humboldt-Universität Berlin, Berlin, Germany).  
IB: 1:1000 (1% milk in TBS)
- NCAM 1B2 polyclonal antibody derived from the extracellular domain of mouse NCAM-Fact (produced in the lab of Prof. Dr. Melitta Schachner).  
IB: 1:5000 (4% milk in TBS)  
ICH: 1:800
- D3 mouse monoclonal antibody recognizes an epitope on 180 kDa isoform within the intracellular domain encoded by exon 18.  
IB: 1:2000 (3% milk in TBS)  
ICH: 1:100  
ELISA: 1:1000 (0.1% BSA in TBST)  
IP: 4 µg/ sample
- P61 rat monoclonal antibody recognizes an intracellular determinant expressed by adult and embryonic NCAM140 and NCAM180 (kindly provided by Christo Goridis, Developmental Biology Institute of Marseille, Marseille, France).  
IB: 1:10 (supernatant in 2% milk in TBS)  
ELISA: 1:100 (0.1% BSA in TBST)
- 5B8 mouse monoclonal antibody produced against the C-terminus of the intracellular domain of NCAM140 and NCAM180 (obtained from Developmental Studies Hybridoma Bank, University of Iowa, Iowa, USA).  
IB: 1:10 (supernatant in 3% milk/ TBS)  
ELISA: 1:100 (0.1% BSA in TBST)

---

H28	rat monoclonal antibody produced against the C-terminus of the intracellular domain of NCAM180 (kindly provided by Christos Goridis, Developmental Biology Institute of Marseille, Marseille, France). IB: 1:10 (supernatant in 3% milk/TBS) IH: 1:100
Penta His	mouse monoclonal antibody that recognizes five consecutive histidine residues (Qiagen, Hilden, Germany). ELISA: 1:1000 (1% BSA in TBST)
PSA (735)	mouse monoclonal anti- $\alpha$ -2,8-polysialic acid IgG2a antibody which only recognizes long chain PSA (kindly provided by Dr. Rita Gerardy-Schahn, Medizinische Hochschule Hannover, Hannover, Germany). ICH: 1:100
PanTrk (C-14)	rabbit polyclonal antibody raised against a peptide mapping within the highly conserved C-terminus (Santa Cruz Biotechnology, Santa Cruz, USA). IB: 1:1000 (3% milk in TBS) IP: 4 $\mu$ g/ sample ICH: 1:100
TrkB (H-181)	rabbit polyclonal antibody raised against a recombinant protein corresponding to amino acids 160-340 located within the extracellular domain of TrkB of human origin (Santa Cruz Biotechnology, Santa Cruz, USA). IB: 1:1000 (3% milk in TBS) ICH: 1:100
TrkB (794)	rabbit affinity purified polyclonal antibody raised against a peptide mapping adjacent to the C-terminus of the precursor form of TrkB gp145 of mouse origin (Santa Cruz Biotechnology, Santa Cruz, USA). IB: is not to recommend for IB due to lack of specificity and weak signal ICH: 1:100
Ubiquitin	mouse monoclonal antibody against amino acids 1-76 representing full length ubiquitin of bovine origin (Santa Cruz Biotechnology, Santa Cruz, USA). IP: 2 $\mu$ g/ sample

### 3.11.2 Secondary antibodies

All horseradish peroxidase-coupled (HRP) secondary antibodies were purchased from Dianova (Hamburg, Germany) and were used in a dilution of 1:10,000. Streptavidin-HRP was

obtained from Sigma-Aldrich (Deisenhofen, Germany) and was used in a dilution of 1:3000. For immunocytochemistry, Cy3 and Cy5 secondary antibodies were obtained from Dianova and were used in a dilution of 1:200.

## 4 Methods

### 4.1 Molecular biology

#### 4.1.1 Bacterial strains

##### 4.1.1.1 Maintenance of bacterial strains

(Sambrook *et al.*, 1989)

Selected bacterial strains were stored as glycerol stocks (LB-medium, 25% (v/v) glycerol) at -70 °C. An aliquot of the stock was streaked on an LB-plate containing the corresponding antibiotics and was incubated overnight at 37 °C. Agar plates covered with grown bacteria were stored up to 6 weeks at 4 °C.

##### 4.1.1.2 Production of competent bacteria

(Inoue *et al.*, 1990)

DH5 $\alpha$  and M15[REP4] bacteria were streaked on LB-plates containing the appropriate antibiotics and incubated overnight at 37 °C. Individual colonies were selected and used for inoculation of an overnight culture that was subsequently added to 100 ml pre-warmed LB medium. Bacterial growth at 37 °C continued until an optical density (OD<sub>600</sub>) of 0.5 was reached (approximately 90 –120 min). After a cooling period on ice for 5 min the culture was transferred to a sterile round-bottom tube and centrifuged at low speed (4,000 x g, 5 min, 4 °C). The cells were gently resuspended in ice-cold TBF1 buffer and kept on ice for another 90 min. To harvest cells a previous centrifugation step was repeated (4,000 x g, 5 min, 4 °C). Cells were resuspended in 4 ml ice-cold TBF2 buffer. Aliquots were snap frozen in liquid nitrogen and stored at -70 °C for no longer than 6 months.

##### 4.1.1.3 Transformation of bacteria

(Sambrook *et al.*, 1989)

Aliquots of competent DH5  $\alpha$  or M15[REP4] bacteria were thawed on ice for 10 min. 50-100 ng of plasmid DNA were supplemented to 100  $\mu$ l of bacteria suspension and incubated for 20 min at 4 °C. After a heat shock at 42 °C for 1 min and consecutive incubation on ice for 2 min, 800  $\mu$ l LB-medium were added to the bacteria following incubation at 37 °C for 30 min with constant movement. The cells were collected by centrifugation at 10,000 x g for 2 min at RT. Cells were resuspended in 100  $\mu$ l LB medium and plated on LB

plates containing the appropriate antibiotics. The plates were incubated at 37 °C overnight to allow single bacteria colonies to grow.

#### **4.1.2 Plasmid isolation of *Escherichia coli***

(Sambrook *et al.*, 1989)

The methods for plasmid DNA purification are based on alkaline lysis of bacteria, on denaturation of protein by chaotropic salts, and on the separation of DNA from contaminants using a glass fiber matrix. For small scale plasmid isolation (Miniprep) 3 ml LB/Amp-Medium (100 µg/ml ampicillin) were inoculated with a single colony and incubated overnight at 37 °C with constant agitation. Bacteria of the overnight culture were pelleted by centrifugation at 12,000 x rpm for 1 min at RT. Plasmids were isolated from the bacteria according to the manufacturer's protocol (Amersham Pharmacia Mini preparation kit). The DNA was eluted from the glass fiber matrix columns by addition of 50 µl 10 mM Tris-HCl, pH 8.0 with subsequent centrifugation (12,000 rpm, 2 min, RT). The concentration of the eluted DNA was about 0.25 µg/µl as determined by UV spectrometry. To quickly obtain higher concentrations of DNA (80 µg total plasmid DNA), the Nucleospin kit (Macherey-Nagel) was chosen and the plasmids from a 15 ml bacterial culture were purified according to the manufacturer's instructions with minor modifications. Thus, the suggested volume of buffers was doubled and the elution buffer was pre-warmed to 70 °C. The concentration of the eluted DNA was about 1.5 µg/µl as determined by UV spectrometry. To prepare large quantities with about 500 µg total plasmid DNA, the Maxiprep kit (Qiagen) was used. Plasmid isolation from 500 ml bacterial cultures was performed as described in the manufacturer's protocol. To gain higher purification of plasmid DNA, successive precipitation and washing steps of the DNA in 70% ethanol at 4 °C were carried out.

#### **4.1.3 DNA Gel-electrophoresis**

(Sambrook *et al.*, 1989)

For separation of DNA fragments agarose gels in horizontal electrophoresis chambers (BioRad) were used. The agarose gels were prepared by heating 1-2% (w/v) agarose (Gibco) in 1x TAE buffer, depending on the size of DNA fragments. TAE buffer was filled in the electrophoresis chambers containing the gel. DNA sample buffer was added to the DNA samples, which were pipetted in the pockets of the gel. The gel was run at constant voltage (10 V/cm gel length) until the orange G dye reached the end of the gel. As a next step, the

gel was dyed in an ethidiumbromide staining solution for 20 min. Having this completed, the gels were documented using the E.A.S.Y. UV-light documentation system (Herolab, Wiesloh, Germany).

#### 4.1.4 Determination of DNA concentrations

An Amersham-Pharmacia spectrometer was used to determine the DNA concentrations. The necessary absolute sample volume for measurement was 50  $\mu$ l. The sample eluate was diluted 1:50 with water and the DNA concentration was determined by measuring the absorbance at 260 nm, 280 nm and 320 nm. The results were considered reliable when the measured absorbance at 260 nm was higher than 0.1 but less than 0.6. Sufficient purity of the DNA preparation was achieved with a ratio of A<sub>260</sub>/A<sub>280</sub> between 1.8 and 2.

#### 4.1.5 DNA Sequencing

DNA sequencing was performed by the sequencing facility of the ZMNH (Step-by-Step protocols for DNA-sequencing with Sequenase-Version 2.0, 5<sup>th</sup> ed., USB, 1990). For preparation, 1  $\mu$ g of DNA was diluted in 7  $\mu$ l ddH<sub>2</sub>O and 1  $\mu$ l of the appropriate sequencing primer (10 pM) was added.

#### 4.1.6 Phage display

A commercial Phage Display Peptide Library (New England Biolabs, Frankfurt, Germany) was screened displaying random 12-mer polypeptides at the pili of M13-like phage particles as fusion protein to the N-terminus of pVIII major coat protein (Hong and Boulanger, 1995). All *in vitro* selection processes, such as biopanning, for clones having selectivity towards the target, namely the intracellular domain of NCAM180 (NCAM180-ID), were performed according the Ph.D.-12<sup>TM</sup> Phage Display Peptide Library Kit instruction manual version 2.0 (New England Biolabs). The Phage Display Peptide Library is characterized by a complexity of  $1.5 \times 10^{13}$  plaque forming units/ ml (pfu/ml) with every phage displaying on the surface the encoding peptide with constant 12-mer sequence length. All three rounds of biopanning and the control by enzyme-linked immunosorbent assay (ELISA) were carried out in Nunc-Immuno<sup>TM</sup> MaxiSorp Tubes (Nunc, Wiesbaden, Germany). First, the target NCAM180-ID (dissolved in 0.1 M sodium hydrogen carbonate, pH 8.6 containing 0.02% sodium azide) was immobilized at a concentration of 100  $\mu$ g/ml and incubated overnight at 4 °C under constant agitation. Blocking with 0.1 M sodium hydrogen carbonate, pH 8.6 containing 5 mg/ml BSA and 0.02% sodium azide for 1 h was followed by a series of six final washes with Tris buffer containing 0.1% Tween 20 and 3  $\mu$ M CaCl<sub>2</sub> at RT. In

parallel, LB medium was inoculated with an individual *E. coli* ER2738 colony at 37 °C under vigorous agitation. An aliquot of peptide ( $4 \times 10^{10}$  pfu/ml) from the phage-display library was diluted in 1 ml Tris buffer containing 0.1% Tween 20 (TBST) and incubated with the target surface for 1 h at RT. After a series of 10 final washes with TBST bound phage clones were selected by unspecific elution using 0.2 M Glycine-HCl, pH 2.2, and subsequent neutralisation using 1 M Tris-HCl, pH 9.1. This eluate was amplified in an 20 ml *E. coli* ER2738 culture for 4 h at 37 °C. The precipitation and purification of the amplified phages were performed as described in the manual. The purified phage solution was used for the next round of biopanning. For the second and third round the washing steps were performed with a Tris buffer containing 0.5% Tween 20 (TBST). After the third round, the eluate was streaked out on Luria-Bertani/ D-Thiogalactosid/ 5-Bromo-4-chloro-3-indolyl- $\beta$ -D-galactopyranosid (LB/IPTG/XGAL) plates. After amplification in *E. coli* ER2738 culture plaques were removed from the plates to test the binding specificity of the interaction between NCAM180-ID and the phage peptide by a phage ELISA. The target solutions such as NCAM180-ID, CHL1-ID for control of cross-interactions and bovine serum albumin (BSA) for control of unspecific binding were immobilized on a polyvinylchloride surface of an ELISA plate (Maxisorb F8, Nunc) for 2 h. Afterwards, the wells were blocked with phosphate buffered saline (PBS), pH 7.3 containing 0.5% BSA for 1 h. Then diluted phage suspensions were applied to the wells and incubated for 1 h. After 10 washing steps with TBST a HRP-conjugated anti-M13 antibody (Pharmacia, Cambridge, USA) was applied for 1 h. Subsequently, 10 washing steps with TBST followed. Finally, visualization of phage binding was performed using an ABTS-solution containing H<sub>2</sub>O<sub>2</sub> (Sigma) as described in the paragraph ELISA. The complete procedure was performed at RT. One clone that selectively bound NCAM180-ID was selected, sequenced and characterized. The criteria for selection was a highly selective interaction between the clone and the target NCAM180-ID but no significant binding to the CHL1-ID control. Unspecific binding was tested with bovine serum albumin (BSA) as control. The phage display analysis was kindly performed by Dr. Jens Lütjohann and Dr. Jens Franke (ZMNH, Hamburg, Germany). Recombinant NCAM180-ID for the phage display screen was kindly provided by Dr. Melanie Richter (ZMNH, Hamburg, Germany).

## 4.2 Protein-biochemistry

### 4.2.1 SDS-polyacrylamide gel electrophoresis

(Laemmli, 1970)

Proteins were separated by use of discontinuous SDS-polyacrylamide gel electrophoresis (SDS-PAGE) using the Mini-Protean III system (BioRad, Munich, Germany). The SDS-polyacrylamide gel with a thickness of 1 mm consists of a 0.8 cm stacking gel containing 5% (v/v) acrylamide and covering a 4.5 cm running gel with 8% or 10% acrylamide. The stacking gel is responsible for the concentration of the proteins. The running gel separates the proteins. After complete polymerization of the gel was completed, the chamber was set up according to the manufacturer's protocol. Prior to analysis the protein samples were heated for 5 min at 95 °C in a sample buffer. The samples were then loaded with a maximum volume of 25 µl in the 15 pockets of the gel. Afterwards, the gel was run at constant voltage of 80 V for 10 min and then at 140 V until the bromphenol blue line migrated to the end of the gel. After completion of the procedure, gels were either stained or subjected to Western blot analysis.

#### **4.2.1.1 Coomassie Blue staining of SDS-polyacrylamide gels**

When SDS-PAGE was completed, the gels were dyed in staining solution for 1 h at RT with constant agitation. The gels were then incubated in destaining solution until the background of the gel almost disappeared. This staining method is sensitive enough to detect 0.1 µg of protein in a single band.

#### **4.2.1.2 Silver staining of SDS-polyacrylamide gels**

(Shevchenko *et al.*, 1996)

Whenever the Coomassie staining was not sensitive enough the Silver staining was utilized which can detect as little as 2 ng of protein in a single band. Following SDS-PAGE, gels were fixed and incubated in fixation solution for 30 min at RT with constant agitation. Gels were intensively rinsed with water and washed on a shaking platform for another hour. Afterwards the gel was quickly sensitised with the reducing sensitising solution for 1 min and washed twice with water. Subsequently, the gel was stained in chilled 0.1% AgNO<sub>3</sub> for 30 min at 4 °C. Finally, the gels were briefly incubated in developing solution and the reaction was stopped with 1% acetic acid.

## 4.2.2 Western Blot-analysis

### 4.2.2.1 Electrophoretic transfer

(Towbin *et al.*, 1979; Burnette, 1981)

Proteins were transferred from the SDS-gel onto a nitrocellulose membrane (Protran, Nitrocellulose BA 85, Schleicher & Schüll, Dassel, Germany) using a Mini Transblot apparatus (Biorad) as described in the manufacturer's protocol. The blotting 'sandwich' was assembled according to the manufacturer's recommendations. Proteins were transferred electrophoretically in blot buffer at constant voltage (85 V for 120 min or 35 V overnight at 4 °C). The pre-stained marker (*BenchMark Prestained Protein Ladder*, Life Technologies or *Precision Plus Protein Standards Dual Color*, Biorad) was used as a molecular weight marker as well as to control the efficiency of the electrophoretic transfer.

### 4.2.2.2 Immunological detection of proteins on Nitrocellulose membranes

(Towbin *et al.*, 1979; Burnette, 1981)

After completion of the electrophoretic transfer, the nitrocellulose membrane was removed from the blotting sandwich. Then the side of the membrane presenting the protein was placed right-side up in a glass jar. The membrane was washed once in TBS and blocked in non-fat dried milk powder solution (3-4% in TBS) for 1 h at RT. Afterwards, the primary antibody was diluted in milk powder solution and incubated either for 2 h at RT or overnight at 4 °C on a shaking platform. The primary antibody was removed and the membranes were washed once for 5 min with TBST and 4 times for 5 min with TBS. The appropriate secondary antibody was employed in milk powder solution for 1 h at RT followed by further washing. Immunoreactive complexes composed of membrane bound target protein, primary antibody and secondary antibody coupled to horseradish peroxidase (HRP) were detected using either the enhanced chemiluminescence detection system (ECL) or ECL with extended duration (Pierce Biotechnology, Rockford, IL, USA) for detection of weak signals. The membrane was covered with detection solution (1:1 mixture of solutions I and II) for 2 min. The solution was discarded and the blot was placed between two plastic foils. The membrane was exposed to X-ray film (Kodak Biomax-ML, Sigma-Aldrich, Steinheim, Germany) for various time periods following development and fixation of the film.

#### 4.2.2.3 Densitometric evaluation of band intensity

The band intensities were densitometrically quantified using the image processing software TINA 2.09 (raytest Isotopenmeßgeräte GmbH, Straubenhardt, Germany) and the evaluation was performed according to the manufacturer's manual. The developed film was scanned and the digitized picture was exported to TINA 2.09.

#### 4.2.3 Recombinant expression of proteins in *Escherichia coli* using the pQE-system

(Ausubel, 1996; Sambrook *et al.*, 1989; *The QIAexpressionist<sup>TM</sup> handbook*, Qiagen, 2001)

The expression of recombinant proteins in *E. coli* was achieved by cloning the cDNA of the desired protein in frame with an ATG start codon and the purification tag of the corresponding expression plasmid. Appropriate host cells were transformed with the expression vector. After host cell growth, the expression of the proteins was induced, and ended with cell lysis. Cell lysates were subjected to SDS-PAGE. Plasmids for the rat NCAM140 and NCAM180 in the pcDNA3 expression vector were kindly provided by Dr. Patricia Maness (University of North Carolina, Chapel Hill, NC, USA) and the plasmid for CHL1 in the pcDNA3 expression vector was kindly provided by Dr. Birthe Schnegelsberg (ZMNH, Hamburg, Germany) was used. The intracellular domains of NCAM140 (bp.2135-2550) and NCAM180 (bp.2135-2850) were amplified by PCR (primers: NCAMIC-Start/BamHI-up 5'-CTA GGA TCC GCC ACC ATG GAC ATC ACC TGC TAC-3' and NCAMXhoI-Stop-dn 5'-GGC GAA TTC TCG AGG TCA TGC TTT GCT CTC-3') introducing BamHI restriction sites at the 5' and 3' end. The PCR product was cloned into the pQE30 plasmid after BamHI digestion. The intracellular domain of CHL1 was amplified by PCR (primers: CHL1-CT/SacI-up 5'-CCC GAG CTC AAG AGG AAC AGA GGT-3' and CHL1-CT/HindIII-dn 5'-CCC AAG CTT TCA TGC CCG GAG TGG-3') and was also ligated to pQE30 after digestion with the appropriate restriction enzymes BamHI/HindIII. The pQE expression vectors encoding the intracellular domains (IDs) of NCAM180 and NCAM140, NCAM exon 18 and the cell adhesion molecule CHL1 (Hillenbrand *et al.*, 1999) (kindly provided by Dr. Markus Delling and Dr. Melanie Richter, ZMNH, Hamburg, Germany) were transformed into *Escherichia coli* M15/ pREP4 to provide the recombinant fragments with an N-terminal 6xHis purification tag. Transformed host cells were streaked out on LB plates containing the appropriate antibiotics (Ampicillin and Kanamycin). A 20 ml LB broth pre-culture with antibiotics was inoculated with a single colony and incu-

bated overnight at 37 °C with constant shaking. The non-induced overnight culture was transferred into a 1 l expression culture and incubated at 37 °C under vigorous shaking until the culture reached an optical density (OD<sub>600</sub>) of 0.6. Protein expression from large scale preparations was induced by adding 1 mM isopropyl-D-thiogalactopyranoside (IPTG). The protein expression was controlled by collecting small aliquots of the culture after IPTG induction every hour. After 4 h of growth at 37 °C, the bacteria were harvested (4,000 x g, 30 min, 4 °C), lysed in sample buffer and applied on a SDS-gel.

#### **4.2.4 Lysis of bacteria**

##### **4.2.4.1 Sonification**

(Frangioni and Neel, 1993)

The bacterial culture was centrifuged (8,000 x g, 4 °C, 10 min) and the pellet was resuspended in SDS sample buffer. The suspension was lysed using a sonicator (Branson Sonifier B15, level 6, 50% pulse, 5 x 20 s, in ice) and the debris was removed by centrifugation (10,000 x g, 4 °C, 10 min). The supernatant was subjected to SDS-PAGE.

##### **4.2.4.2 French press**

(Ausrubel, 1996)

Prior to the use of the French press, bacteria were resuspended in native lysis buffer (see 3.2). Subsequently, bacteria were compressed (Spectronic Instruments/SLM Aminco) at 10,000 psi for 5 min on ice and lysed using a pre-cooled French-Pressure-20K-chamber. After centrifugation (20,000 x g, 30 min, 4 °C), proteins were purified in soluble form under native conditions using nickel-chelate-resin (Ni-NTA beads, Qiagen, Hilden, Germany) according to the handbook 'The QIAexpressionist™' (Qiagen). However, washing buffers with an increasing imidazole gradient were chosen to modify the washing procedure slightly. Following dialysis against PBS, pH 7.3 protein solutions were concentrated using Centricon filter devices (Millipore Corp., Bedford, MA, USA) and stored at -20 °C.

#### **4.2.5 Determination of protein concentration (BCA)**

The protein concentration of cell lysates was determined using the BCA kit (Pierce, Biotechnology, Rockford, IL, USA). Solution A and B of the BCA kit were mixed in a ratio of 1:50 to get the final BCA solution. 10 µl of the samples were applied to 200 µl BCA solution in microtiter plates and incubated for 30 min at 37 °C. All experiments were performed with BSA standards with concentrations varying from 100 µg/ml to 1 mg/ml. The absorb-

ance of each sample was measured at 562 nm using an ELISA reader (Micronaut Skan Type 352, Merlin, Bornheim-Hersel, Germany).

#### **4.2.6 Preparation of phosphorylated intracellular domain of TrkB (pTrkB-ID)**

(Iwasaki *et al.*, 1997, 1998; Rong *et al.*, 2001)

Native TrkB-ID was prepared in a baculovirus expression system (a kind gift of Dr. Shini-chi Koizumi, Novartis Pharma K.K., Tsukuba Research Institute, Ibaraki, Japan) and phosphorylated at the tyrosine residues in the catalytic site as reported before by Iwasaki *et al.* (1997). The kinase activity of recombinant TrkB-ID was confirmed, the time course of autophosphorylation was analyzed and quantified by immunoblotting using anti-P-Tyr antibody and panTrk antibody showing a time-dependent increase of tyrosine phosphorylated TrkB in an autophosphorylation assay. Furthermore, the effect of ATP concentration on maximal autophosphorylation was tested. Recombinant TrkB-ID at a concentration of 1.0 µg/ml was phosphorylated by incubation for 30 min at 30 °C in a freshly prepared phosphorylation buffer (see 3.2) directly prior to its immobilization in ELISA experiments.

#### **4.2.7 ELISA (Enzyme-linked immunosorbent assay)**

Unphosphorylated or phosphorylated TrkB-ID (TrkB-ID/ pTrkB-ID) were immobilized on a polyvinylchloride surface in a 96-well microtiter plate (Maxisorb F8, Nunc, Wiesbaden, Germany) at a concentration of 1.0 µg/ml overnight at 4 °C and under constant agitation. After removal of unbound proteins by washing 5 times for 5 min at RT with TBST washing buffer (see 3.2) the wells were blocked for 1 h at 37 °C with blocking buffer. From this point on, the following steps were performed at RT under constant agitation. Potential binding proteins such as NCAM180-ID or CHL1-ID for control were diluted in TBST prior to incubation for 2 h. Unspecifically bound proteins were removed by five washing steps of 5 min with TBST. Specific primary antibodies and their respective HRP-coupled secondary antibodies were used for the detection of bound proteins. Primary antibodies were incubated for 1 h followed by five washing steps of 5 min with TBST. After an incubation of 1 h with secondary antibodies, a series of three washes of 5 min with TBST and two with TBS followed. NCAM180-ID was detected using the NCAM180 specific antibody D3 and antibodies reacting with epitopes specific for the two isoforms NCAM140 and NCAM180 (5B8 and P61). The TrkB peptide 2 (synthesized by Dr. Jochen Heukeshoven, Heinrich-Pette-Institut, Hamburg, Germany) containing the putative binding site (QHFVH)

from the page display analysis (see 3.3.2) was dissolved in 50% DMSO and also substrate-coated. After overnight coating with 250 ng/ml TrkB peptide at 4 °C under constant agitation a blocking solution was added for 1 h at RT. Further incubation steps were again performed at RT and under constant agitation. His-tagged NCAM180-ID, NCAM140-ID, CHL1-ID were added for 1 h prior to three washes for 5 min with TBST. After bound IDs were detected using anti-Penta His antibody a series of three final washes of 5 min with TBST and two with TBS followed. For visualization of protein binding in all ELISA experiments, 100 µl of freshly prepared ABTS (Sigma-Aldrich, Taufkirchen, Germany) staining solution was applied. The detection reaction of HRP was quantified by measuring the absorbance at 405 nm using an ELISA reader (Merlin).

#### 4.2.8 Epitope mapping

Using a set of synthetic NCAM peptides (synthesized by Dr. Jochen Heukeshoven, Heinrich-Pette-Institut, Hamburg, Germany), encompassing the entire intracellular domain of NCAM140, we have mapped on NCAM-ID the regions recognized by various NCAM antibodies (D3, P61 and 5B8). The synthesized peptides divide the intracellular domain of NCAM140 into three parts: an N-terminal part (NCAM peptide 1), a part in the middle of NCAM140-ID (NCAM peptide 2), and a C-terminal part (NCAM peptide 3) (see 3.3.1 and 5.2). The only difference between NCAM140-ID and NCAM180-ID is characterized by the presence of NCAM exon 18, which is specifically recognized by the NCAM180 specific antibody D3. In addition, antibodies reacting with epitopes specific for the two isoforms NCAM140 and NCAM180 (5B8 and P61) were also used for this epitope mapping. The binding specificity of the 3 NCAM140 peptides representing together the complete NCAM140-ID was tested separately with the 3 anti-NCAM antibodies in order to determine the binding site of the said antibodies (see 5.2). In brief, the NCAM peptides were dissolved in PBS and immobilized on a polyvinylchloride surface in a 96-well microtiter plate (Nunc) at 4 °C under constant agitation. After overnight incubation a blocking step followed by adding PBS, pH 7.4 containing 1% BSA for 1 h at RT. After bound NCAM140-ID peptides were detected using primary anti-NCAM antibodies (D3, P61 and 5B8) and the respective secondary antibodies, visualization of peptide binding was performed as described in the paragraph ELISA.

#### 4.2.9 Brain homogenization

Mostly brains from 2- to 3-month- old NCAM wildtype mice (NCAM<sup>+/+</sup>) and NCAM deficient mice (NCAM<sup>-/-</sup>) (Cremer *et al.*, 1994) were used for homogenization. For

experiments in which TrkB deficient mice (TrkB<sup>-/-</sup>) were needed as controls, brains of newly born TrkB wildtype mice (TrkB<sup>+/+</sup>) and TrkB deficient mice (TrkB<sup>-/-</sup>) were used since TrkB<sup>-/-</sup> mice barely survive one week (Klein *et al.* 1993). After decapitation of the mice the brains were removed from the skulls and immediately homogenized in a Dounce homogenizer (Weaton, Teflon pestle, 2 ml, 5 ml or 10 ml) on ice. In the first cross-linking experiments using TrkB peptides for coupling to the cross-linker Sulfo-SBED brain homogenate was prepared either in PBS with the protease inhibitors Complete<sup>TM</sup> or in lysis buffer 1 (see 3.2). Then the homogenate was centrifuged for 15 min at 1,000 x g and 4 °C before adding Triton X-100 at a final concentration of 1%. For later cross-linking experiments and proteolysis assays, mice brains were homogenized at 4 °C in lysis buffer inhibiting dephosphorylation (P+) or inhibiting tyrosine kinase phosphorylation (P-). The lysis condition inhibiting dephosphorylation (P+) is characterized by the presence of protein tyrosine phosphatase and protease inhibitors in the lysis buffer (Haier and Nicolson, 2000; Hyuer *et al.*, 1997). For proteolysis assays and co-immunoprecipitations (see 5.7), nuclei were removed by centrifugation for 15 min, at 600 x g and 4 °C after homogenization. After re-centrifugation of the supernatant for 45 min at 25,000 x g and 4 °C, the membrane pellet was resuspended in RPMI medium (for proteolysis assays) or in P+ lysis buffer (for co-immunoprecipitations). For detection of the interaction between full-length TrkB and NCAM180-ID using the cross-linking approach (see 5.6) and co-immunoprecipitations (see 5.7), the P+ lysis buffer additionally contained 20 µM of the matrix metalloprotease inhibitor GM 6001 and 1 µM of the γ-secretase inhibitor DAPT (Calbiochem, La Jolla, California, USA). The other lysis buffer (P-) inhibiting Trk phosphorylation contained the specific Trk inhibitor K252a (Calbiochem) (Tapley *et al.*, 1992).

#### **4.2.10 Isolation of brain subfractions enriched with synaptosomes, synaptosomes from mossy fibers, myelin and nuclei**

(Huttner *et al.*, 1983; Kleene *et al.*, 2001)

For subcellular fractionation and enrichment of synaptosomal compartments, synaptosomes of mossy fibers, myelin, nuclear or mitochondrial fractions of at least 10 adult C57BL/6J mice were sacrificed to collect their brains. The mice brains were removed from the skull and were transferred into an ice-cold homogenization buffer. From this point on, the material was kept at 4 °C. Each brain was individually homogenized with 12 strokes in a Dounce homogenizer (Weaton, Teflon pestle, 10 ml) in 3 ml homogenization buffer containing 0.32 M sucrose without detergent or protease.

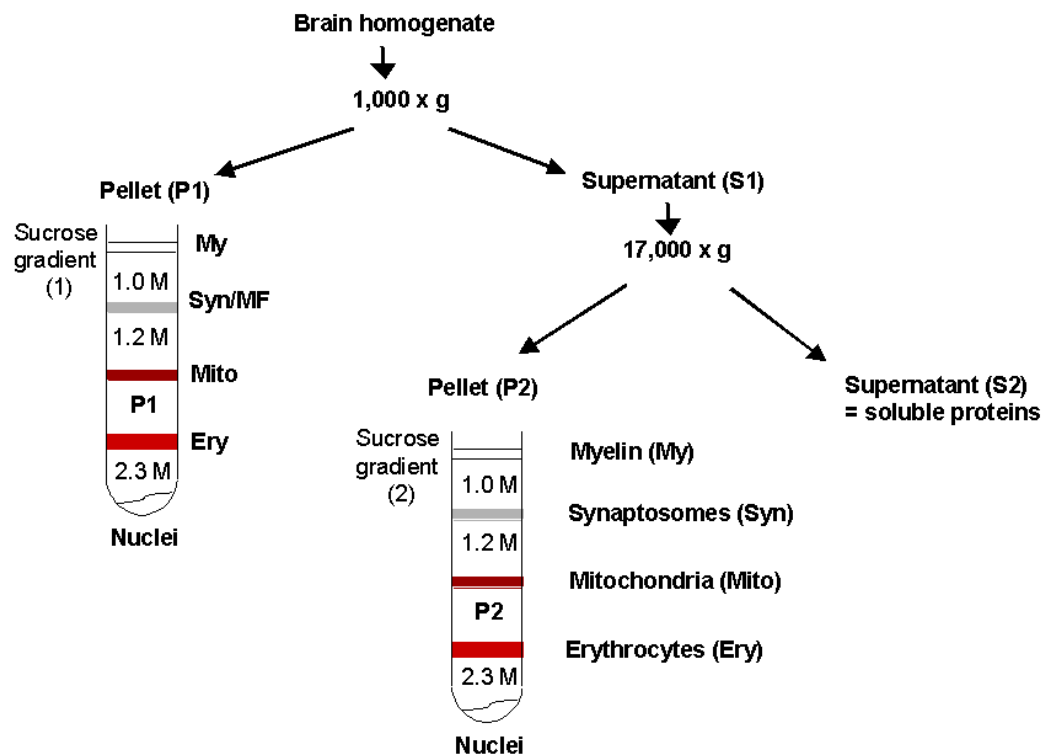


**Figure 6. Isolation of brain subfractions enriched with synaptosomes, synaptosomes from mossy fibers, myelin, mitochondria and nuclei using a discontinuous sucrose gradient.**

To gain the particular synaptosomal fraction from the mossy fibers (Syn/MF) a resuspended '1,000 x g pellet' (P1) was applied on a sucrose gradient (1). After centrifugation of the supernatant a '17,000 x g pellet' (P2) was applied on another sucrose gradient (2) in order to harvest the regular synaptosomal fraction (Syn). An ultracentrifugation step of the sucrose gradients followed for 2 h at  $100,000 \times g$  and  $4^\circ\text{C}$ . Both subfractions (Syn/MF and Syn) were collected at the 1.0/1.2 M interfaces. The nuclei remained as pellet at the bottom of both gradients and were pooled.

The homogenate was centrifuged for 10 min at  $1,000 \times g$  and  $4^\circ\text{C}$ . The resulting supernatant was centrifuged at  $17,000 \times g$  for 15 min. The pellet of the  $17,000 \times g$  centrifugation step (P2) was resuspended in a homogenization buffer and was homogenized 1:2 with 2.27 M sucrose buffered solution for isolation of myelin, synaptosomes, mitochondria, erythrocytes and nuclei (sucrose gradient (2) is depicted in Fig.6). However, the isolation of synaptosomes from mossy fibers required the pellet of the  $1,000 \times g$  centrifugation step (P1) (sucrose gradient (1) is depicted in Fig.6). Both resuspended pellets (P1 and P2) were applied to discontinuous sucrose gradients. Fig.6 shows the 4 different layers of a discontinuous sucrose gradient (from top to bottom) consisting of 1.0 M, 1.2 M, 1.6 M (with P1 or P2), and 2.3 M buffered sucrose. The interface between the 2.3 M sucrose solution and the resuspended pellet (P1/P2) was disturbed by inserting a glass pasteur pipette into the interface several times. After ultracentrifugation for 2 h at  $100,000 \times g$ , the turbid material that

contained the isolated organelles from the different interfaces was collected, diluted 1:2 with the homogenization buffer, and pelleted by centrifugation for 30 min at 100,000 x g. The pellet of the nuclear fraction was resuspended in Roeder C solution, whereas the other pellets of the subfractions were resuspended in Tris plus buffer.

#### 4.2.11 Preparation of a nuclear extract

Several sucrose step gradients were performed in order to get a sufficient amount of subfractions enriched with nuclei (see 4.2.10) of brains from 10-20 adult wild-type NCAM<sup>(+/+)</sup> and NCAM<sup>(-/-)</sup> mice. The subfractions that contained enriched nuclei were resuspended in Roeder C solution and were homogenized with 12 strokes in a glass Dounce homogenizer. After extraction for 30 min at 4 °C a centrifugation step followed for 30 min at 200,000 x g and 4 °C. The resulting supernatant consisting of the nuclear extract was employed for immunoprecipitations (see 5.13).

#### 4.2.12 Biochemical cross-linking with Sulfo-SBED

(Das and Fox, 1979; Santhoshkumar and Sharma, 2002; Hurst *et al.*, 2004)

The trifunctional cross-linker sulfo-SBED (Perbio Science, Bonn, Germany) containing a biotin moiety, a Sulfo-NHS active ester and a photoactive aryl azid was either coupled to TrkB peptides (see 3.3.2) or to recombinant proteins of interest such as the IDs of NCAM. Since the cross-linker was light-sensitive the procedure was performed in darkness until after photoactivation by using UV light. Sulfo-SBED was separately dissolved in 100% DMSO at a concentration of 0.03-0.04 mg/μl before adding dissolved TrkB peptides (1 mg in 0.5 ml 0.1 M PBS, pH 7.2) or recombinant IDs (200 μg ID dissolved in 1 x PBS) to 5 μl dissolved Sulfo-SBED in each sample. The reaction mixture was incubated for 1 h at RT. Unbound cross-linker was removed by using a polyacrylamid column PD-10 (Amersham Pharmacia Biotech, Uppsala, Sweden) equilibrated with PBS (4.2.12). After application of PBS to the column, 0.5 ml eluted fractions were collected and protein-containing fractions were pooled and concentrated to the original volume using Centricon tubes (Millipore GmbH, Schwalbach, Germany). Alternatively, overnight microdialysis in PBS (see 4.2.13) was chosen to abolish the non-reacted Sulfo-SBED as recommended in the manufacturer's sample protocol. Then the potential binding proteins within either brain homogenate, Triton-soluble brain lysate (1%), synaptosomal subfraction or specifically prepared brain lysate (4.2.9) were added for conjugation to the peptide-cross-linker-complex (4.2.12) or protein-cross-linker-complex (4.2.13). Photoactivation for 15 min un-

der UV (365 nm) resulted in the biotin labels being transferred to the interacting protein. To isolate the potential interacting proteins, the conjugated complexes were incubated with magnetic streptavidin DYNA-beads (DynaL Diagnostics, Hamburg, Germany) (30  $\mu$ l beads/ sample) for 1 h at 4 °C on a rotating wheel. Afterwards, the Eppendorf tubes containing the sample-beads-suspension were placed into the magnetic tube holder to collect magnetic DYNA-beads on one side of the tubes. The supernatant was carefully removed without disturbing the bead clot. This procedure was followed by three washing steps using PBS. The disulfide bond within the active ester of sulfo-SBED can be photolytically cleaved under reducing conditions of the sample buffer resulting in a biotin label attached to the binding proteins. These potential binding partners attached to the TrkB peptides (see 4.2.12) or to NCAM-ID (4.2.13) were isolated and separated by SDS-PAGE under reducing conditions resulting in a transfer of the biotin group to the potential binding partner(s). Immunoblot analysis was performed using Streptavidin-HRP for detection of biotin labeled proteins. For detection of the hypothesized binding proteins such as NCAM and TrkB the following antibodies were used: the NCAM180 specific D3 antibody and the anti-NCAM 1B2 antibody recognizing all NCAM isoforms (4.2.12) and the TrkB specific antibody and panTrk antibody recognizing all Trk family members (4.2.13).

#### **4.2.13 Biochemical cross-linking using TrkB peptides for coupling**

Synthesized TrkB peptides were (kindly synthesized by Dr. Jochen Heukeshoven, Heinrich-Pette-Institut, Hamburg, Germany and by Dr. Christian Schafer, Copenhagen, Denmark) employed in the first cross-linking experiments (see 5.4). Brain homogenate, Triton-soluble brain lysate (1%) (4.2.9) or isolated synaptosomal subfraction (4.2.10) from 2- to 3-month-old C57BL/6J mice was added so that the potential binding partners within this prepared brain material bind to the eluted fractions containing the TrkB peptide–cross-linker–complex. The samples were incubated for 30 min at RT before photoactivation (in contrast to 4.2.13).

#### **4.2.14 Biochemical cross-linking using NCAM-ID for coupling**

Recombinant intracellular domains of NCAM180 (NCAM180-ID), NCAM140 (NCAM140-ID), and CHL1 (CHL1-ID) for controls were utilized for coupling to the cross-linker sulfo-SBED (Perbio Science). In the first series of cross-linking experiments brain homogenate was prepared under P+ and P– lysis buffer (see 4.2.9) before adding to the IDs and incubated for 30 min at RT.

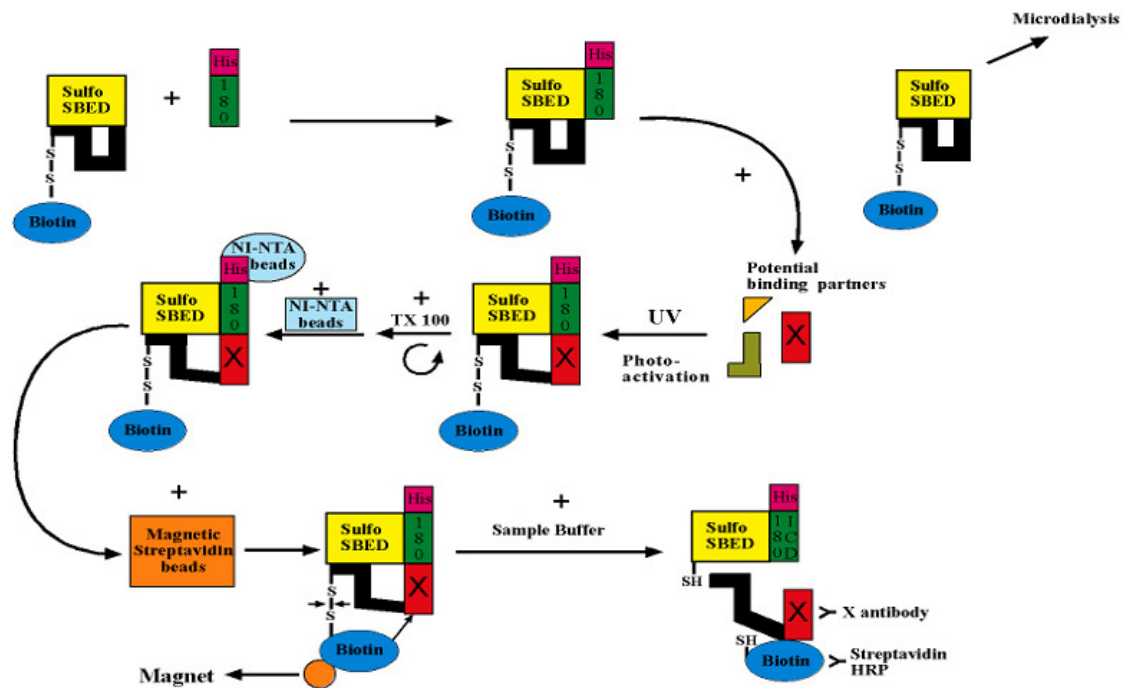


**Figure 7. Principle of optimized cross linking protocol using Sulfo-SBED.**

The trifunctional cross-linker sulfo-SBED containing a biotin moiety, a Sulfo-NHS active ester and a photoactive aryl azid was coupled to the His-tagged intracellular domains of NCAM180 (indicated in green for NCAM180-ID and purple for the respective His-tag) or CHL1 for control. Isolated brain membranes containing potential binding partners to NCAM180-ID (180) were incubated at 37 °C for 2 h before adding complexes of cross-linker and intracellular domain. After cross-linking under UV light, Triton X-100 (TX100) was added to the samples followed by a brief centrifugation to remove nuclei. Subsequently, two purification steps were performed: First, using Ni-NTA beads and then, using magnetic streptavidin beads. The potential binding partner(s) conjugated to the intracellular domains were isolated and separated by SDS-PAGE under reducing conditions resulting in a transfer of the biotin group to the potential binding partner(s). Immunoblot analysis was performed using a specific antibody (depicted as X antibody) for detection of the potential binding protein and Streptavidin-HRP for detection of the biotin labels transferred to these binding proteins.

According to a subsequent and optimised cross-linking protocol (Fig.7) brain membranes were not only isolated under P+ lysis conditions but also in the presence of 1  $\mu$ M the  $\gamma$ -secretase inhibitor DAPT and 20  $\mu$ M matrix metalloprotease inhibitor GM 6001 (Calbiochem, La Jolla, California, USA) followed by centrifugation for 45 min at 25,000 x g and 4 °C. The pellet was resuspended in RPMI medium (PAA Laboratories, Pasching, Austria) containing additionally the following inhibitors: DAPT, GM 6001, Complete<sup>TM</sup> EDTA-free. The isolated membranes containing the potential binding partners (Fig.7, one potential binding partner is indicated as a red rectangle) were incubated for 2 h at 37 °C before adding the complexes of coupled cross-linker-ID. After photoactivation under UV Triton X-100 was added to the samples at a final concentration of 1%. After 45 min incubation on ice membranes were centrifuged for 5 min at 200 x g and 4 °C for removal of

nuclei. Subsequently, two purification steps were performed for 1 h at 4 °C on a rotating wheel: First, Ni-NTA beads (350 µl beads/ sample) (Qiagen) were used for isolation of all complexes carrying the ID with the His-tag and then magnetic streptavidin DYNA-beads (DynaL Diagnostics) were applied as described before (see 4.2.12) in order to isolate the potential binding proteins with the attached biotin label.

## **4.2.15 Immunoprecipitation**

### **4.2.15.1 Coupling of antibodies to Protein A/G Sepharose beads**

(Schnegelsberg, 2001)

To couple covalently monoclonal anti-NCAM H28 antibody to Protein A/G Sepharose beads 200 µg of the antibody was incubated with 400 µl beads overnight at 4 °C followed by 3 washing steps with 200 mM sodium tetraborate, pH 9.0. All incubation steps were performed under constant agitation on a rotating wheel. Coupling solution was added to the bead-antibody-mixture and incubated for 3 h at RT. The reaction was stopped by 2 washing steps and an incubation of 2 h with 0.2 M ethanolamin, pH 8.0. Finally, the coupled antibodies were washed twice with PBS and were stored in PBS containing 0.02% NaN<sub>3</sub> at an H28 antibody concentration of 1 µg/ µl at 4 °C for up to 2 weeks.

### **4.2.15.2 Co-immunoprecipitation after covalent coupling of anti-NCAM H28 antibody to Protein A/G Sepharose beads**

25-50 µl of coupled beads were added to either brain lysate, cerebella lysate or homogenate with varying detergent conc. (0.2%, 0.5% or 1%) and were diluted in RIPA buffer up to a total volumen of 1 ml. After 1-2 h incubation under constant agitation at 4 °C the samples were briefly centrifuged for 1 min at 14,000 rpm. The remaining pellet was washed twice with ice-cooled washing buffer 1 and 3 times with washing buffer 2. Beads were extracted with 5 x SDS-PAGE sample buffer. After boiling at 95 °C for 5 min samples were separated by SDS-PAGE and subsequent immunoblotting.

### **4.2.15.3 Co-immunoprecipitation without antibody coupling using Protein A/G agarose beads**

For immunoprecipitations using either an NCAM180 specific D3 antibody or a panTrk antibody for precipitation, brain lysate was prepared according to the optimized cross-linking protocol (see 4.2.9 and 4.2.13). After 2 h of incubation at 37 °C, brain membranes were pre-cleared by incubation with Protein A/G agarose Plus (Santa Cruz Biotechnology). Tri-

ton X-100 was added to the pre-cleared supernatant at a final concentration of 0.5%. A panTrk antibody or an NCAM180 specific D3 antibody was applied for precipitation and samples were incubated for 3 h on a rotating wheel at 4 °C. Prewashed Protein A/G agarose beads were added and incubated overnight at 4 °C under constant agitation. Beads were then washed once with a washing buffer 3 (3.2) and three times with PBS. Proteins were eluted from the beads with 2 x SDS-PAGE sample buffer. After boiling at 95 °C for 5 min, samples were separated by SDS-PAGE and subjected to immunoblotting (4.2.2). The primary antibodies were either an NCAM180 specific D3 antibody or a panTrk antibody which were incubated overnight at 4 °C followed by incubation of the secondary HRP-conjugated goat anti-mouse or anti-rabbit antibodies for 1 h at RT.

#### **4.2.15.4 Immunoprecipitation using an ubiquitin antibody and brain lysate**

For immunoprecipitations using an ubiquitin antibody for precipitation, the above immunoprecipitation protocol (see 4.2.15.3) was followed, except that before immunoprecipitation the brain lysate was incubated in the absence or the presence of the following proteasome inhibitors ALL, MG262 and MG132 at a concentration of 50 µM for 2 h at 37 °C.

#### **4.2.15.5 Immunoprecipitation using NCAM180 specific D3 antibody and nuclear brain extract**

Prior to the immunoprecipitations the nuclear brain extract was incubated with sodium dodecyl sulfate (SDS) at a final concentration of 1% for 5 min at 95 °C. Afterwards, the nuclear extract was diluted in freshly prepared P+ lysis buffer followed by the incubation with the NCAM180 specific D3 antibody for 3 h on a rotating wheel at 4 °C, the above immunoprecipitation protocol (see 4.2.15.3) was followed. After SDS-PAGE immunoblot analysis was performed the NCAM180 specific D3 antibody was used for detection of intracellular NCAM fragments in the nuclear extract.

#### **4.2.16 Proteolysis assay using isolated brain membranes**

(modified according to Probstmeier *et al.*, 1989)

Brain membranes of adult C57BL/6J mice brains were isolated under either P+ or P- lysis conditions as described before (see 4.2.9). Various proteasome inhibitors such as ALLN, MG262 (kind gift from Dr. Ingolf Bach, ZMNH, Hamburg, Germany) and MG132 (Calbiochem) were added to the resuspended membranes and incubated for 2 h at 37 °C. For control, one sample was kept at 4 °C and another at 37 °C without inhibitors. After incubation, the samples were separated into supernatant and membrane fraction by centrifugation

for 1 h, at 100,000 x g and 4 °C. The supernatants were subjected to acetone precipitation by incubating 1 volume of the sample with 7 volumes of ice-cold acetone overnight at -20 °C. After centrifugation for 30 min, at 4,100 x g and 4 °C the pellets were dried for 15 min at RT and resuspended in a 2 x sample buffer. After an incubation time of 20 min the samples were finally boiled at 95 °C for 15 min. Proteins from the supernatants and the membrane fractions (pellets) were subjected to immunoblot analysis using the NCAM specific antibody and panTrk antibody.

## 4.3 Cell culture

### 4.3.1 LMTK-/LMTK-PST cell culture

The original LMTK cells were adherent mouse fibroblasts (ATCC, LGC Promchem, Wessel, Germany) which were stably transfected into polysialyltransferases expressing fibroblast cells (LMTK-PST) (pFlagHa-ST8SiaIV, full length, N-terminally, FlagHa-tagged PST) by Martina Muehlenhoff (a kind gift of Martina Muehlenhoff and Dr. Rita Gerardy-Schahn, Medizinische Hochschule Hannover, Hannover, Germany). PST (ST8Sia IV) and STX (ST8Sia II) are the two polysialyltransferases responsible for NCAM polysialylation (Close and Colley, 1998). LMTK-/LMTK-PST cells were cultured in DMEM with 10% FCS (fetal calf serum) and 2% Penicillin/Streptomycin (P/S) 37 °C, 5% CO<sub>2</sub> and 90% relative humidity in 75 cm<sup>2</sup> flasks (Nunc) with 15 ml medium or in six-well plates (d = 35 mm; area = 9,69 cm<sup>2</sup>) with 2 ml medium. After 2-3 days when cells had reached approximately 95% confluency, they were passaged. Therefore, medium was removed and cells were detached by incubation with 2 ml versene for 5 min at 37 °C. The cells were centrifuged (200 x g, 5 min, RT) and the pellet was resuspended in 10 ml new medium. The cells were split 1:10 for maintenance or seeded in six-well plates for transfection (1 ml per well). For immunocytochemical experiments coverslips (d=14 mm) were coated with poly-L-lysine to seed the cells on. First, the coverslips were cleaned by vigorous shaking with acetone and then dried for 2 h at 160 °C. Afterwards, coverslips were cooled down before adding the sterile filtered coating solution poly-L-lysine (50 µg/ml in PBS). Coating of the coverslips was performed by constant agitation at 4 °C overnight. Finally, the coverslips were gently washed three times with ddH<sub>2</sub>O and dried under a sterile hood. At last an incubation of 30 min under UV light followed. The cells were seeded with a density of 30% confluency 24 h before use.

### 4.3.2 Transfection of CHO cells, N2a cells and LM-TK cells

(Lipofectamine Plus manual, Life technologies; Shih *et al.*, 1997)

The Lipofectamine Plus kit (Life Technologies) was chosen for transient transfection of LM-TK-/LM-TK-PST cells, CHO cells and N2a cells (Hawley-Nelson *et al.*, 1993). One day before transfection,  $2 \times 10^5$  cells were seeded per 35 mm dish. Equal amounts of DNA were used for double transfection. When the cells had grown to 80-90% confluency (usually after 18-24 h), they were washed with HBSS and the medium was exchanged against DMEM without FCS and any antibiotics. The cells were transfected with 2  $\mu$ g total DNA per 35 mm well. 6  $\mu$ l Plus reagent and 4  $\mu$ l Lipofectamine were used in each transfection assay as described in the manufacturer's transfection protocol. After 4 h the transfection was stopped by adding 1 ml DMEM containing 10% FCS and 2% P/S and cells were incubated for 24 h. To detach the cells, 500  $\mu$ l versene were added per well. The suspension was split either 1:2 for biochemical analysis or 1:6 for immunocytochemistry to seed on coverslips.

### 4.3.3 Primary hippocampal cell culture

(Lochter *et al.*, 1991; Brewer *et al.*, 1993)

For preparation of the dissociated hippocampal cultures, several mice of postnatal day 1-3 were used. Hippocampal preparation was performed by Galina Dityateva (ZMNH, Hamburg, Germany) as described in the above-said literature. First, the mice were decapitated, their brains removed from the skulls and cut along the midline. The dissected hippocampi were split into 1 mm thick pieces. Second, the hippocampi were washed twice with dissection solution and digested with trypsin and DNaseI for 5 min at RT. After removal of the digestion solution, hippocampi were again washed twice and the reaction was stopped by adding trypsin inhibitor afterwards. Third, hippocampi were resolved in dissection solution containing DNaseI. Various glass pasteur pipettes with successively smaller diameters were used to dissociate hippocampal cells by trituration to a homogeneous suspension. The last step of the procedure was the removal of cell debris and the plating of the cells. The hippocampal suspension was centrifuged (80 x g, 15 min, 4 °C) and the pellet resuspended in dissection buffer. Cells were counted in a Neubauer cell chamber and plated to provide a density of 1,000 cells/mm<sup>2</sup>.

#### 4.3.4 Primary cerebellar cell culture

(Lochter *et al.*, 1991; Müller-Husmann *et al.*, 1993)

C57BL/6J mice of postnatal day 6-8 were decapitated to prepare dissociated cerebellar granule cells for culture. The skull was cut along the midline and the cerebella were dissected from the brains. The cerebella were transferred to ice-cold Hanks' balanced salt solution (HBSS) (PAA Laboratories, Cölbe, Germany) in order to clean them from meninges, choroid plexus, and blood vessels. After cutting the cerebella into several big pieces cell separation followed. First, the cerebella were washed with ice-cold HBSS. Second, the cerebella were digested with trypsin/DNaseI solution for 15 min at RT. After removal of the trypsin/DNaseI solution, Cerebella were again washed three times with ice cooled HBSS. Third, the cerebella were dissociated in DNaseI solution using glass pasteur pipettes with successively smaller diameters. The suspension was centrifuged for 15 min, at 100 x g and 4 °C and the pellet resuspended in dissection buffer. As a last step the cells were counted in a Neubauer cell chamber. The cell suspension ( $1$  or  $2 \times 10^5$  cells/ml) was distributed to a 12-well plate (Nunc, Roskilde, Denmark). Each well contained one glass cover slip (15 mm in diameter; Hecht, Sondheim, Germany) substrate-coated with poly-L-lysine (PLL) (Sigma-Aldrich, Taufkirchen, Germany), which was covered with 1 ml of cell suspension and cultured in chemically defined serum-free medium. As positive control, laminin (Sigma-Aldrich; 2 µg/ml) was coated in addition to PLL while as negative control only PLL was given as substrate for neurite outgrowth. For investigation of NCAM-induced neurite outgrowth, PLL-coated coverslips were additionally coated with 10 µg/ml native mouse NCAM (kindly provided by Achim Dahlmann, ZMNH, Hamburg, Germany), which was immunoaffinity-purified from adult mouse brain (Rathjen and Schachner, 1984). Two hours after seeding cells were stimulated for 30 min with 50 ng/ml BDNF (50 µM stock solution dissolved in ddH<sub>2</sub>O) (Sigma-Aldrich, St Louis, MO, USA) (Lee and Chao, 2001; Kong *et al.*, 2001; Snider, 1994) followed by inhibitor treatment. The proteasome inhibitor MG132 was added for 1 h at a concentration of 100 ng/ml (Calbiochem) and the matrix metalloprotease inhibitor GM 6001 was applied for 1 h at a concentration of 1 µM and 10 µM (1 mM stock solution dissolved in DMSO) after BDNF stimulation. The cells were allowed to grow for 24 h at 37 °C and 5% CO<sub>2</sub>. After this time period, cells were fixed with 25% glutaraldehyde in PBS, pH 7.3 for at least 30 min and stained with 1% toluidine blue and 1% methylene blue in 1% borax (pH 7.4) for 1 h at RT. After three final washes with H<sub>2</sub>O and the cells were dried at RT. They were imaged with a Kontron microscope (Zeiss, Jena, Germany) and analysed with Carl Zeiss Vi-

sion KS 400 V2.2 software. For each experimental value, the length of total neurites per cell was measured. In each experiment at least 50 cells with neurites longer than the cell body diameter were separately measured on two coverslips. Analysis only included cells that were not in contact with other cells.

### 4.3.5 Cerebellar microexplant culture

(Fischer *et al.*, 1986)

Cerebella were taken from 6- to 8-day-old C57BL/6J mice and transferred to ice-cold HBSS (PAA Laboratories). Meninges, choroid plexus, and blood vessels were removed. The cerebellar tissue was forced through a Nitrex net with a pore width of 300  $\mu\text{m}$ . The small cerebellar pieces were washed twice with Hanks' balanced salt solution, followed by a washing step with cerebellar microexplant culture medium (see 3.6.) (Sigma-Aldrich, Steinheim, Germany) (Bix and Clark, 1998). The tissue pieces were collected by sedimentation and 30-40 pieces were first only plated onto PLL-coated glass coverslips (15 mm diameter) for negative control. Secondly, PLL-coated coverslips were additionally coated with 2  $\mu\text{g/ml}$  laminin (Sigma-Aldrich) for positive control and thirdly additionally coated with 10  $\mu\text{g/ml}$  mouse NCAM that was immunoaffinity-purified from adult mouse brain (Rathjen and Schachner, 1984) in  $\sim 150 \mu\text{l}$  of culture medium/coverslip. Native mouse NCAM was obtained from Achim Dahlmann (ZMNH, Hamburg, Germany). Just before plating, the coating solution was removed, and the coverslips were rinsed once with HBSS. To guarantee adhesion microexplants were incubated for 16 h. Afterwards, 1 ml of culture medium lacking fetal calf serum was added to the explants. Cells were stimulated for 30 min with 50 ng/ml BDNF (50  $\mu\text{M}$  stock solution dissolved in ddH<sub>2</sub>O) (Sigma-Aldrich) (Lee and Chao, 2001; Kong *et al.* 2001). Endoneuraminidase N that specifically degrades  $\alpha$ -2,8-polysialic acid attached to NCAM (kindly provided by Dr. Rita Gerardy-Schahn, Medizinische Hochschule Hannover, Hannover, Germany) was applied at 85 ng/ml (85  $\mu\text{g/ml}$  stock solution dissolved in PBS). After further maintenance for 24 h, the explants were fixed with 2% glutaraldehyde and 2% paraformaldehyde in PBS. Then explants were stained with 1% toluidine blue and 1% methylene blue in 1% borax, pH 7.4. Microexplants were only analyzed if they had had no contact to other microexplants. Neurite outgrowth was analyzed and quantified by measuring the lengths of the 10 longest neurites of 15 explants in each experiment with an IBAS Image analysis system (Kontron, Zeiss, Jena, Germany).

## 4.4 Immunocytochemistry

### 4.4.1 Immunocytochemistry of living cells

Twenty-four hours after transfection, LM-TK cells were seeded on 6-well dishes with a confluency of ~ 30% so that they reach a density of about 60% the next day. Then, they were washed once with 1 ml of serum free DMEM and then incubated with 1 ml of serum free media for either for 6 h or overnight in the CO<sub>2</sub>-incubator. Coverslips with the attached cells were rinsed with DMEM without FCS and placed in a humid chamber covered with Parafilm. 150 µl of pre-warmed DMEM without FCS containing the primary antibody in the appropriate dilution were added on the coverslips followed by incubation for 15 min at 37 °C in the CO<sub>2</sub>-incubator. Afterwards, coverslips were put into 12-well dishes and washed three times with DMEM without FCS. After putting the coverslips again in a humid chamber covered with Parafilm, the coverslips were covered with 100 µl DMEM without FCS containing the fluorescent dye-coupled secondary antibody in a 1:200 dilution. This was followed by incubation for 15 min at 37 °C in the dark. After rinsing three times with DMEM without FCS, the coverslips were fixed and mounted with Aqua Poly-Mount medium (Polysciences Inc., Warrington, PA, USA) on glass slides.

### 4.4.2 Immunocytochemistry of fixed cells

To investigate whether TrkB and NCAM were closely located within the cell membrane, immunocytochemistry of fixed LM-TK cells co-transfected with NCAM and TrkB and hippocampal neurons was performed. The incubation was carried out in a humid chamber covered with Parafilm. Blocking was performed using 150 µl PBS containing 3% BSA and 0.02% Triton X-100 for 30 min at RT. After removal of the blocking buffer, the coverslips were covered with 150 µl antibody solution containing the appropriate primary antibody and incubated for 1 h at 4 °C (for hippocampal neurons overnight). The bound primary antibody was detected with secondary antibodies labeled with fluorescent dye Cy3 (later Cy5). The medium was removed from the coverslips and they were washed three times with PBS. The cells were fixed with 1 ml 4% ice-cold paraformaldehyde in PBS for 15 min at RT. After two rinses with PBS the coverslips were incubated with 150 µl second primary antibody solution for 1 h at RT in darkness. After having been washed three times with PBS, the coverslips were incubated with 150 µl antibody solution containing the fluorescent dye-labeled secondary antibody (Cy5) for 1 h at RT in darkness. Finally, the cells were washed three times with PBS, fixed and mounted on glass slides with Aqua Polymount (Polysciences Inc.). Glass slides were stored in darkness at 4 °C.

#### **4.4.3 Confocal laser-scanning microscopy**

All images of LM-TK cells and hippocampal neurons were obtained with a Zeiss LSM510 argon-crypton confocal laser-scanning microscope equipped with a 60 x oil-immersion objective lens. Images were scanned with a resolution of 512 x 512. The detector gain and the pinhole were adjusted to give an optimal signal to noise ratio.

#### **4.5 Computer-based sequence analysis**

Computer-based sequence analysis and alignments of DNA sequences and protein sequences was performed using the Lasergene-programe (DNASTAR, Inc., [www.dnastar.com](http://www.dnastar.com)). For the search of SUMOlation sites the SUMOplot<sup>TM</sup> Prediction was chosen (ABGENT, San Diego, CA, USA, [www.abgent.com](http://www.abgent.com)). The following databases were used: Medline-, BLASTN- and BLASTP Server of NCBI (National Center for Biotechnology Information, [www.ncbi.nlm.nih.gov](http://www.ncbi.nlm.nih.gov)).

## 5 Results

### 5.1 Phage display analysis revealed a TrkB peptide showing selective binding towards NCAM180-ID

To find specific binding partners for the ID of the 180-kDa isoform of NCAM (NCAM180-ID), a commercial phage display peptide library (New England Biolabs) was screened for selectivity towards the target NCAM180-ID (kindly performed by Dr. Jens Lütjohann and Dr. Jens Franke (ZMNH, Hamburg, Germany)). The library consists of inserts of random 12-mer peptides fused to the minor N terminus of the M13 phage VIII major coat protein.

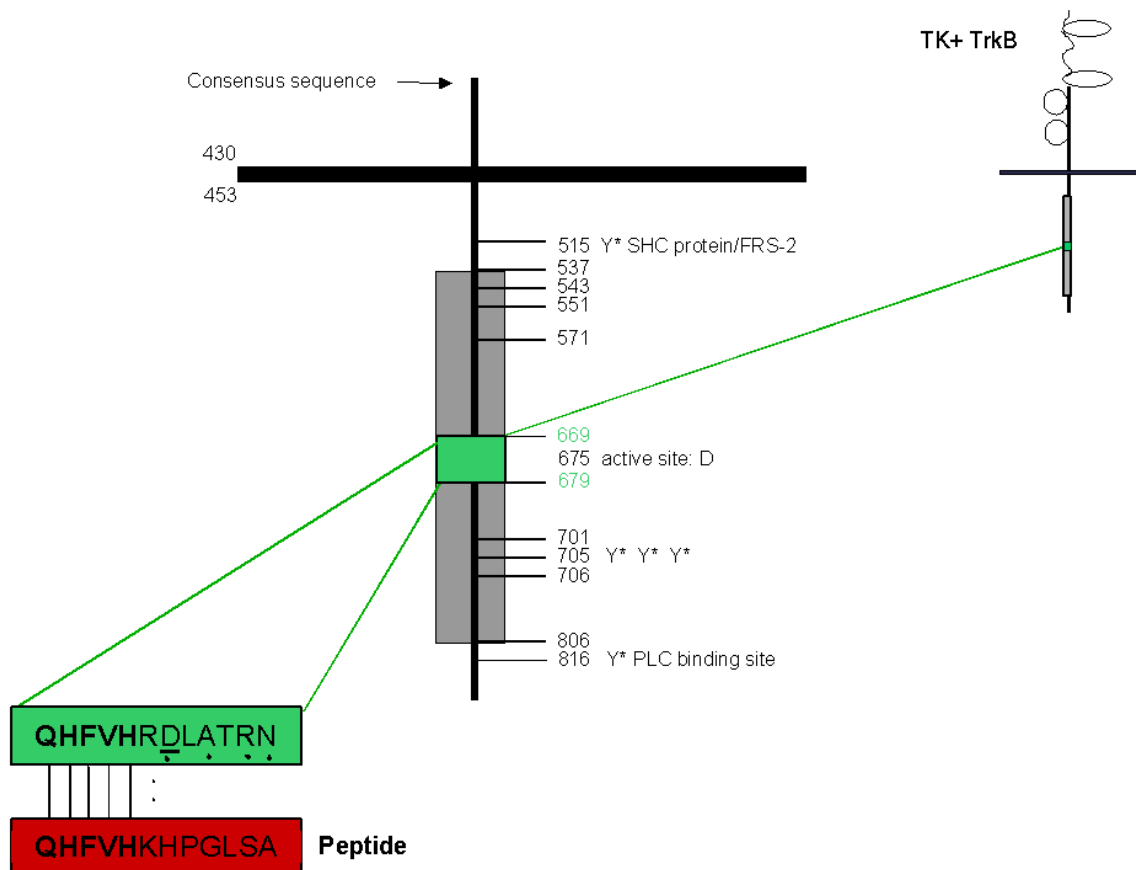


**Figure 8. Schematic representation of the ID of mouse TrkB (TrkB ID).**

The sequence of the peptide (highlighted box in red) discovered by phage display analysis using NCAM180-ID as bait shows significant similarity to a sequence in TrkB-ID (highlighted box in green). This sequence is located in the tyrosine kinase domain, contains the active site aspartate (D) and is flanked by the potential tyrosine autophosphorylation sites (Y\*). The sequence contains five identical amino acids (I), one highly conserved amino acid (:), and four weakly conserved amino acids (.).

Each phage displays one 12-mer peptide on the surface (Hong and Boulanger, 1995). One clone with excellent selectivity in binding to NCAM180-ID was selected, sequenced and characterized. The criterion for selection was a highly selective interaction between the phage and the target NCAM180-ID but no significant binding to the CHL1-ID control; additionally, no unspecific binding to the BSA control was shown by phage ELISA. By means of sequence alignment, the sequence of the displayed peptide of this selected phage (Fig. 8, highlighted box in red) showed similarity to a peptide sequence in TrkB-ID (Fig. 8, highlighted box in green). This peptide sequence within TrkB-ID is located in the tyrosine kinase domain, contains the active site aspartate (Fig. 8; underlined D) and is flanked by the autophosphorylated tyrosine residues (Fig. 8; Y\*). It contains five identical amino acids (QHFVH), one highly conserved amino acid (R) and four weakly conserved amino acids (D, A, R, N). This TrkB peptide identified by phage display analysis was used for future binding studies and biochemical experiments.

## 5.2 Epitope mapping

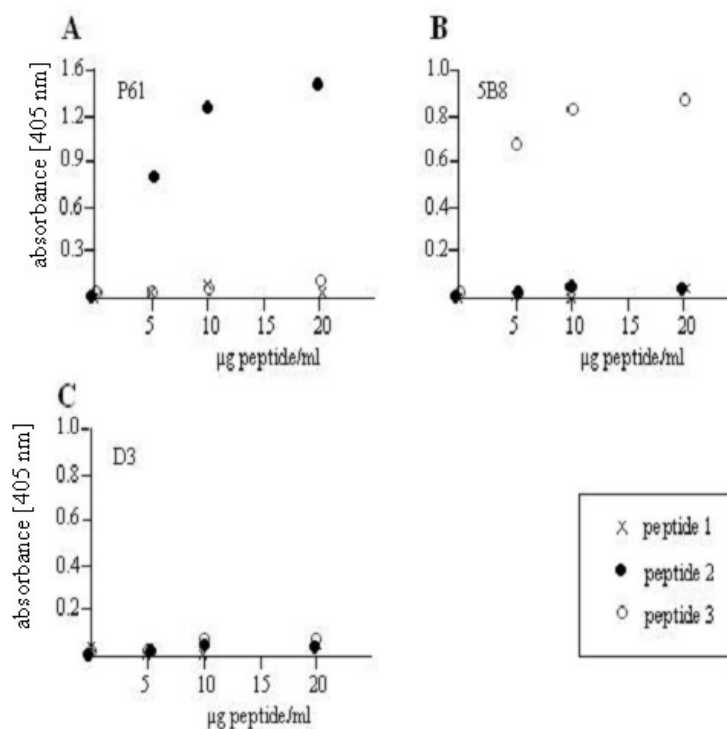


**Figure 9. Epitope mapping.**

Binding of various NCAM antibodies to NCAM peptides representing NCAM140-ID was tested by using an ELISA approach. All NCAM peptides were substrate-coated and incubated with the anti-NCAM antibodies P61, 5B8 and D3. The antibody P61 (A) only showed binding with the N-terminally located peptide 2 within NCAM140-ID, whereas the antibody 5B8 (B) specifically recognized the C-terminally located peptide 3. The NCAM180/exon 18-specific antibody D3 did not bind to any of the peptides (C).

After the identification of a peptide within TrkB-ID that binds to NCAM180-ID, the next step was to find the exact binding site within NCAM180-ID that binds to the discovered TrkB peptide (see 5.1). For this purpose, a set of synthetic peptides (kindly synthesized by Dr. Jochen Heukeshoven, Heinrich-Pette-Institut, Hamburg, Germany) encompassing the entire ID of NCAM140 was mapped with various NCAM antibodies specific to NCAM-ID (Figs. 9 and 10). The only difference between the IDs of NCAM140 and NCAM180 is the presence of an additional 261-amino acid insert in NCAM180-ID, encoded by NCAM exon 18. Three synthesized peptides (1–3) were used for epitope mapping of different NCAM antibodies (D3, P61 and 5B8) (Fig. 10) and subsequently for binding studies.

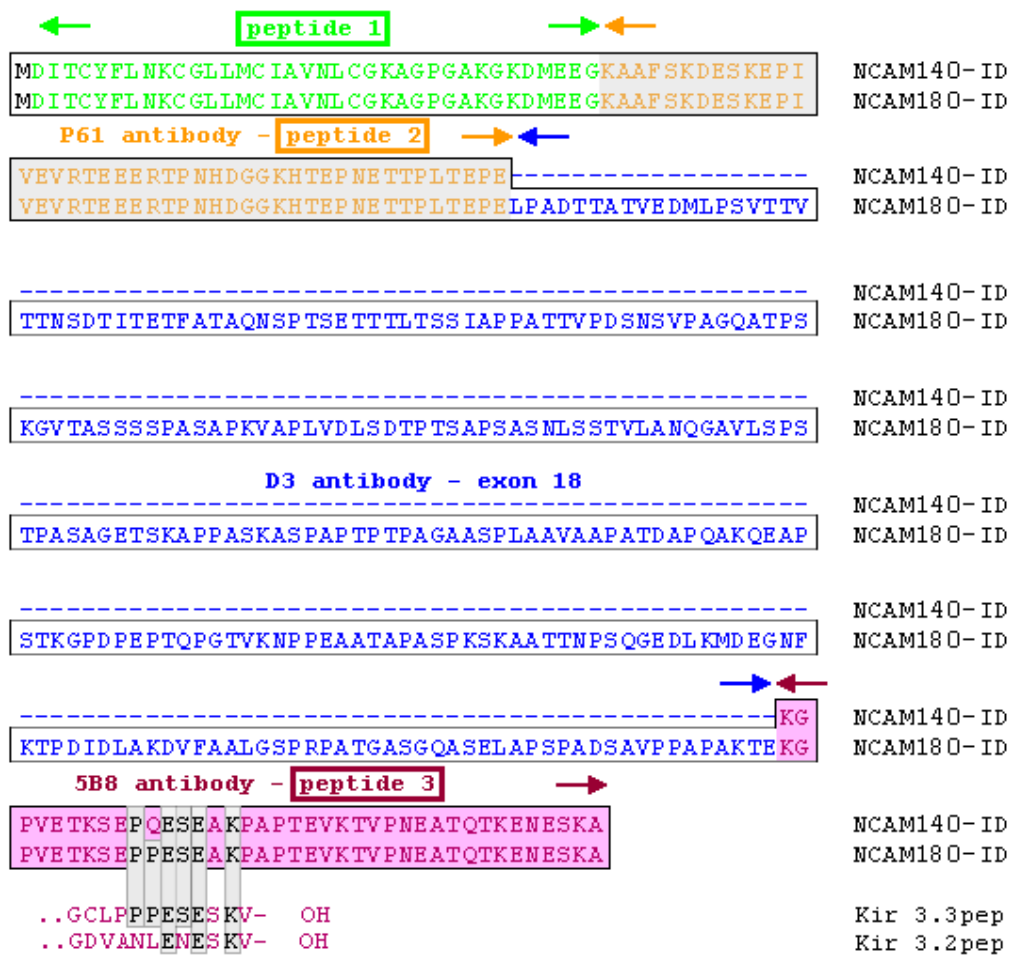


**Figure 10. Comparison of the IDs of mouse NCAM180 and NCAM140.**

The only difference between the IDs of NCAM140 and NCAM180 is the presence of an additional 261-amino acid insert in the intracellular region of NCAM180, encoded by NCAM exon 18. The three synthesized peptides 1–3 used for epitope mapping of the three different anti-NCAM antibodies D3, P61 and 5B8 are indicated. The epitopes of P61 and 5B8 were mapped by using peptides covering aa 766–810 and aa 811–849/1077–1115. D3 recognizes an epitope within the coding sequence of exon 18. A sequence at the extreme C terminus of the Kir3.3 channel shows high similarity to a sequence present in the C-terminal part of NCAM180-ID and NCAM140-ID.

The specific binding between the antibody P61 and peptide 2 (Fig. 9A) determined the exact epitope of P61 as covering aa 766–810 of NCAM140/180. The 5B8 antibody specifically bound and recognized peptide 3 covering aa 811–849 and 1077–1115 of NCAM140 and NCAM180, respectively (Fig. 9B). As expected, D3 did not show any binding to the NCAM140 peptides since the antibody is known to recognize an epitope within the coding sequence of exon 18 (Fig. 9C). Furthermore, thanks to the epitope mapping, a peptide motif in NCAM180 and NCAM140 was discovered (Fig. 10) as having similarity to the C-terminal part of one of the inwardly rectifying potassium channels, namely the Kir3.3 isoform (personal communication Dr. Ralf Kleene, ZMNH, Hamburg, Germany). After identifying the exact epitopes of the anti-NCAM antibodies D3, P61 and 5B8 by epitope mapping, these antibodies were subsequently used for binding studies (see 5.3).

### 5.3 Binding study of recombinant NCAM180-ID to TrkB-ID and a TrkB peptide using an ELISA approach

An ELISA, *i.e.* an *in vitro* assay, was decided on to prove a direct binding of NCAM180 and TrkB. For this purpose, recombinant NCAM180-ID, NCAM140-ID, NCAM exon 18 and CHL1-ID proteins were expressed and produced in *E. coli*. Native TrkB-ID was prepared in a baculovirus expression system (Iwasaki *et al.*, 1997) (a kind gift of Dr. Shinichi Koizumi, Novartis Pharma K.K., Tsukuba Research Institute, Ibaraki, Japan) and phosphorylated at the tyrosine residues in the catalytic site as reported by Iwasaki *et al.* (1997, 1998).

First, a TrkB peptide (kindly synthesized by Dr. Jochen Heukeshoven, Heinrich-Pette-Institut, Hamburg, Germany) discovered in the phage display analysis as containing the putative NCAM180-ID binding site was substrate-coated at a concentration of 250 ng/ml on absorbent plastic surfaces (see 3.3.2; TrkB peptide 2). The TrkB peptide was then incubated with the putative binding partner NCAM180-ID containing a His-tag in addition to His-tagged NCAM140-ID and CHL1-ID and BSA that were used as negative controls. Detection of the potential interaction partner was performed using a specific mouse anti-Penta His antibody that recognizes five consecutive histidine residues in proteins. NCAM180-ID specifically bound to the TrkB peptide, in contrast to the other isoform, NCAM140-ID, or CHL1-ID (Fig. 11A). Second, based on the results from the epitope mapping, the respective anti-NCAM antibodies (D3, P61 and 5B8) were targeted in ELISA binding studies, in order to determine where the specific binding site of the TrkB peptide is located within NCAM180-ID. The TrkB peptide was immobilized at a concentration of

2.5 µg/ml on an absorbent surface and subsequently incubated with NCAM180-ID (Fig. 11B), NCAM140-ID, or NCAM exon 18 (data not shown since there was no binding). Binding of NCAM180-ID to the TrkB peptide was assessed using the exon 18-specific antibody D3 and the antibodies P61 and 5B8 recognizing specific epitopes within the IDs of NCAM180 and NCAM140. Dose-dependent binding was detected between NCAM180-ID and the TrkB peptide when bound NCAM180-ID was assessed by either the exon 18-specific antibody D3 or the P61 antibody with the N-terminally located epitope. Surprisingly, when the antibody 5B8 with the C-terminally located epitope was used for detection, there was no specific binding signal (Fig. 11B). This indicates that the antibody 5B8 could not bind either because the epitope was occupied by the TrkB peptide or because the peptide was in competition with the antibody 5B8 for the common substrate NCAM180-ID. Third, recombinant TrkB-ID was substrate-coated at a concentration of 1 µg/ml on an absorbent surface and incubated with the putative binding partner NCAM180-ID or with NCAM exon 18. Binding of NCAM180-ID or exon 18 to TrkB-ID was assessed using the NCAM180/exon 18-specific antibody D3. Interestingly, only NCAM180 bound to TrkB-ID, but not exon 18 alone (Fig. 11C). This result again confirms that the binding site is definitely located within the shared parts of NCAM180- and NCAM140-ID.

To investigate the influence of the phosphorylation state of TrkB on the binding to NCAM180-ID, unphosphorylated and phosphorylated TrkB-ID (TrkB-ID/pTrkB-ID) was used after *in vitro* preparation. Unexpectedly, no difference in binding to NCAM180-ID was observable between TrkB-ID and pTrkB-ID (data not shown). This indicates that the binding between NCAM180-ID and TrkB-ID may not depend on the phosphorylation state of TrkB-ID. Furthermore, binding between TrkB and NCAM180-ID was only detectable when TrkB-ID or TrkB peptide was used for immobilization, and not *vice versa* (data not shown).

In summary, a direct interaction of NCAM180-ID and TrkB-ID or TrkB peptide was shown in different ELISA assays. Since the antibody D3 recognizes an epitope within the coding sequence of exon 18 but the NCAM exon 18 did not bind to TrkB-ID, the binding site of NCAM180-ID and TrkB-ID has to be located in an overlapping region between NCAM exon 18 and the N terminus of NCAM180-ID and NCAM140-ID.

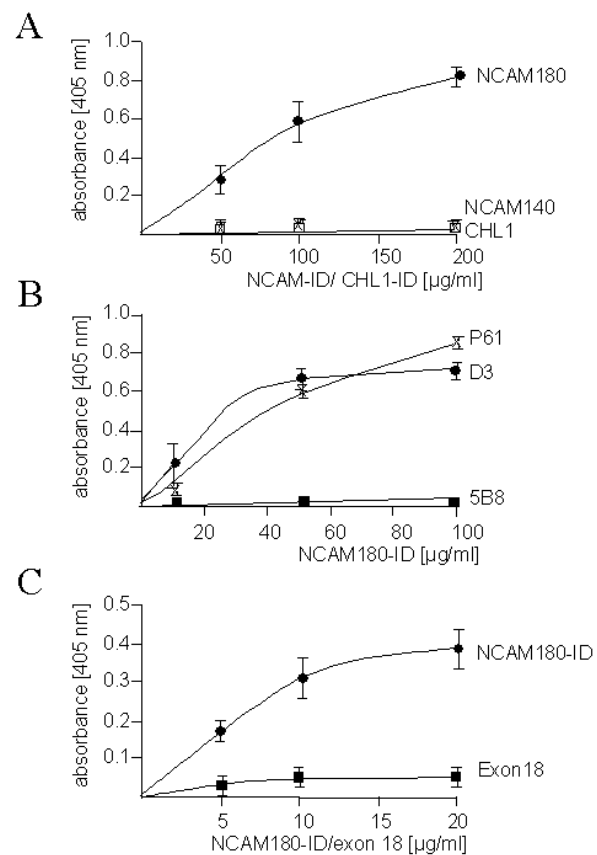


**Figure 11. Binding of NCAM180 ID to a TrkB peptide and to TrkB ID.**

The TrkB peptide (A, B) and TrkB-ID (C) were substrate-coated and incubated with NCAM180-ID (A–C), recombinant exon 18 (C), NCAM140-ID and CHL1-ID (A). (A) Binding of His-tagged NCAM180-, NCAM140-, CHL1-ID to substrate-coated TrkB peptide was analyzed using an anti-Penta His antibody for detection. (B) Binding of NCAM180-ID to the TrkB peptide was assessed using the exon 18-specific antibody D3 and the antibodies P61 and 5B8 recognizing specific epitopes within the IDs of NCAM180 and NCAM140. (C) Binding of NCAM180-ID or exon 18 to TrkB-ID was analyzed by using the NCAM180/exon 18-specific antibody D3. NCAM180, but not exon 18 alone, does bind TrkB-ID. All experiments were reproduced at least three times. Error bars represent SEM.

## 5.4 Cross-linked TrkB peptide did not interact with NCAM180-ID

To confirm the interaction between TrkB and NCAM180-ID, a TrkB peptide (see 3.3.2) was cross-linked to the trifunctional cross-linker Sulfo-SBED containing a biotin moiety. Brains were lysed in PBS that contained only the protease inhibitor mix Complete<sup>TM</sup> (Roche Diagnostics, Mannheim, Germany). Subsequently, the nuclei were removed before adding Triton X-100 at a final concentration of 1%. The Triton-soluble brain lysate from adult NCAM<sup>+/+</sup> mice or NCAM<sup>-/-</sup> control mice was added to the TrkB peptide–cross-linker complex.

Although hypothesized from the ELISA experiments as a potential binding partner, no NCAM180 was isolated after UV cross-linking of the TrkB peptide and SDS-PAGE. A representative cross-linking experiment using TrkB peptide 1 (3.3.2) with subsequent Western blot analysis is shown in Fig. 12. Streptavidin-HRP was used for detection of biotin-labeled proteins (lanes 1 and 2), the D3 antibody for detection of NCAM180 (lanes 3 and 4), and the anti-NCAM antibody 1B2 for detection of all NCAM isoforms (lanes 5 and 6). The arrows indicate co-isolated NCAM in wild-type (NCAM<sup>+/+</sup>) brain lysate, which is localized within the TrkB peptide complex (lanes 3 and 5), whereas the NCAM<sup>-/-</sup> control (lanes 4 and 6) did not show any unspecific band. If NCAM180 had received biotin labels from the cross-linked TrkB peptide, a respective band at 180 kDa would have been detectable using streptavidin-HRP, as a result of the biotin transfer from the TrkB peptide to NCAM180. The prominent bands with a molecular weight of 120 kDa that were detected with the biotin groups by streptavidin-HRP (Fig. 12, lanes 1 and 2) were not NCAM specific since there was a positive signal also in the NCAM<sup>-/-</sup> control.

This cross-linking approach was also tested using the following: Triton-soluble brain lysate, enriched synaptosomal brain subfraction, and with all four TrkB peptides (3.3.2) as bait. None of these experiments showed a direct interaction between TrkB peptide and NCAM180.

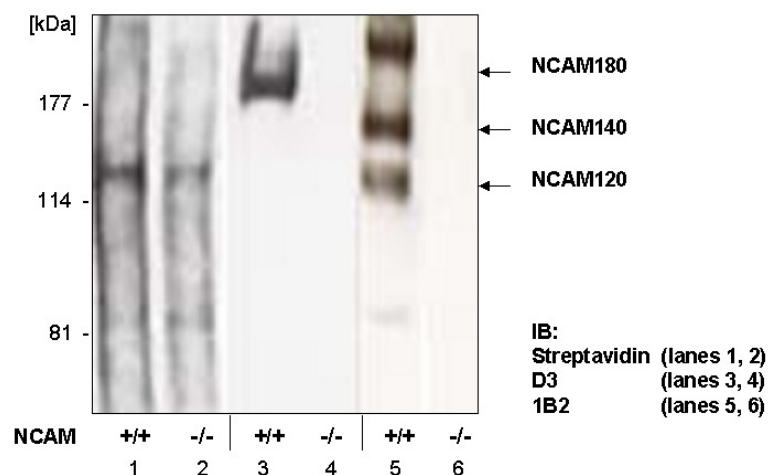


**Figure 12. No specific binding between cross-linked TrkB peptide and NCAM180.**

Triton-soluble brain lysate of adult wild-type (NCAM<sup>+/+</sup>) and NCAM<sup>-/-</sup> mice were used for sulfo-SBED cross-linking. The cross-linker was coupled to the TrkB peptide 1 and biotin-labeled binding partners were subjected to Western blot analysis using streptavidin-HRP (lanes 1 and 2), the NCAM180-specific D3 antibody (lanes 3 and 4), and the anti-NCAM antibody 1B2 recognizing all NCAM isoforms (lanes 5 and 6). The prominent band at 120 kDa detected by streptavidin-HRP was not NCAM specific since this band was observed in the NCAM<sup>-/-</sup> control as well. There is no specific band detected by streptavidin-HRP at a molecular weight of 180 kDa in NCAM<sup>+/+</sup> mice which would prove a direct interaction between NCAM180 and TrkB peptide 1.

## 5.5 Binding of a Trk fragment to NCAM180-ID under P+ lysis conditions in a modified cross-linking approach

Since the previous cross-linking approach did not confirm the direct interaction between TrkB and NCAM180 that was indicated by the ELISA experiments, the cross-linking protocol was altered. In this new cross-linking approach, the trifunctional cross-linker Sulfo-SBED containing a biotin moiety was coupled to the IDs of NCAM180 (Fig. 13A, B), NCAM140 (Fig. 13B) and CHL1 for control (Fig. 13A, B). To test if the binding capacity of TrkB to other molecules, such as NCAM180, was influenced by the phosphorylation state of TrkB, two lysis conditions for brain homogenate preparation were investigated, one inhibiting dephosphorylation (P+) and the other inhibiting tyrosine kinase phosphorylation (P-) (Fig. 13A). After UV cross-linking and SDS-PAGE, the biotin-labeled binding partners were subjected to Western blot analysis. Streptavidin-HRP was used for detection of biotin-labeled proteins (Fig. 13A, lanes 1–4; Fig. 13B, lanes 1–3), a panTrk antibody for recognition of the highly conserved C termini of all Trk family members (Fig. 13A, lanes 5–8; Fig. 6B, lanes 4–6), the D3 antibody for NCAM180 detection (Fig. 13B, lanes 7–9), and a specific antibody for Kir3.3 detection (Fig. 13B, lanes 10–12).

Fig. 13A shows a direct binding between NCAM180-ID and a Trk fragment (lanes 1, 2 and 5, 6), whereas the CHL1-ID control (lanes 3, 4 and 7, 8) did not show any binding. The arrowhead indicates biotin-labeled proteins and a Trk fragment with a molecular weight of 80 kDa that prominently binds to NCAM180-ID under P+ conditions (lane 6). Under P- conditions, less Trk fragment binding to NCAM180-ID was detectable (lane 5). Therefore, from this point on, cross-linking experiments were performed under P+ conditions.

The direct binding between NCAM180-ID and the Trk fragment was confirmed in Fig. 13B where the upper arrowhead indicates the biotin-labeled proteins (lane 1) and the Trk fragment (lane 4) with a molecular weight of 80 kDa that prominently binds to NCAM180-ID, but not to NCAM140-ID (lanes 2, 5) and the control CHL1-ID (lanes 3, 6). The upper arrowhead also points to an NCAM fragment that is associated with NCAM180-ID (lane 7) but not detected in the controls. Additionally, the lower arrowhead indicates a Kir3.3 channel monomer binding to NCAM180 (lane 10). These results were confirmed in two independent experiments (Fig. 13). So far, only the interaction between NCAM180-ID and a Trk fragment with a molecular weight of approximately 80 kDa has been shown.

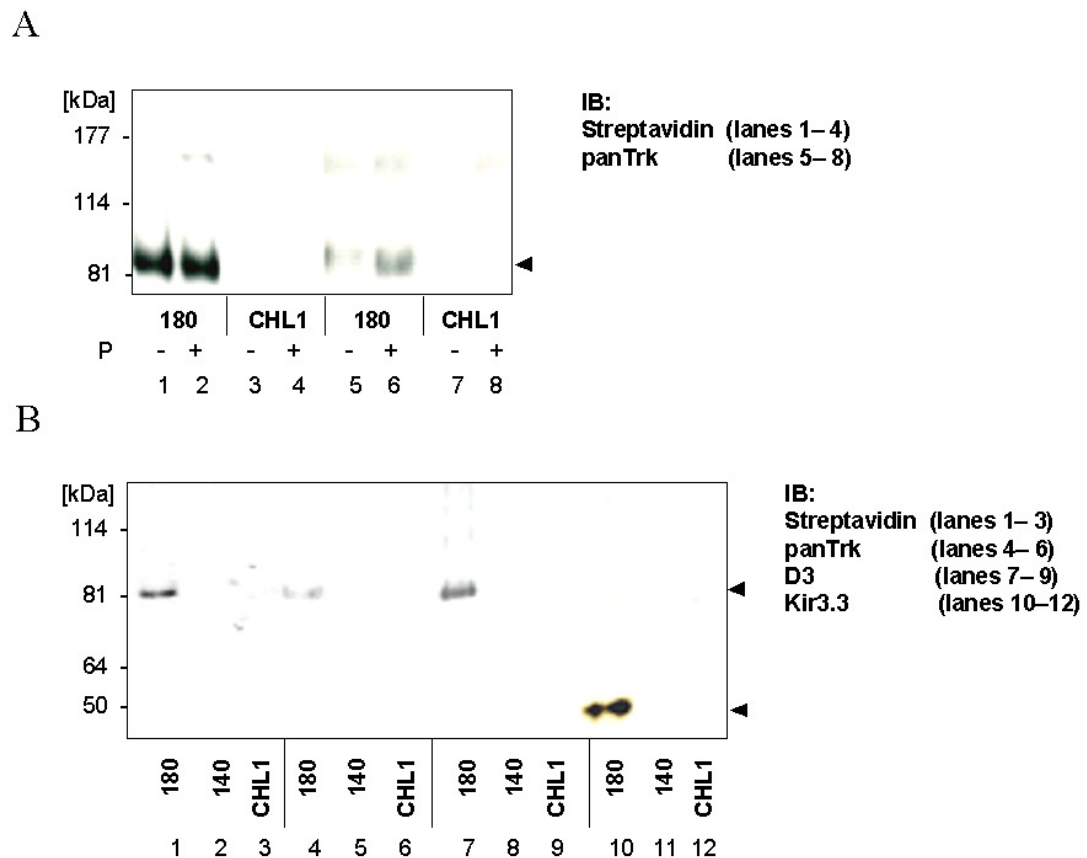


**Figure 13. Binding of the intracellular TrkB fragment to NCAM180 ID.**

(A) Cross-linking experiments were performed under lysis conditions inhibiting dephosphorylation (P+) or inhibiting tyrosine kinase phosphorylation (P-). The trifunctional cross-linker sulfo-SBED containing a biotin moiety was coupled to NCAM180-ID or to CHL1-ID as control. Brain homogenate from NCAM<sup>+/+</sup> mice was added to the protein–cross-linker complex, and after UV cross-linking, the potential binding partners were isolated and separated by SDS-PAGE under reducing conditions resulting in a transfer of the biotin group to the cross-linked partner molecules. Western blot analysis using streptavidin-HRP (for detection of biotin-labeled proteins) and a panTrk antibody is shown. The arrowhead points at the Trk fragment that prominently binds to NCAM180-ID (180) under conditions inhibiting dephosphorylation (P+), whereas the CHL1-ID control (CHL1) does not show a similar band. (B) The cross-linking experiment was performed under P+ conditions using the IDs of NCAM180, NCAM140 or CHL1 as bait. Western blots using streptavidin-HRP, the panTrk antibody, the NCAM180-specific antibody D3 or a Kir3.3-specific antibody are shown. The upper arrowhead indicates the Trk fragment that prominently binds to NCAM180-ID but not to NCAM140-ID or the control CHL1-ID. The upper arrowhead also points to an NCAM fragment that is associated with NCAM180-ID. The lower arrowhead indicates a Kir3.3 monomer binding to NCAM180. These results were confirmed in two independent experiments.

## 5.6 NCAM180-ID interacts with full-length TrkB under P+ lysis conditions and in the presence of specific protease inhibitors in an optimized cross-linking approach

After showing a direct interaction between a Trk fragment and NCAM180-ID, the previous cross-linking protocol had to be optimized further in order to eventually show a binding

between full-length TrkB and NCAM180-ID. The hypothesis was that TrkB is proteolytically cleaved before or after binding to NCAM180-ID. Therefore, proteolysis was investigated in parallel to the establishment of optimized conditions for the cross-linking experiments (see 5.10). The aim was to find experimental conditions that avoid the production of processed fragments.

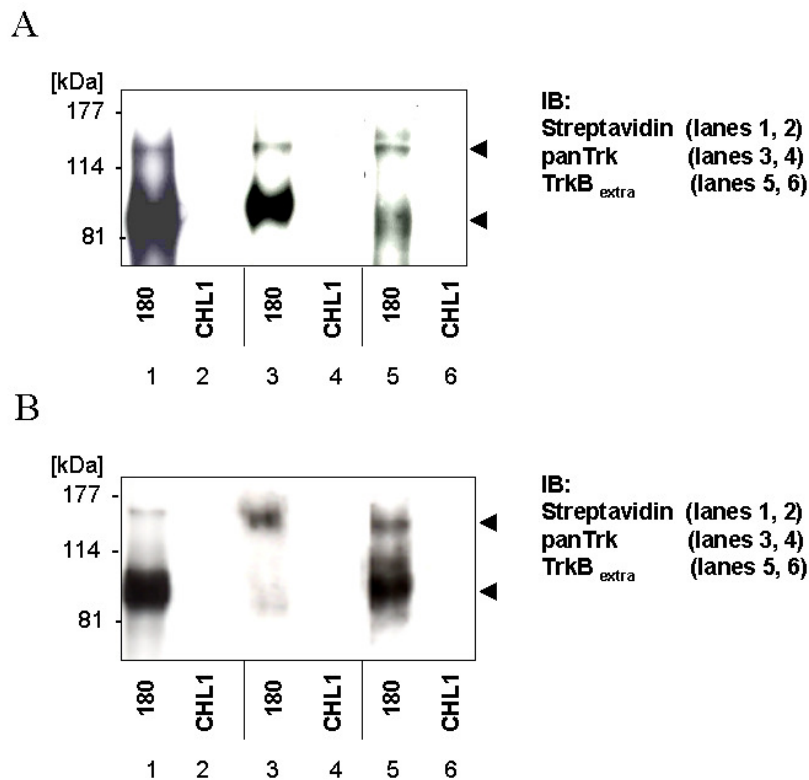


**Figure 14. An interaction between NCAM180 ID and full-length TrkB.**

Isolated membranes (A) and the mossy fiber fraction (B) of adult wild-type brains were prepared under lysis conditions inhibiting dephosphorylation (P+) and in the presence of protease inhibitors, for cross-linking experiments. The cross-linker sulfo-SBED was coupled to NCAM180-ID (180) and CHL1-ID (CHL1) as described before. The potential biotin-labeled binding partners were analyzed by Western blot using Streptavidin-HRP (lanes 1, 2), the panTrk antibody (lanes 3, 4) and a TrkB-specific antibody (lanes 5, 6). The lower arrowhead points to the Trk fragment and the upper arrowhead shows the full-length TrkB that binds to NCAM180-ID.

According to an optimized cross-linking protocol, brain membranes from 2–3-month-old C57BL/6J mice were isolated under P+ conditions and in the presence of a  $\gamma$ -secretase inhibitor (DAPT) and a matrix metalloprotease inhibitor (GM 6001). The isolated membranes were incubated at 37°C for 2 h before adding the coupled cross-linker–ID complexes. After UV cross-linking, Triton X-100 was added before incubation of the samples

for 45 min on ice, followed by removal of the nuclei. Potential binding partner(s) bound to NCAM180-ID and control CHL1-ID were isolated and separated by SDS-PAGE and immunoblotted as previously described (Fig. 14). Detection of the biotin labels transferred to the putative binding partner(s) was analyzed by streptavidin-HRP (lanes 1, 2), the panTrk antibody (lanes 3, 4) and a TrkB-specific antibody (lanes 5, 6) (Fig. 14).

The interaction between full-length TrkB and NCAM180-ID could be proven in isolated membranes (Fig. 14A) and the mossy fiber subfraction (Fig. 14B) of adult wild-type mice under lysis conditions inhibiting dephosphorylation (P+) and in the presence of specific protease inhibitors (DAPT and GM 6001). When the mossy fiber fraction was isolated by using a sucrose density gradient, the same protease inhibitors were applied to the P+ homogenization buffer. In addition to the interaction between full-length TrkB and NCAM180, the already previously detected interaction between the Trk fragment and NCAM180-ID was also observable using this approach. Proteolytic processing seems to have an impact on the interaction between these proteins.

## 5.7 Verification of the NCAM180-Trk interaction by co-immunoprecipitation

Co-immunoprecipitation was chosen as another method to confirm the interaction between NCAM180 and TrkB already shown by biochemical cross-linking. For that reason, various tissue preparations were used, such as brain homogenates, isolated brain subfractions, Triton-soluble brain lysates, or cell culture lysates from N2a cells or NCAM- and TrkB-transfected CHO cells. Either NCAM or TrkB was precipitated out of an *in vivo* situation by using either an anti-NCAM or an anti-TrkB antibody attached to beads. To subsequently detect the co-precipitated respective other protein (TrkB or NCAM) within the isolated immune complexes, the respective other antibody against TrkB or NCAM was used. Various co-immunoprecipitation approaches were systematically tested until a successfully working protocol was established for the detection of the interaction between NCAM and TrkB. For co-immunoprecipitations, one has the possibility to covalently couple the antibody to beads or to add the antibodies in excess to the beads. The first approach was to covalently couple the antibody to beads. A rat monoclonal anti-NCAM antibody, H28, was covalently coupled to Sepharose A/G beads. Fig. 15 shows a representative Western blot of this approach. In this case, detergent-soluble cerebellum lysates from adult NCAM<sup>+/+</sup> and NCAM<sup>-/-</sup> mice were incubated with the coupled beads. After SDS-PAGE, subsequent immunoblotting was performed using the polyclonal anti-NCAM antibody 1B2 (Fig. 15,

lanes 1–4) for precipitation control, and a specific anti-TrkB antibody (a gift from Dr. Joseph Kiss, University of Geneva, Geneva, Switzerland) for detection of co-precipitated TrkB. This approach resulted in a satisfactory precipitation of all NCAM isoforms (Fig. 15, lane 3) but no Trk protein was detectable in the co-precipitates (Fig. 15, lane 7). Then, in the other approaches, besides a variety of beads (Sephacrose beads, magnetic DYNA-beads or agarose beads), different anti-NCAM (H28 and 1B2 since D3 was at that time not available) and six anti-TrkB antibodies with three different epitopes within TrkB (a gift from Dr. Joseph Kiss, University of Geneva, Geneva, Switzerland) were tested for precipitation and immunoblotting. Immunoprecipitations worked best with the rat monoclonal anti-NCAM antibody H28, in contrast to the anti-TrkB antibodies which did not work for precipitation. Unfortunately, most of the anti-TrkB antibodies showed unspecific bands, high background and only weak TrkB-specific bands (data not shown). Hence, a rabbit polyclonal antibody specific for TrkB and a rabbit polyclonal panTrk antibody were commercially purchased and tested. Both antibodies showed good results for immunoblotting. In addition, the panTrk antibody was very useful for immunoprecipitation. Moreover, the monoclonal NCAM180-specific antibody D3 (kindly produced by Stefan Hennig and Gaby Loers, ZMNH, Hamburg, Germany) was very useful for immunoprecipitation and immunoblotting. Although the immunoprecipitations with these antibodies worked well, none of these co-immunoprecipitation approaches indicated an interaction between the two molecules NCAM and TrkB (data not shown). Thus, as for the cross-linking experiments, special conditions (see 3.2.9 and 3.2.13) were necessary to be able to detect, for the first time, an interaction between the two full-length transmembrane proteins. Consequently, a new co-immunoprecipitation protocol was developed, based on these optimized experimental conditions and on results gained from the cross-linking experiments. Brain membranes were isolated either from adult NCAM wild-type (NCAM<sup>+/+</sup>) and NCAM-deficient (NCAM<sup>-/-</sup>) mice or from newborn TrkB wild-type (TrkB<sup>+/+</sup>) and TrkB-deficient (TrkB<sup>-/-</sup>) mice. Brain lysates were always prepared using P+ lysis conditions inhibiting dephosphorylation, as previously described (3.2.9 and 4.2.13).

First, the brain lysates derived from adult NCAM<sup>+/+</sup> and NCAM<sup>-/-</sup> mice containing Trk (Fig. 16A, lanes 7, 8) as well as NCAM180 (Fig. 16A, lane 3) were incubated with the panTrk antibody (Fig. 16A, lanes 5, 6 and 9, 10) for immunoprecipitation. Immune complexes were isolated using Protein A/G agarose Plus beads. To analyze for co-precipitation of Trk and NCAM180, the immune complexes were subjected to Western blot analysis with the NCAM-specific antibody D3 (Fig. 16A, lanes 1–4; Fig. 16B, lanes 1, 2). The im-

munoprecipitations were successfully performed because Trk was detectable in the immune complexes that were eluted from the Protein A/G agarose Plus beads (Fig. 16A, lanes 5, 6). To exclude unspecific binding, brain lysate of NCAM<sup>-/-</sup> mice was used as control, showing no corresponding unspecific band (Fig. 16A, lane 4; Fig. 16 B, lane 2). The analysis of the co-immunoprecipitates (Fig. 16A, lanes 3, 4; Fig. 16B, lanes 1, 2) using the NCAM-specific antibody D3 revealed that Trk did not only co-precipitate with full-length NCAM180 but also with an NCAM fragment (see 5.6) (Fig. 16A, B; indicated by arrows) in the brain lysates of adult NCAM<sup>+/+</sup> mice (Fig. 16A, lane 3; Fig. 16B, lane 1). These results were reproduced in three independent experiments.

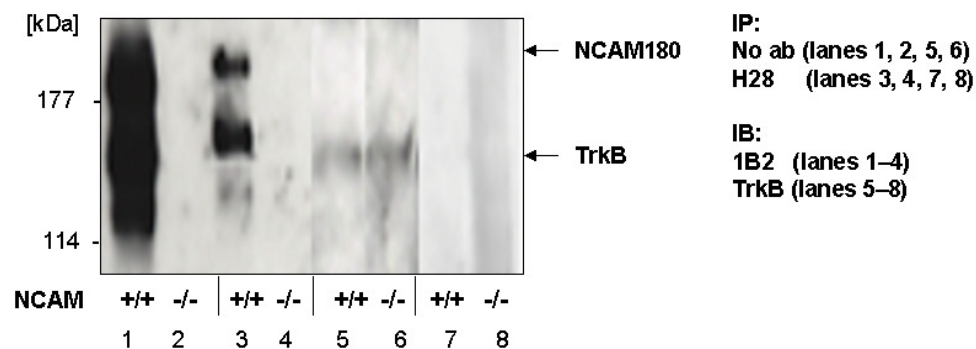


**Figure 15. Immunoprecipitation of NCAM180 and NCAM140, but no co-immunoprecipitation of Trk.**

Lysates of cerebella from adult NCAM<sup>+/+</sup> and NCAM<sup>-/-</sup> mice were incubated with the monoclonal anti-NCAM antibody H28 covalently coupled to Sepharose A/G beads. After SDS-PAGE, Western blot analysis (IB) was performed using the polyclonal anti-NCAM antibody 1B2 (lanes 1-4) for precipitation control and a specific anti-TrkB antibody (gift from Dr. Joseph Kiss, Geneva, Switzerland) (lanes 5-8) for detection of TrkB in the supernatant of the precipitates (lanes 5, 6) and in the eluates of the precipitates (lanes 7, 8). NCAM was present in the supernatant of the precipitates (lanes 1, 2). NCAM immunoprecipitation (IP) of NCAM140 and NCAM180 isoforms was successfully performed (lane 3). The NCAM<sup>-/-</sup> controls (lanes 2, 4 and 8) showed no signal, as expected; however, unexpectedly, the co-immunoprecipitation of Trk and NCAM was not detectable (lane 7).

Furthermore, there are preliminary data from a *vice versa* co-immunoprecipitation approach. For this purpose, NCAM180 was immunoprecipitated, using the NCAM-specific antibody D3, from brain lysates of newborn wild-type mice (TrkB<sup>+/+</sup>) and control TrkB<sup>-/-</sup> mice, and later subjected to Western blot analysis using the rabbit polyclonal panTrk antibody. It was not possible to use brain tissue of adult mice since the control TrkB<sup>-/-</sup> mice barely survive one week. The co-immunoprecipitation protocol already described for the experiments shown in Fig. 16 was used. For the analysis of the immunoprecipitates, Western blot analysis was performed using the NCAM-specific antibody D3 to control for successful precipitation (Fig. 17, lanes 1, 2), and the panTrk antibody to detect Trk in the

immunoprecipitation complexes of NCAM180 (Fig. 17, lane 3). In the case of 1-day-old mice, co-immunoprecipitations did not show any results. Only a weak but detectable signal of Trk was discoverable in the co-immunoprecipitates of brain lysates from 3-day-old  $\text{TrkB}^{+/+}$  mice (Fig. 17, lane 3) and not in the  $\text{TrkB}^{-/-}$  control (Fig. 17, lane 4). These data have to be considered as preliminary since the experiments were not reproduced twice due to a lack of sufficient numbers of 3-day-old control  $\text{TrkB}^{-/-}$  mice.

Thus, the co-immunoprecipitation results enrich the body of evidence for an interaction between TrkB and NCAM180 in the ‘natural environment’ of cell membranes within the brain.

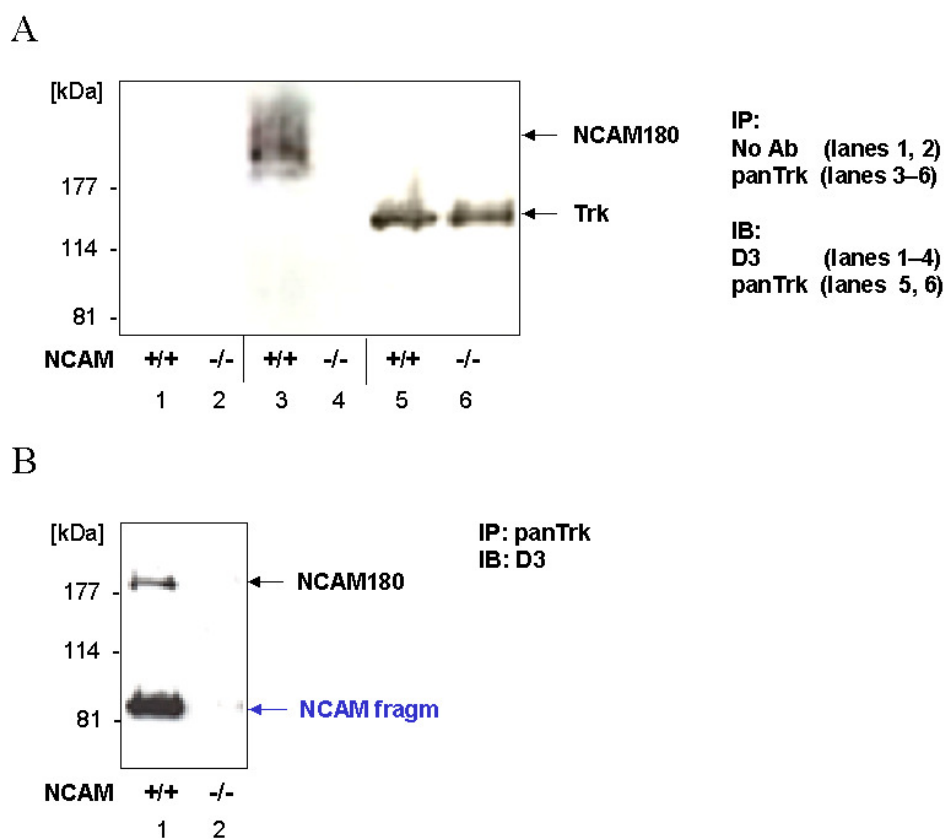


**Figure 16. Co-immunoprecipitation of Trk and NCAM180.**

Brain lysates of adult  $\text{NCAM}^{+/+}$  and  $\text{NCAM}^{-/-}$  mice were incubated with the panTrk antibody for immunoprecipitation, followed by incubation with protein A/G agarose. After SDS-PAGE, Western blot analysis (IB) was performed using the NCAM180-specific antibody D3 (A, lanes 1–4; B, lanes 1, 2) for analysis of putative co-immunoprecipitates (A, lane 3; B, lane 1) and the panTrk antibody (A, lanes 5, 6) for precipitation control. Eluates from protein A/G agarose treated without antibodies for negative controls (A, lanes 1, 2) and the eluates containing immunoprecipitates (A, lanes 3–6; B, lanes 1, 2) were analyzed. The panTrk antibody labeled a band at 145 kDa in the precipitates, indicating that the precipitation worked (A, lanes 5, 6) (indicated by an arrow). The NCAM180-specific D3 antibody detected NCAM180 in the co-precipitates (A, lane 3). In three other experiments, not only NCAM180 but also an NCAM fragment (NCAM fragm) was co-precipitated (B, lane 1, indicated by a blue arrow). There were no unspecific bands in the  $\text{NCAM}^{-/-}$  controls (A, lanes 2, 4; B, lane 2) as well as in the negative control without antibodies (A, lanes 1, 2).

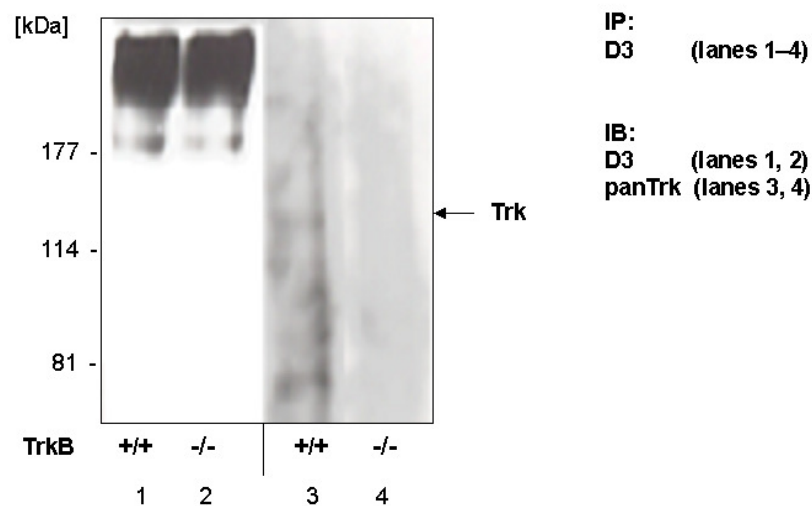


**Figure 17. Co-immunoprecipitation of NCAM180 and TrkB.**

Brain lysates of 3-day-old TrkB<sup>+/+</sup> and TrkB<sup>-/-</sup> mice were incubated with the NCAM-specific antibody D3 for immunoprecipitation (lanes 1–4), followed by incubation with Protein A/G Plus agarose. After SDS-PAGE, immunoblot analysis (IB) of the immunoprecipitates was performed using the panTrk antibody (lanes 3, 4) and the NCAM-specific antibody D3 for precipitation control (lanes 1, 2). The panTrk antibody labeled a very weak band at 145 kD in the precipitates of TrkB<sup>+/+</sup> mice (lane 3) but not in the TrkB<sup>-/-</sup> control (lane 4). The NCAM180-specific antibody D3 detected NCAM180 in the immunoprecipitates, indicating that the precipitation worked (lanes 1, 2).

## 5.8 No spatial relationship between NCAM and TrkB shown in co-localization and co-capping experiments

To confirm the binding of NCAM180 and TrkB under natural conditions in the *in vivo* environment of the cell membrane, co-localization and co-capping experiments using cellular model systems were chosen. For NCAM capping, an NCAM-specific antibody was used to cross-link NCAM on the cell surface and was detected with the respective Cy3-labeled secondary antibody. After antibody application, formation of NCAM caps was observed as clusters of fluorescent spots on the cell surface (Figs. 18–20). TrkB expression was assessed on the same cells by indirect immunofluorescence staining with antibodies specific for TrkB and a Cy5-labeled secondary antibody. TrkB protein was hypothesized to be recruited to the NCAM cap and to be indicated by the yellow color in the overlay image gained by confocal immunofluorescence microscopy. If a potential re-distribution of TrkB after antibody-induced pre-clustering of NCAM took place, this would demonstrate the physical *in vivo* association of TrkB and NCAM and be a hint for their putative interaction. Capping was successfully induced by antibodies specific for NCAM (Figs. 18, 19B) or PSA-NCAM (Fig. 20B), in contrast to the antibodies specific for TrkB which did not in-

duce satisfactory pre-clustering of TrkB protein (data not shown). Since polysialylation of NCAM into  $\alpha$ -2,8-linked PSA-NCAM has been suggested to facilitate the presentation of BDNF to TrkB (Charles *et al.*, 2000; Muller *et al.*, 2000; Vutskits *et al.*, 2001), a mouse fibroblast cell line (LMTK) was chosen that expressed polysialyltransferases (LMTK-PST) (a kind gift of Martina Muehlenhoff and Dr. Rita Gerardy-Schahn, Medizinische Hochschule Hannover, Hannover, Germany). ST8SiaII and ST8SiaIV are the two polysialyltransferases responsible for NCAM polysialylation (Close and Colley, 1998). The first co-capping experiments were performed on these LMTK and LMTK-PST cells to investigate the possibility that PSA on NCAM may be essential for the potential binding between NCAM and TrkB. For this purpose, LMTK/LMTK-PST cells were transiently transfected with a rat Flag-tagged full-length TrkB construct (pFlag T+ TrkB; generous gift of Dr. Eero Castrén, Kuopio, Finland) and a mouse full-length NCAM180 construct or an NCAM120 construct for control. Co-capping experiments were started by pre-incubation with the polyclonal rabbit anti-NCAM antibody 1B2. When the secondary rabbit Cy3-labeled antibody was applied, clustering of the primary and secondary antibodies was induced and TrkB was detected by using a mouse monoclonal anti-Flag M2 antibody and its corresponding secondary mouse Cy5-labeled antibody. Antibody-induced clustering of NCAM in the cell membrane of TrkB- and NCAM-co-transfected cells did not result in TrkB co-clustering in the NCAM180 and NCAM120 patches, indicating that the two transmembrane proteins, NCAM180 and TrkB, did not specifically associate with each other in the cell membrane of LMTK/LMTK-PST cells. Additionally, there was no difference detectable between LMTK (data not shown) and LMTK-PST cells, indicating that PSA did not improve the capability of NCAM and TrkB to interact with each other. Co-transfected NCAM180 and TrkB did not co-cap on the surface of PST-expressing LMTK cells (Fig. 18).

As a next step, the co-localization studies of NCAM and TrkB were continued using hippocampal primary cell cultures. Hippocampi taken from 1–3-day-old wild-type mice were prepared, dissociated and cultured for 3 days. Then, wild-type hippocampal neurons were incubated with the rat monoclonal anti-NCAM antibody H28 (Fig. 19B) or with a mouse monoclonal anti-PSA antibody (Fig. 20B). After antibody-induced clustering of NCAM or PSA-NCAM, TrkB distribution was analyzed using a rabbit polyclonal antibody specific for TrkB-ID (Allendoerfer *et al.*, 1994) and its corresponding secondary rabbit Cy3-conjugated antibody. However, pre-clustering of NCAM did not initiate an accumulation of TrkB in defined patches within the cell membrane (Figs. 19A, 20A). There was almost no

yellow staining visible in the overlay image, suggesting that there was no observable interaction of NCAM and TrkB (Figs. 19C, 20C; indicated by arrows). Even BDNF stimulation of TrkB (50 ng/ml for 15 min) prior to pre-clustering of NCAM did not induce or facilitate a re-distribution of TrkB in the cell membrane of hippocampal neurons (data not shown).

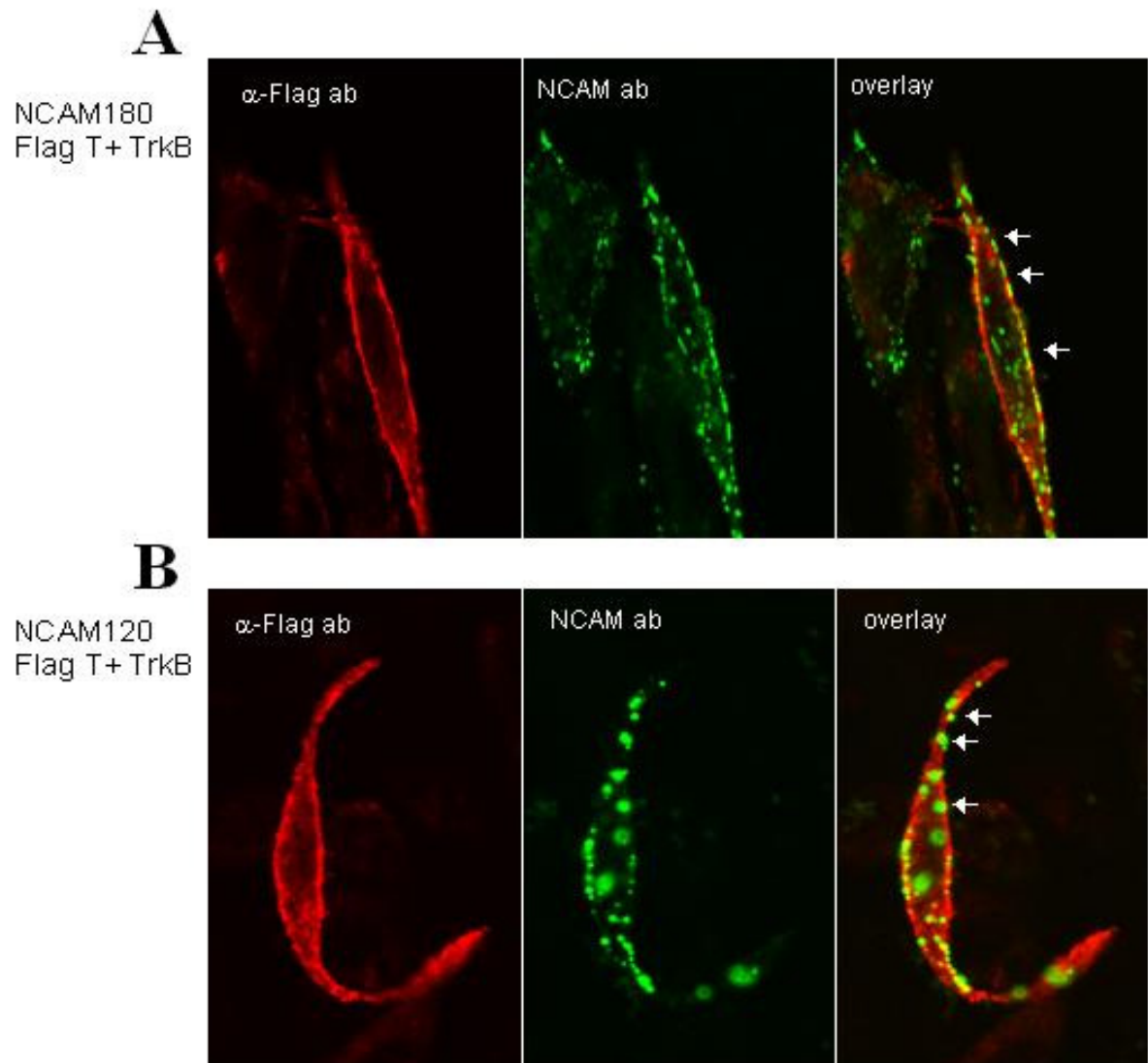


**Figure 18. Clustering of NCAM did not induce a re-distribution of TrkB in co-transfected LMTK-PST cells.**

Representative confocal immunofluorescence images of LMTK-PST cells transfected with Flag-tagged full-length TrkB and NCAM180 (A) or Flag-tagged full-length TrkB and NCAM120 for control (B). Pre-clustering was induced by incubation with polyclonal anti-NCAM antibodies (green). LMTK-PST cells were fixed, permeabilized and stained for TrkB (red) using a mouse monoclonal anti-Flag antibody. TrkB did not specifically co-distribute with NCAM180 clusters, which is indicated by arrows showing basically no yellow overlap of the staining for NCAM and TrkB.

To sum up, after antibody-induced pre-clustering of NCAM or PSA-NCAM, no re-distribution of TrkB into defined areas within the cell membrane was detectable. This result was found using (1) PST-expressing LMTK fibroblast cells co-transfected with NCAM180 and Flag-tagged full-length TrkB and (2) hippocampal neurons. Taken together, all these co-capping experiments showed neither a direct nor an indirect association of the two transmembrane proteins, NCAM180 and TrkB.

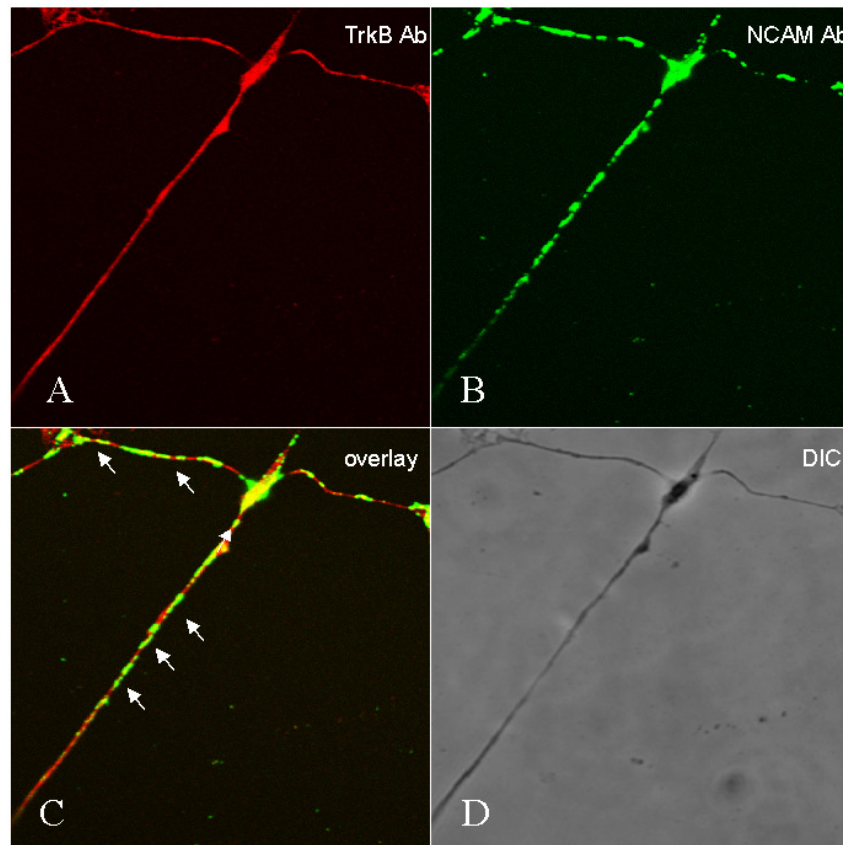


**Figure 19. Clustering of NCAM did not induce a re-distribution of TrkB in primary hippocampal neurons.**

Representative confocal immunofluorescence images of dissociated wild-type hippocampal neurons from 1–3-day-old mice (3 days in culture). Pre-clustering was induced by incubation with the rat monoclonal anti-NCAM antibody H28 (A, green). Later, neurons were fixed, permeabilized and stained for TrkB using a rabbit monoclonal antibody (B, red). The overlay image (C, yellow) showed no re-distribution of TrkB to the distinct NCAM clusters, indicating no physical interaction between NCAM and TrkB (arrows). The phase contrast image is shown in (D).

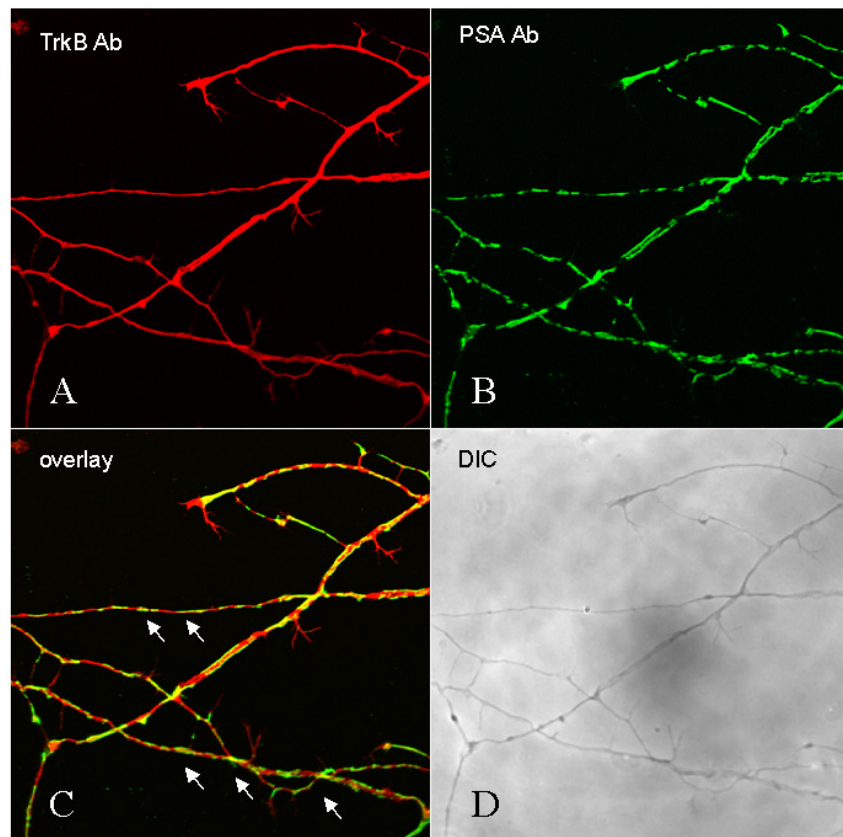


**Figure 20. Clustering of PSA-NCAM did not induce a re-distribution of TrkB in primary hippocampal neurons.**

Representative confocal images of dissociated wild-type hippocampal neurons from 1–3-day-old mice (3 days in culture). Pre-clustering was induced by incubation with the mouse monoclonal anti-PSA-NCAM antibody 735 (A, green). Later, neurons were fixed, permeabilized and stained for TrkB using a rabbit monoclonal TrkB-specific antibody (B, red). The overlay image (C, yellow) basically showed no re-distribution of TrkB to the distinct PSA-NCAM clusters, indicating no physical interaction between PSA-NCAM and TrkB (arrows). The phase contrast image is shown in (D).

## 5.9 Isolation of the Trk and NCAM fragments for protein sequencing

To determine the sequence of the 80-kDa Trk and NCAM fragments discovered in the biochemical cross-linking experiments, cross-linking samples were analyzed using SDS-PAGE followed by silver staining according to Shevchenko (Shevchenko *et al.*, 1996). Silver staining was performed for isolation and exact identification of the sequence of the fragments that specifically bound to NCAM180-ID and not to the CHL1 control. The silver-stained protein band with an approximate molecular weight of 80 kDa was cut out of the 8% polyacrylamide gel (indicated by a red arrow in Fig. 21). The proteins within this band were sequenced using matrix-assisted laser desorption/ionization-mass spectroscopy

(MALDI-MS) (Jensen *et al.*, 1997). Protein sequencing was carried out by Dr. Fritz Buck, Institut für Zellbiochemie und Klinische Neurobiologie, UKE, Hamburg, Germany. However, the protein quantity of the 80-kDa fragment was too low for MALDI-MS to reveal its exact sequence identity.

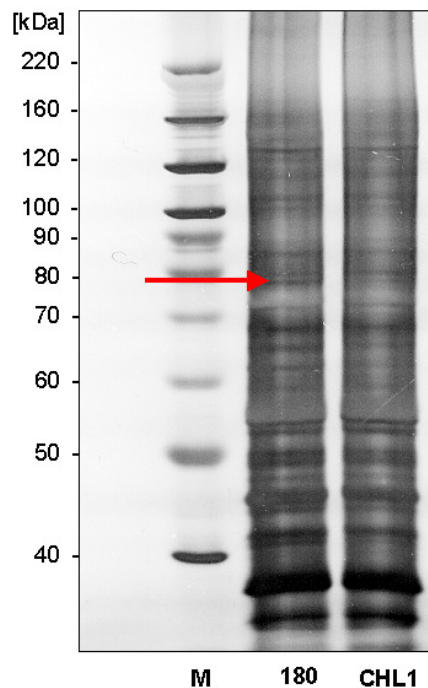


**Figure 21. Silver staining for subsequent protein sequencing of the Trk and NCAM fragments discovered in the cross-linking experiments.**

Eluates from the cross-linking experiments prepared under P+ lysis conditions were subjected to SDS-PAGE. Silver staining was performed after separation of the proteins. An 80-kDa band is indicated by the red arrow and is visible in the NCAM180-ID (180) sample but not in the CHL1 control (CHL1). This fragment was cut out of the polyacrylamid gel (8%) for subsequent sequence analysis. M, molecular weight marker. Molecular weights are indicated in the left margin.

## 5.10 Proteolysis of Trk and NCAM in addition to ectodomain shedding of TrkB

One way to explain the production and the regulation of the Trk and NCAM fragments was to investigate whether these proteins undergo proteolysis. During this kind of posttranslational modification, especially transmembrane proteins are cleaved by a variety of proteases, leading to the release of active protein fragments which are pivotal for a wide range of cellular processes. The release of extracellular domains of membrane-anchored proteins during proteolytic processing is called ectodomain shedding (Pickart, 2001; Hoppe *et al.*, 2000).

To investigate proteolytic processing *in vitro*, proteolysis assays were performed (see 4.2.16). Therefore, brain membranes of adult C57BL/6J mice were incubated at 4°C to inhibit proteolysis for control and at 37°C to enhance proteolytic processes (Fig. 22). After incubation of the membranes, they were separated into supernatant and membrane pellet samples, followed by Western blot analysis using the NCAM180-specific antibody D3 for detection of intracellular NCAM, and the panTrk antibody (Fig. 22). An antibody against a specific epitope in the intracellular part of TrkB (TrkB (794)<sub>intra</sub>) was tested, but this antibody failed to detect full-length TrkB in various controls (data not shown); it was therefore not useful for Western blot analysis. That being the case, the panTrk antibody which recognizes the highly conserved C termini of all Trk family members was the only antibody available for the detection of TrkB-ID or released intracellular TrkB fragments. Unfortunately, apart from this antibody, no alternative antibody recognizing a specific epitope in the intracellular part of TrkB was commercially available. The arrow in Fig. 22 indicates the 80-kDa fragment after proteolytic processing of full-length NCAM180 (180 kDa) and Trk (145 kDa). Samples from the membrane pellet that were incubated at 4°C showed no 80-kDa NCAM fragment, or only low amounts of it. In contrast, the samples incubated at 37°C generated a significantly higher amount of the proteolytically processed membrane-bound fragment (Fig. 22A, compare lane 3 to lane 4). The same effect was seen for the supernatant analyzed for the Trk fragment using the panTrk antibody: After incubation at 4°C, only low amounts of the 80-kDa Trk fragment were found in the supernatant (lane 5), whereas incubation at 37°C yielded a significantly higher amount of this fragment in the supernatant (lane 6). No significant difference in the amount of Trk fragment was detected in the membrane pellet incubated at 4 or 37°C (lanes 7 and 8). The densitometric quantification of the immunoreactive bands of the NCAM and Trk fragments (arrow) from three independent experiments is presented in Fig. 22B.

To identify the proteases that were responsible for the proteolytic cleavage, brain membranes were incubated at 37°C in the presence of specific protease inhibitors, in additional *in vitro* proteolysis assays. In the cross-linking experiments, the matrix metalloprotease inhibitor GM 6001 (GM 6001) and the  $\gamma$ -secretase inhibitor DAPT (DAPT) seemed to be essential factors, when added to the P+ lysis buffer, for the successful detection of the interaction between full-length TrkB and NCAM180-ID (see 5.6). Therefore, these inhibitors were tested in *in vitro* proteolysis assays (Figs. 23, 24). For this purpose, brain membranes of adult C57BL/6J mice were prepared under P+ lysis conditions inhibiting dephosphorylation, followed by incubation at 4°C (Fig. 23, lanes 1, 6) or at 37°C (Fig. 23, lanes 2–5 and

7–10) in the absence or presence of the matrix metalloprotease inhibitors GM 6001 (Fig. 23, lanes 3, 8) and 1,10-phenanthroline (Fig. 23, lanes 4, 9) and of the  $\gamma$ -secretase inhibitor DAPT (Fig. 23, lanes 5, 10). The supernatants and pellets were analyzed by Western blot using an antibody specific for the extracellular part of TrkB (Fig. 23A) and the panTrk antibody (Fig. 23B). After incubation at 4°C, no soluble 80-kDa TrkB fragment was generated, but after incubation at 37°C, the fragment was released in high amounts into the supernatant (Fig. 23A, compare lane 1 to lane 2). The shedding of the 80-kDa soluble extracellular TrkB fragment (Fig. 23A, shown by red arrow) was inhibited by the GM 6001 (lane 3) and 1,10-phenanthroline (lane 4), whereas DAPT had no effect (lane 5). Proteolytic processing of intracellular Trk fragments occurred neither in the supernatant nor in the membrane pellet, as verified by using the panTrk antibody under P+ conditions (Fig. 23B). Furthermore, the inhibitor GM 6001 was also tested under P– lysis conditions. The membranes were pelleted, followed by Western blot analysis of the supernatants and pellets using an antibody specific for the extracellular part of TrkB (Fig. 24A) and the panTrk antibody for detection of intracellular Trk (Fig. 24C). GM 6001 had an inhibitory effect on TrkB shedding under P+ conditions (Fig. 24A, lanes 2, 4, 6) and also under P– conditions (Fig. 24A, lanes 1, 3, 5). Both membrane pellet and supernatant prepared under P– conditions contained an intracellular 80-kDa Trk fragment (Fig. 24C, lanes 1, 3, 5) in comparison to P+ conditions under which no intracellular Trk fragment was generated (Figs. 23, 24C). Both the intracellular soluble and the intracellular membrane-bound Trk fragment were not inhibited by GM 6001. Since it is known that TrkA undergoes proteolysis (Cabrera *et al.*, 1996) and that calmodulin (CaM), a Ca<sup>2+</sup> binding protein, is involved in the modulation of this process (Diaz-Rodriguez *et al.*, 2000). The effect of the CaM inhibitor CGS9343B (CGS) (Novartis Pharma, Basel, Switzerland) on proteolysis was investigated in *in vitro* proteolysis assays (Fig. 24B). Western blot analysis of the supernatants and pellets prepared under P+ and P– lysis conditions was performed using an antibody specific for the extracellular part of TrkB. No influence of the CaM inhibitor (CGS) on TrkB shedding was observable (Fig. 24B).

In summary, shedding of a soluble extracellular 80-kDa TrkB fragment has been shown under P+ and P– conditions, with an inhibitory effect of the matrix metalloprotease inhibitor GM 6001. Surprisingly, when brain membranes were prepared under P+ condition there was no generation of the processed intracellular Trk fragment, in contrast to P– conditions, under which processing lead to the generation of both a soluble and a membrane-associated

80-kDa Trk fragment. GM 6001 did not influence the release of either the soluble or the membrane-associated intracellular Trk fragment.

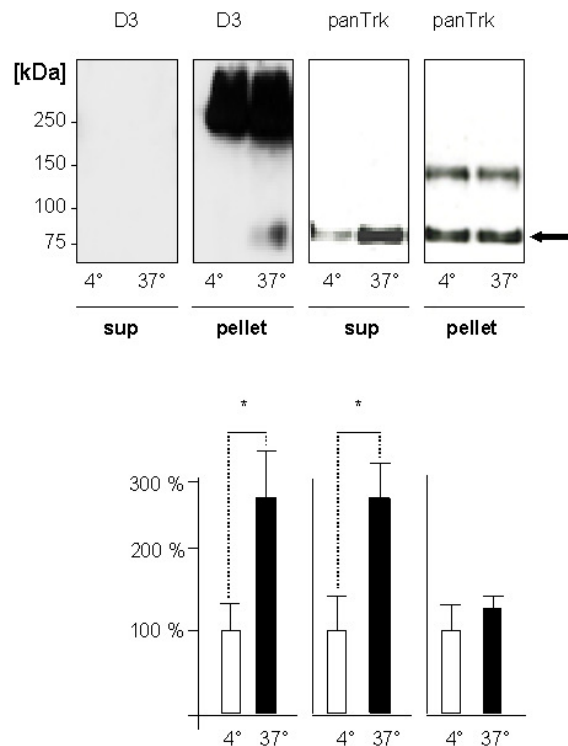


**Figure 22. Proteolysis of Trk and NCAM.**

Brain membranes of adult C57BL/6J mice were prepared under P- lysis conditions and were incubated at 4 or 37°C. Samples were separated into supernatant (sup) and membrane pellet (pellet) and subjected to Western blot analysis using the NCAM180-specific antibody D3 and the panTrk antibody. The arrow indicates the 80-kDa fragment after proteolytic processing of full-length NCAM180 (180 kDa) and Trk (145 kDa). The densitometric quantification of the immunoreactive bands of the NCAM180 and Trk fragments (arrow) is presented below the corresponding representative Western blots. These results were confirmed in three independent experiments. The *asterisks* indicate a statistically significant difference (Student's *t*-test; \*,  $p < 0.05$ ). Error bars represent SEM.

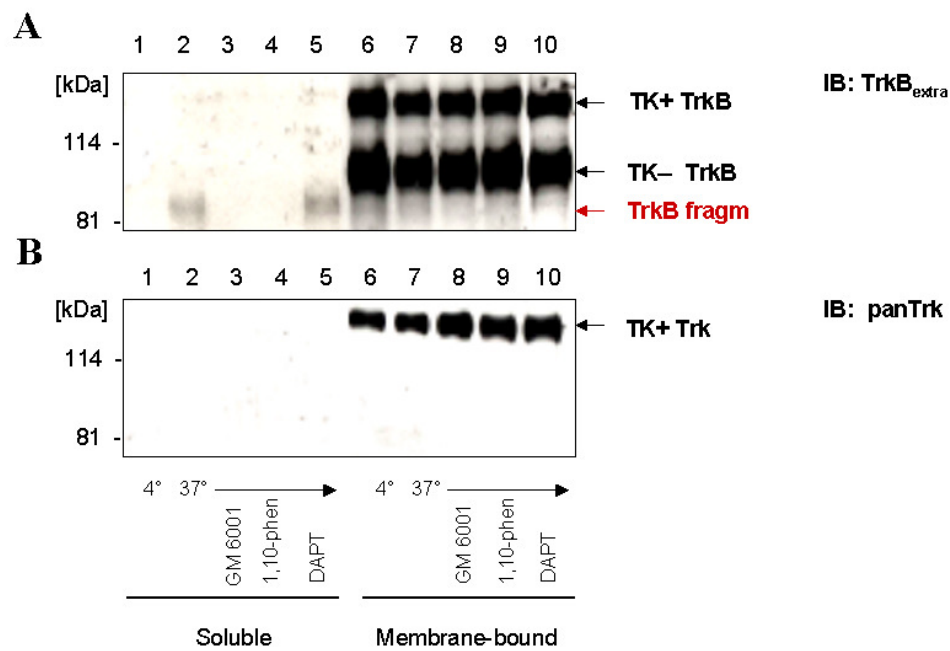


**Figure 23. Ectodomain shedding of TrkB.**

Brain membranes of 2–3-month-old C57BL/6J mice were prepared under P+ lysis conditions and incubated for 2 h at 4°C (lanes 1, 6) or at 37°C (lanes 2–5, 7–10) in the absence (controls, lanes 2, 7) or presence of the matrix metalloprotease inhibitors GM 6001 (50  $\mu$ M; lanes 3, 8) or 1,10-phenanthroline (5 mM; lanes 4, 9), or of 1  $\mu$ M of the  $\gamma$ -secretase inhibitor DAPT (lanes 5, 10). The samples were separated into supernatant (lanes 1–5) and membrane pellet (lanes 6–10). The supernatants and pellets were analyzed by immunoblotting (IB) using an antibody specific for the extracellular part of TrkB (TrkB<sub>extra</sub>) (A) and the panTrk antibody (panTrk) (B). Full-length (TK+ TrkB) and truncated TrkB (TK- TrkB) were membrane associated, whereas the shedding of TrkB resulted in an 80-kDa soluble extracellular TrkB fragment (TrkB fragm, shown by red arrow). The matrix metalloprotease inhibitors GM 6001 and 1,10-phenanthroline inhibited the shedding, in contrast to the  $\gamma$ -secretase inhibitor DAPT which had no effect (A). With the panTrk antibody, only full-length Trk (TK+) was detectable in the membrane pellet, but no proteolytic processing of intracellular Trk fragments was shown under P+ conditions (B).

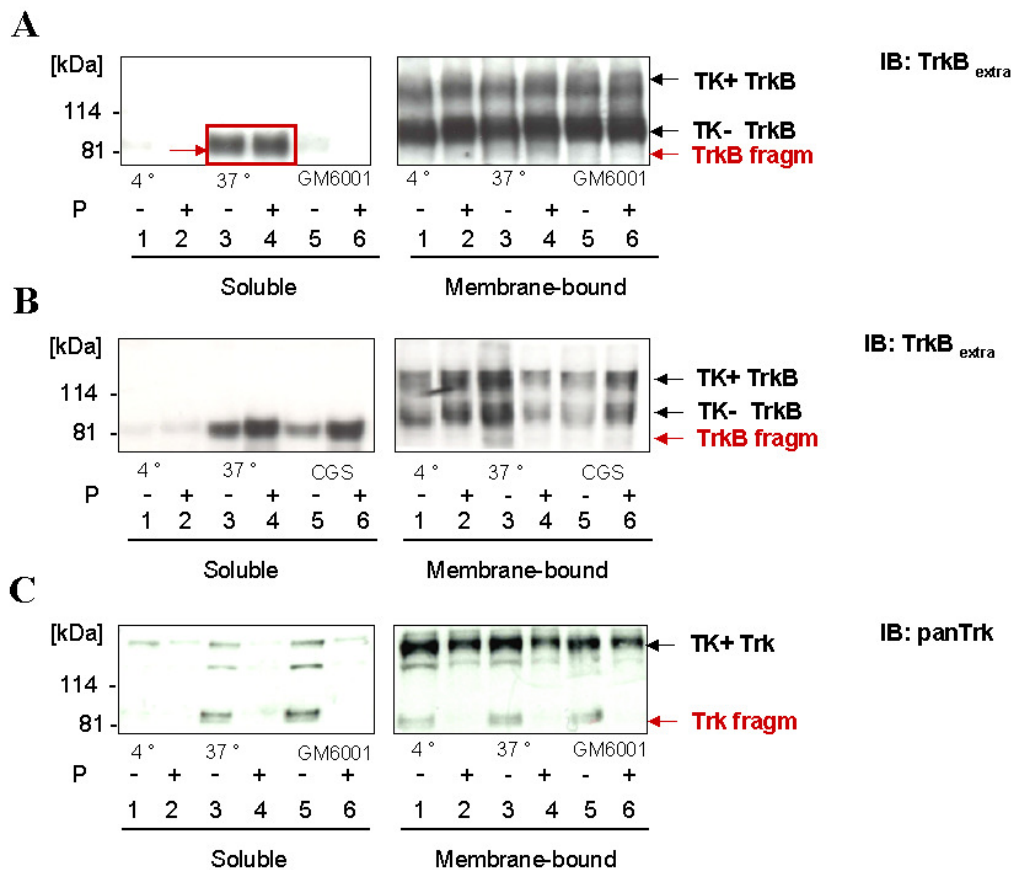


**Figure 24. Proteolysis of Trk and ectodomain shedding of TrkB.**

Brain membranes of 2–3-month-old C57BL/6J mice were prepared under P+ and also under P– lysis conditions and incubated for 2 h at 4°C (lanes 1, 2) or at 37°C (lanes 3–6) in the absence (controls, lanes 3, 4) or presence of 50  $\mu$ M of the matrix metalloprotease inhibitor GM 6001 (GM 6001) (lanes 5, 6). The samples were separated into supernatant (soluble) and membrane pellet (membrane-bound). The supernatants and pellets were analyzed by immunoblotting (IB) using an antibody specific for the extracellular part of TrkB (TrkB<sub>extra</sub>) (A) and the panTrk antibody (panTrk) (B). Full-length (TK+ TrkB) and truncated TrkB (TK– TrkB) were membrane associated, whereas the shedding of TrkB resulted in an 80-kDa soluble extracellular TrkB fragment (TrkB fragm) under P+ and P– conditions (indicated by the red arrow pointing to the red square) (A). Under P+ conditions there was no processed intracellular Trk (Trk fragm) observable but only TK+ Trk (B). Under P– conditions, two intracellular Trk fragments (indicated by the red arrow) were processed: an 80-kDa membrane-bound and an 80-kDa soluble Trk fragment, neither of which was inhibited by GM 6001 (B).

## 5.11 Ubiquitin/proteasome-dependent proteolysis of Trk and NCAM

Besides the classical ubiquitination of proteins and their degradation within the proteasome, a completely different processing pathway termed ‘regulated ubiquitin/proteasome-dependent processing’ (RUP) has recently been described (Hoppe *et al.*, 2000; Pickart, 2001; Klimschewski, 2003). Therefore, the question was addressed whether full-length Trk and NCAM undergo RUP resulting in the generation of processed 80-kDa protein frag-

ments. To investigate whether the detected NCAM and Trk fragments were indeed the products of ubiquitin-dependent proteolysis, specific proteasome inhibitors were tested in *in vitro* proteolysis assays.

After incubation of brain membranes of adult C57BL/6J mice for 2 h at 4°C or at 37°C in the absence or presence of the proteasome inhibitors ALL (ALL), MG262 (262) and MG132 (132), under lysis conditions inhibiting tyrosine kinase phosphorylation (P<sup>-</sup>) (Fig. 25) and conditions inhibiting dephosphorylation (P<sup>+</sup>) (data not shown), membranes were pelleted. The separated supernatants and pellets were analyzed by Western blot using the NCAM-specific antibody D3 (Fig. 25C) and the panTrk antibody (Fig. 25A, B). Release of a processed soluble 80-kD fragment was only detected in the supernatant analyzed for Trk protein (shown in Fig. 25B), whereas in the supernatant analyzed for NCAM no released soluble 80-kDa NCAM fragment was detectable (not shown). Under P<sup>+</sup> lysis conditions, only full-length Trk (TK<sup>+</sup> Trk) but no intracellular Trk fragment was observable in the membrane pellet (data not shown). This result confirms previous ones (Figs. 23B, 24C) under lysis conditions inhibiting dephosphorylation (P<sup>+</sup>). Samples from the membrane pellets that were incubated at 4°C showed no 80-kDa NCAM fragment, or only low amounts of it. In contrast, in the samples incubated at 37°C, a significantly higher amount of the proteolytically processed membrane-bound fragment was observable (Fig. 25C, compare lane 1 to lane 2). When the proteasome inhibitors were tested, only the inhibitor MG262 (Fig. 25C, lane 4) showed an inhibitory effect on the generation of the 80-kDa NCAM fragment. There was no difference between P<sup>+</sup> and P<sup>-</sup> lysis conditions when the membrane pellet was analyzed for the generation of the NCAM fragment. Accordingly, only the experiment under P<sup>-</sup> conditions is shown in Fig. 25C. The analysis of the supernatant using the panTrk antibody revealed that the increased amount of 80-kDa Trk fragment generated at 37°C without proteasome inhibitors was inhibited by the proteasome inhibitor MG132 (Fig. 25B, lane 5). When the membrane pellet was incubated at 37°C in the presence of the proteasome inhibitors MG262 (Fig. 25A, lane 4) and MG132 (lane 5), a significant difference was detected in comparison to the untreated 37°C sample (Fig. 25A, lane 2). After incubation at 37°C with MG262, higher amounts of the membrane-associated 80-kDa Trk fragment were found in the supernatant (lane 4), whereas incubation with MG132 at 37°C yielded a significantly lower amount of this fragment (lane 5). These experiments were performed twice, independently.

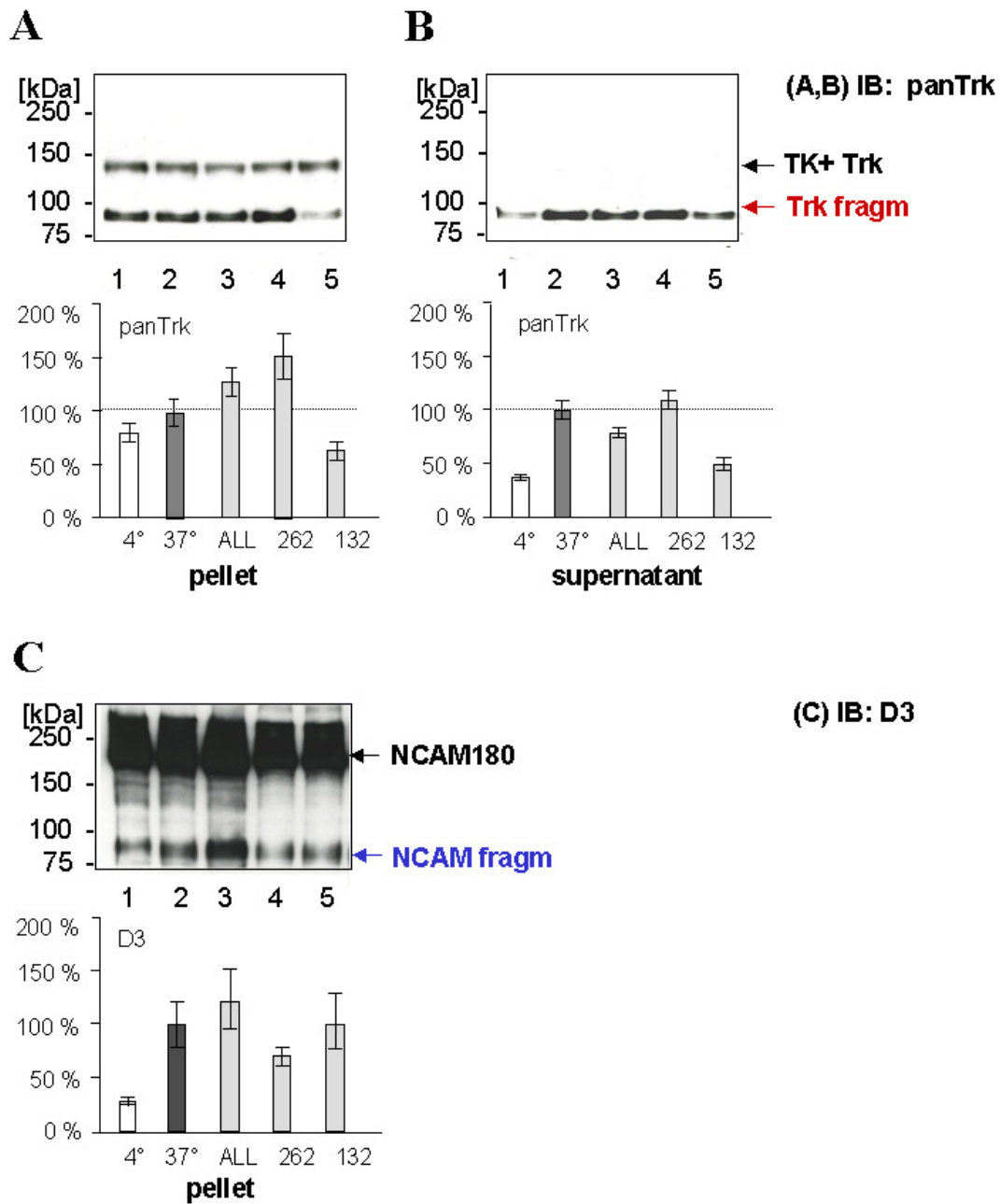


**Figure 25. Densitometric quantification of proteasome-dependent proteolysis of Trk and NCAM under P- lysis conditions.**

Brain membranes of adult C57BL/6J mice were incubated at 4°C (lane 1) and at 37°C (lanes 2–5) in the absence (lane 2) or presence of the proteasome inhibitors ALL (lane 3), MG262 (lane 4) and MG132 (lane 5), under lysis conditions inhibiting tyrosine kinase phosphorylation (P-). All proteasome inhibitors were used at a concentration of 50  $\mu$ M. The samples were separated into supernatant and membrane pellet. The supernatants (only the supernatant analyzed for Trk fragments is shown (B) since no soluble fragments were detected in the supernatant analyzed for NCAM fragments) and pellets (A, C) were analyzed by Western blot analysis using the panTrk antibody (A, B) and the NCAM180-specific antibody D3 (C). Arrows indicate the 80-kDa fragments after proteolytic processing of full-length NCAM180 (180 kDa) and Trk (TK+ Trk) (145 kDa). Similar results were obtained in at least two independent experiments. The densitometric quantification of the amounts of the 80-kDa fragments after proteolytic processing of full-length NCAM180 (180 kDa) (C) and Trk (145 kDa) (A, B) is presented below the corresponding representative Western blots of two independent experiments. Error bars represent SEM.

## 5.12 Ubiquitination of full-length NCAM

Since the proteasome inhibitors seem to have an effect on the generation of the NCAM and Trk fragments, the involvement of ubiquitin in this process was investigated. When proteasome-dependent proteolysis plays a role, the proteins that undergo this process will be labeled with one or several ubiquitin molecules by various enzymes (*e.g.* ubiquitin ligases). The hypothesis was that the ubiquitin labels should be detectable on the protein fragments and thus prove the participation of Trk and NCAM in proteasome-dependent proteolysis. To determine whether Trk, NCAM and their respective fragments were ubiquitinated, immunoprecipitation experiments were performed using a monoclonal mouse anti-ubiquitin antibody. Brain extracts were prepared from NCAM<sup>+/+</sup> and NCAM<sup>-/-</sup> mice under lysis conditions inhibiting dephosphorylation (P+) and inhibiting tyrosine kinase phosphorylation (P-). After incubation of the brain lysates, first without (Fig. 26A, lanes 1, 6–9) and then with proteasome inhibitors (Fig. 26A lanes 2–5, Fig. 26B), and subsequent immunoprecipitation with the anti-ubiquitin antibody, immune complexes were isolated using protein A/G agarose beads. Sample buffer was used for the elution of the bound proteins from the beads. To analyze whether the precipitated, ubiquitin-labeled proteins also comprised NCAM180 and Trk, the immune complexes were subjected to Western blot analysis with the NCAM-specific antibody D3 or the panTrk antibody.

When the immunoprecipitation was performed without any additional proteasome inhibitors during membrane incubation (Fig. 26A, lanes 1, 6–9), the NCAM180-specific antibody successfully precipitated NCAM180 detected by the D3 antibody (lanes 3, 5, 7, 9); however, when using the monoclonal mouse anti-ubiquitin antibody for immunoblotting, only a smear and no specific attachment of ubiquitin to NCAM180 was detectable (data not shown). After precipitation with the anti-ubiquitin antibody, no co-precipitated NCAM180 was observable (Fig. 26A, lanes 2, 4, 6, 8), indicating that NCAM180 is not ubiquitin-labeled under these conditions. Then, membranes were incubated with various proteasome inhibitors before precipitation. Fig. 20 shows immunoprecipitations after using the proteasome inhibitors ALL (A), MG132 and MG262 (B) for membrane treatment and then using the anti-ubiquitin antibody for subsequent precipitation, followed by Western blot analysis using the NCAM180-specific antibody D3 (Fig. 26) or the panTrk antibody (data not shown). When brain extracts of adult wild-type (NCAM<sup>+/+</sup>) mice were prepared under P+ and P- lysis conditions and treated with the inhibitor ALL, no ubiquitin label was seen on NCAM180 (Fig. 20A). However, when brain extracts of adult NCAM<sup>+/+</sup> and NCAM<sup>-/-</sup> mice were prepared under P+ lysis conditions and treated with the inhibitors MG132

(Fig. 26B, lanes 1-4) and MG262 (Fig. 26B, lanes 5-8), immunoprecipitation of ubiquitin also precipitated full-length NCAM180 (indicated by the arrow, lanes 3, 7), indicating that NCAM was ubiquitin-labeled under these conditions. The NCAM<sup>-/-</sup> control was negative (lanes 4, 8). Immunoprecipitations performed to detect ubiquitin molecules attached to Trk or Trk fragment were not successful (data not shown).

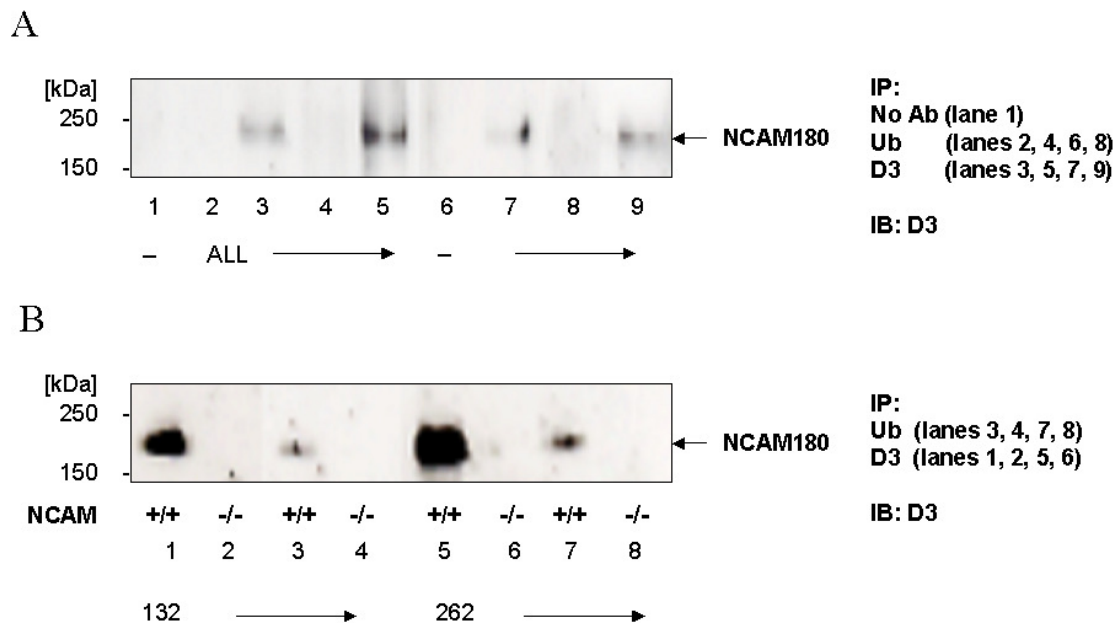


**Figure 26. Ubiquitination of full-length NCAM180.**

(A) Brain extracts of adult NCAM<sup>+/+</sup> mice were prepared under P+ and P- lysis conditions and were first incubated in the absence (A, lanes 1, 6-9) and then in the presence of the proteasome inhibitor ALL (A, lanes 2-5) before immunoprecipitations. (B) Brain lysates of adult NCAM<sup>+/+</sup> and NCAM<sup>-/-</sup> mice were prepared under P+ lysis conditions and incubated with the proteasome inhibitors MG132 (lanes 1-4) and MG262 (lanes 5-8). Ubiquitin was precipitated with a mouse monoclonal anti-ubiquitin antibody (Ub), and NCAM180 was precipitated with the NCAM180-specific antibody D3 for control. Fractions were subjected to SDS-PAGE and immunoblotting for analysis of anti-ubiquitin antibody-precipitated NCAM180, using the D3 antibody. Eluate from protein A/G agarose that had been treated without antibodies for negative control did not show any unspecific band (A, lane 1), while the NCAM180-specific D3 antibody detected NCAM180 in the anti-NCAM antibody precipitates (A, lanes 3, 5, 7, 9 and B, lanes 1, 5). Eluates from protein A/G agarose that had been pre-incubated either without (A, lanes 1, 6-9) or with the proteasome inhibitor ALL (A, lanes 2-5) did not show any ubiquitination of NCAM180 (A, lanes 2, 4, 6, 8). However, in the presence of MG132 and MG262, full-length NCAM180 was precipitated with the anti-ubiquitin antibody in three other experiments (B, lanes 3, 7, indicated by an arrow); however, ubiquitinated NCAM fragment was never detectable. There were no unspecific bands in the NCAM<sup>-/-</sup> controls (B, lanes 2, 4, 6, 8).

In summary, when the regular P+ or P- lysis conditions were used, NCAM was not precipitated by the monoclonal mouse anti-ubiquitin antibody. In contrast, when the proteasome inhibitors MG132 and MG262 were added to the lysis buffer, it was possible to detect ubiquitin conjugated to full-length NCAM180. However, no ubiquitin-labeled NCAM180 fragments were observable. This is probably due to the lower total amount of available

fragment and the high turnover rate of deconjugation of ubiquitin from the target proteins by de-ubiquitinating enzymes. Together, these data suggest that NCAM180 is likely to be involved in ubiquitin-dependent proteolysis.

### 5.13 Potential nuclear localization of the intracellular NCAM fragment

It is known that transmembrane receptors (*e.g.* p75<sup>NTR</sup> and Notch) play a pivotal role in signal transduction processes and undergo ‘regulated intramembrane proteolysis’ (RIP) involving site-specific and membrane-localized proteases. The IDs of these receptors are cleaved and the generated soluble fragments migrate into the nucleus to influence transcription (Hoppe *et al.*, 2001; Kanning *et al.*, 2003; Brown *et al.*, 2003; Selkoe and Kopan, 2003; Zampieri *et al.*, 2005). Recent studies have illuminated that the CAM L1 is also processed by RIP. Kalus (2005) showed, by using immunoprecipitations and immunohistochemistry, that after RIP an intracellular L1 fragment was generated and transported from the plasma membrane to the nucleus. Given that proteolytic processing seems to be involved when NCAM180-ID binds to TrkB-ID (see 5.6. and 5.10), the functional relevance of the processed intracellular NCAM and Trk fragments was investigated. Based on the observation that the ID of L1 was finally conveyed to the nucleus, the question arose whether the final destiny of the processed NCAM fragment was also the nucleus. Hence, immunoprecipitations were performed using the NCAM180-specific antibody D3 in isolated nuclear extracts. When only ten adult NCAM<sup>+/+</sup> and control NCAM<sup>-/-</sup> mouse brains were used for nuclear extract preparation, no intracellular NCAM fragment was detectable in this nuclear extract after immunoprecipitation with the NCAM180-specific antibody D3 (data not shown). However, when the nuclear extract was gained from the isolation of 20 adult NCAM<sup>+/+</sup> mouse brains, a weak but detectable intracellular NCAM fragment was found in the precipitate of this nuclear extract (Fig. 27, lane 4, indicated by the blue arrow). The synaptosomal fraction from NCAM<sup>+/+</sup> brains acted as control (Fig. 27, lanes 1, 2) instead of a nuclear extract from NCAM<sup>-/-</sup> brains. Another control for detection of unspecific binding was a nuclear extract, in which only protein A/G agarose beads without antibodies were applied (Fig. 27, lane 3). No unspecific bands were visible in the control without antibodies (Fig. 27, lane 1, 3), and the 180-kDa full-length isoform of NCAM was observable, as expected, in the control synaptosomal fraction (Fig. 27, lane 2). However, this preliminary result has to be reproduced using in parallel a nuclear extract that was gained from at least 20 control NCAM<sup>-/-</sup> mice.

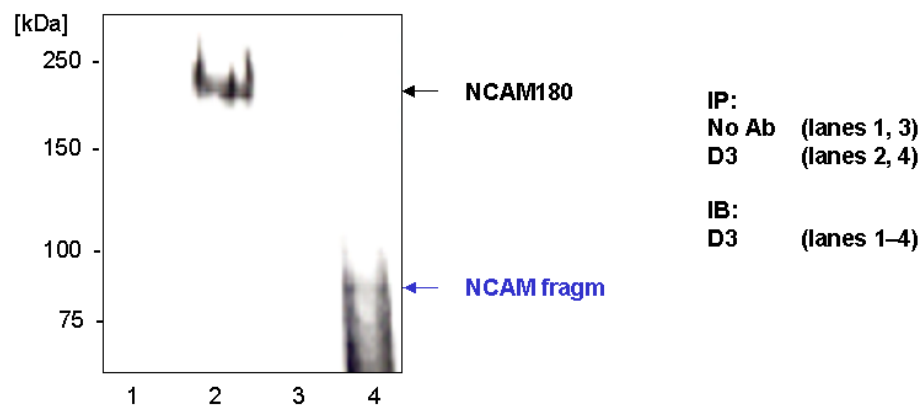


**Figure 27. Immunoprecipitation of intracellular NCAM180 fragment in nuclear extract.**

Nuclear brain extract (lanes 3, 4) and the synaptosomal subfraction (lanes 1, 2) of adult NCAM<sup>+/+</sup> mice were incubated with the NCAM-specific antibody D3 for immunoprecipitation (lanes 2, 4) or without antibody (lanes 1, 3) for controls. This was followed by incubation with Protein A/G Plus agarose. After SDS-PAGE, immunoblot analysis (IB) of the immunoprecipitates was performed using the NCAM-specific antibody D3 (lanes 1–4). A faint but detectable NCAM fragment (NCAM fragm, indicated by a blue arrow) was observable in the immunoprecipitate from the nuclear extract (lane 4) but not in the control precipitate without antibody (lane 3). The NCAM180-specific antibody D3 labeled full-length NCAM180 (NCAM180) in the immunoprecipitate of the synaptosomal fraction, indicating that the NCAM precipitation worked (lane 2).

## 5.14 The effect of BDNF stimulation on NCAM-induced neurite outgrowth

### 5.14.1 Using dissociated cerebellar cell culture

It is known that multiple interactions of CAMs such as NCAM (Cunningham *et al.*, 1987; Doherty *et al.*, 1990; Diestel *et al.*, 2003) as well as extracellular matrix and neurotrophic factors like BDNF with its respective receptor TrkB (Cohen *et al.*, 1994; Williams *et al.*, 2005) govern neurite outgrowth on the neuronal cell surface. To investigate the functional role of the interaction between NCAM and TrkB, the effect of BDNF on NCAM-dependent neurite outgrowth was tested. Neurite outgrowth did not occur in cerebellar neurons of NCAM-deficient mice. Consequently, homophilic binding is a prerequisite for NCAM-dependent neurite outgrowth (Williams *et al.*, 1994). Since it was shown that cerebellar neurons are responsive to neurotrophins and since especially TrkB and BDNF are highly expressed in the cerebellum (Kaplan *et al.*, 1991a; Kaplan *et al.*, 1991b; Segal *et al.*, 1995), dissociated primary cerebellar cell culture was initially chosen as a model system. However, the dissociated cell culture model (see 3.3.4) failed as an experimental approach as the positive control, laminin, did not yield the expected results. Therefore, as another positive control, native CHL1 protein was assayed, but also without success, followed by various

other optimization approaches (data not shown). Finally, we turned to a more robust model system, the cerebellar microexplant culture system, to analyze further the effects of BDNF on NCAM-dependent neurite outgrowth.

#### 5.14.2 Using cerebellar microexplant culture

To answer the question whether the interaction between NCAM and TrkB is involved in NCAM-dependent neurite outgrowth, a cerebellar microexplant culture system was chosen.

Fig. 28 presents the analysis of five independent neurite outgrowth assays, showing that BDNF stimulation inhibited the NCAM-induced neurite outgrowth in comparison to the unaffected positive control, laminin.

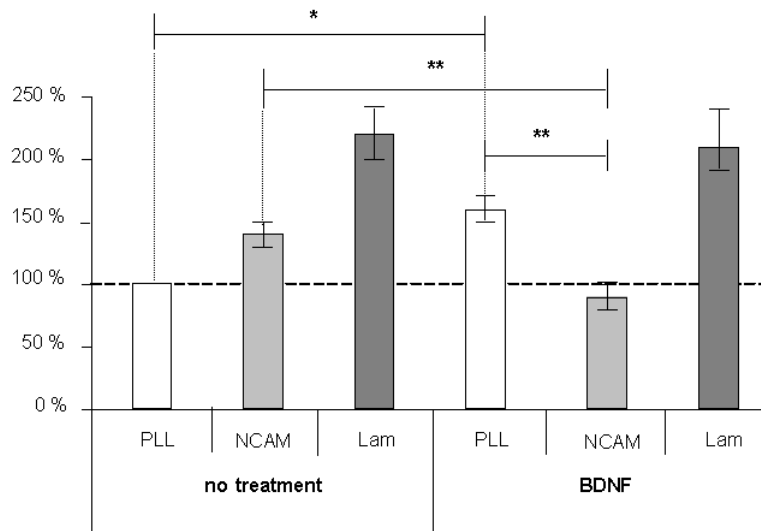


**Figure 28. Effect of BDNF on NCAM-induced neurite outgrowth.**

Cerebellar microexplant cultures were plated onto glass coverslips coated with PLL or a combination of PLL and NCAM (NCAM) or PLL and laminin (Lam). After maintenance in culture for 16 h, cells were incubated for 30 min with BDNF (50 ng/ml). After another 24 h of incubation, the explants were fixed and stained. The average neurite length on PLL substrate without treatment was defined as 100% and served as comparison for the other samples. Neurite outgrowth from the explants was quantified by measuring the ten longest neurites of 15 aggregates in five independent experiments. Error bars represent standard deviation and asterisks denote a statistical significance (Student's *t*-test; \*\*,  $p < 0.01$  and \*,  $p < 0.05$ ).

Promotion of neurite outgrowth of sensitive neuronal populations is known as an activity of neurotrophins (Kuffler, 1994; Lundborg *et al.*, 1994), although inhibitory effects of neurotrophins on neurite growth have also been described (Griffin and Letourneau, 1980). This inhibition of NCAM-induced neurite outgrowth was highly significant. However, poly-L-lysine (PLL) without treatment, which was used as a negative control, showed a positive effect on neurite outgrowth after BDNF treatment (Fig. 28). Furthermore, the involvement

of  $\alpha$ -2,8-linked PSA on NCAM-dependent neurite outgrowth after BDNF stimulation was documented by using the PSA-specific Endo-N enzyme that splits PSA chains from NCAM. The inhibitory influence of BDNF was slightly reduced after Endo-N treatment (Fig. 29). Loss of PSA seems to lead to less inhibition of NCAM-dependent neurite outgrowth after BDNF stimulation. To exclude effects by endogenous BDNF, neurite outgrowth assays were performed in the presence of K252a, which specifically inhibits Trk tyrosine kinase activity when used at low concentrations (Tapley *et al.*, 1992; Segal *et al.*, 1995). Blockage of endogenous BDNF resulted in a minor but still significant inhibitory effect of BDNF on NCAM-dependent neurite outgrowth (Fig. 29). The analysis of the neurite outgrowth assays confirmed the hypothesis of a functional interplay between NCAM and TrkB.

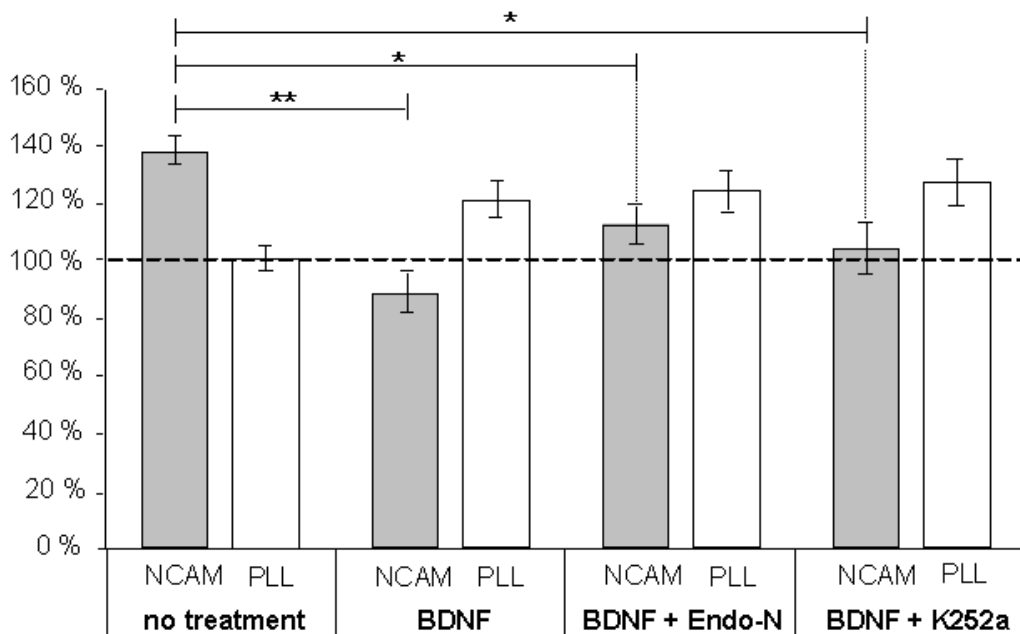


**Figure 29. Effect of BDNF with or without Endo-N and K252a on NCAM-induced neurite outgrowth.**

Cerebellar microexplant cultures were plated onto glass coverslips coated with PLL (PLL) or a combination of PLL and NCAM (NCAM). After incubation for 16 h, cells were incubated for 30 min with BDNF. The tyrosine kinase inhibitor K252a was added for 1 h (100 nM) before BDNF stimulation (50 ng/ml) and the enzyme Endo-N was applied at 85 ng/ml. After another 24 h of incubation, the explants were fixed and stained. The average neurite length on PLL substrate without treatment was defined as 100% and served as comparison for the other samples. The effect of BDNF stimulation with or without Endo-N and K252a on neurite outgrowth from the explants was quantified by measuring the ten longest neurites of 15 aggregates in at least two independent experiments. Error bars represent standard deviation and asterisks denote a statistical significance (ANOVA and Tukey; \*\*,  $p < 0.01$ , \*,  $p < 0.05$ ).

## 6 Discussion

For quite some time now, a potential interaction between the two molecules NCAM and TrkB has been speculated about. Based on several lines of evidence, it has been hypothesized that the binding would take place extracellularly. One explanation model proposed a direct interaction between PSA-NCAM and BDNF/TrkB causing altered signaling. Another model suggested that PSA-NCAM indirectly facilitates the binding and activation of BDNF *via* modification of cell adhesion (Charles *et al.*, 2000; Muller *et al.*, 2000; Vutskits *et al.*, 2001).

In contrast, the hypothesis we set out to prove in this study proposes an intracellular interaction between NCAM and TrkB. First, observations from a phage display analysis provided evidence that TrkB may be considered as a potential binding partner of NCAM180: A peptide in TrkB-ID was identified that bound to a peptide in NCAM180-ID. Then, the interaction between TrkB-ID and NCAM-ID was shown by using *in vitro* binding studies, biochemical cross-linking, and co-immunoprecipitation assays, followed by functional assays.

### 6.1 Characterization of the NCAM180–TrkB interaction

According to the results of the phage display analysis, the identified peptide sequence within TrkB-ID that bound to NCAM180-ID is located within the activation loop in the tyrosine kinase domain and is flanked by the active site and the autophosphorylated tyrosine residues (see 5.1, Fig. 8). Since this is the putative binding site within TrkB-ID, the activation or phosphorylation state of TrkB is very likely to play an important role in regulating the binding between the two proteins. Often phosphorylation is either a prerequisite for an interaction between certain proteins or it regulates their binding capability, *e.g.* Fyn only binds to TrkB after autophosphorylation (Iwasaki *et al.*, 1998).

Since TrkB is able to tyrosine phosphorylate various binding partners, one may speculate that the tyrosine near the juxtamembrane region of NCAM is phosphorylated by TrkB during or before the interaction. A recent study (Diestel *et al.*, 2004) showed, by using phospho-amino acid analysis, that indeed the tyrosine at position 734 of human NCAM180 (Y734) can be phosphorylated. When Y734 was exchanged to phenylalanine (Y734F), NCAM180 was, consequently, not tyrosine phosphorylated and non-stimulated NCAM-mediated neurite outgrowth was enhanced in addition to higher FGFR and extracellular signal-regulated kinase 1 (ERK1) activity. In this case, the interactions with cytoskeletal

components were decreased. Since downstream activation of the transcription factor CREB was not observed, it is very likely that at least one so far unknown other FGFR-independent pathway is activated (Diestel *et al.*, 2004). One could hypothesize that this unknown pathway may be involved in the binding between NCAM180 and TrkB. Furthermore, tyrosine-phosphorylated NCAM180 rather stabilizes cell–cell contacts *via* cytoskeletal components (*e.g.* spectrin) (Pollerberg *et al.*, 1987) than promote neurite outgrowth. Probably, phosphorylation of Y734 within NCAM180-ID leads to the stabilization of an NCAM180-specific tertiary structure (Diestel *et al.*, 2004).

ELISA experiments (see 5.3) revealed that NCAM180-ID bound to TrkB-ID, or to the TrkB peptide discovered in the phage display analysis as containing the putative NCAM180-ID binding site. Interestingly, in the ELISA experiments, NCAM180 but not the NCAM exon 18 alone bound to TrkB-ID (see 5.3, Fig. 11C). Furthermore, binding was detected between NCAM180-ID and the TrkB peptide when bound NCAM180-ID was assessed by either the exon 18-specific antibody D3 or the P61 antibody with the N-terminally located epitope. Surprisingly, no specific binding signal was detected when the antibody 5B8 with the C-terminally located epitope was used (Fig. 11B). This indicates that the antibody 5B8 could not bind either because the epitope was occupied by the TrkB peptide or because the peptide was in competition with the antibody 5B8 for the common substrate NCAM180-ID. These results confirm that the binding site within NCAM is definitely located in an overlapping region between NCAM exon 18 and the C terminus of NCAM180-ID and NCAM140-ID.

To investigate the influence of the phosphorylation state of TrkB on the binding to NCAM180-ID, unphosphorylated and phosphorylated TrkB-ID (TrkB-ID/pTrkB-ID) was used in the ELISA after *in vitro* preparation. Unexpectedly, no difference in binding to NCAM180-ID was observable between TrkB-ID and pTrkB-ID (data not shown). This implies that the binding between NCAM180-ID and TrkB-ID may not depend on the phosphorylation state of TrkB-ID. However, one has to take into consideration that conformational changes in an *in vitro* assay such as the ELISA might differ from those in an *in vivo* assay. For instance, the cross-linking and co-immunoprecipitation assays showed that lysis buffer conditions inhibiting dephosphorylation (P+) facilitated the detection of the binding between the two proteins in comparison to conditions inhibiting tyrosine kinase phosphorylation (P–). A direct interaction between a Trk fragment and NCAM180-ID under P+ lysis conditions has been shown in a modified cross-linking approach (see 5.5).

According to the hypothesis that TrkB is proteolytically cleaved before or after binding to NCAM180-ID, the cross-linking protocol was further optimized in order to show a binding between full-length TrkB and NCAM180-ID. Not only the phosphorylation conditions but also the presence of certain protease inhibitors such as the matrix metalloprotease inhibitor GM 6001 and the  $\gamma$ -secretase inhibitor DAPT in the lysis buffer was shown to be necessary in order to detect the interaction between full-length TrkB and NCAM180-ID (see 5.6, Fig. 14). The specificity of the NCAM binding to TrkB was checked by using the ID of CHL1 and NCAM140 as negative controls in the above-mentioned assays. Taken together, these results implicate that the interaction requires conditions in which phosphorylation is enhanced (*via* inhibition of dephosphorylation) without the necessity of having TrkB phosphorylated itself. This might also indicate that TrkB tyrosine phosphorylates NCAM180.

The cross-linking experiments did not only show a direct interaction between full-length TrkB (TK+ TrkB) and NCAM180-ID but also with the truncated isoform (TK- TrkB). This is surprising since we could prove, in accordance with our hypothesis, that the interaction would take place intracellularly. In addition, TK- TrkB does not contain the binding site within TrkB-ID that was revealed in the phage display analysis. One explanation would be that TK- TrkB has formed heterodimers with TK+ TrkB before, during or after the interaction with NCAM180. For instance, Ohira *et al.* (2001) have shown in monkey cortex that TK+ TrkB and TK- TrkB extracellularly form hetero- and homodimers with each other. Probably, TK+ TrkB meets NCAM180-ID as a heterodimer with extracellularly bound TK- TrkB. In that case the biotin label attached to the cross-linker-NCAM180-ID complex would have been transferred to the direct binding partner, namely the heterodimer complex consisting of full-length and truncated TrkB. One has to take into account that a prerequisite for such interplay between TK+ TrkB, TK- TrkB and NCAM180 would be the corresponding tertiary protein structure that would allow this. This presumption, which needs solid proof, should be investigated in future studies. The functional role of TK- TrkB, which is still elusive, might influence or even regulate the interaction between TK+ TrkB and NCAM180. Such future investigations might be interesting from a functional point of view since the expression of the TrkB isoforms changes during development. TK- TrkB becomes more prevalent with increasing age and during adulthood whereas TK+ TrkB is the predominant form during development (Allendorfer *et al.*, 1994; Escandón *et al.*, 1994). Moreover, TK- TrkB receptors have been shown to be up-regulated in the hippocampus of Alzheimer's and Huntington's disease patients (Connor *et al.*, 1996). So far, an increasing amount of data indicates that the truncated isoforms could either trap the

catalytic TK+ TrkB by homophilic interaction or act as dominant-negative inhibitors (Fryer *et al.*, 1997).

Furthermore, it is important to mention that the above-mentioned interactions were also detectable in the isolated particular synaptosomal fraction from mossy fibers (see 5.6, Fig. 14B). When the isolated mossy fiber fraction was used for cross-linking experiments, the amount of Trk fragment bound to NCAM-ID was lower and the amount of TK+ TrkB was higher in comparison to the isolated brain fraction. This implicates that the interaction in the hippocampal mossy fiber fraction might be involved in synaptic plasticity (Lysetskiy *et al.*, 2005).

In order to explain why the above-mentioned inhibitors, GM 6001 and DAPT, turned out to be essential components of the lysis buffer for detection of the interaction between full-length TrkB and NCAM180-ID, *in vitro* proteolysis assays were performed. For the first time in this study, the shedding of TrkB was shown, which was in fact independent of the phosphorylation conditions (see 5.10). The generation of an 80-kDa soluble extracellular TrkB fragment was inhibited by GM 6001, whereas DAPT applied alone had no effect. It is very likely that the shedding of the extracellular part of TrkB initiates the regulated intramembrane proteolysis (RIP) as it has been described for another member of the neurotrophin receptor family, p75<sup>NTR</sup> (Schechterson *et al.*, 2002). The cleavage of p75<sup>NTR</sup> is modulated by the sequential action of (1)  $\alpha$ -secretase leading to the production of an ectodomain fragment and (2)  $\gamma$ -secretase leading to the subsequent presenilin-dependent cleavage of intracellular fragments which are liberated into the cytosol. This reveals a new mechanism for transmitting neurotrophin signals from the cell surface to intracellular sites, with implications of intracellular and nuclear signaling functions *via* specific proteases (Chao, 2003; Kanning *et al.*, 2003). Furthermore, presenilin seems to be necessary for TrkB receptor maturation (Naruse *et al.*, 1998). However, in this study, a positive or negative effect on proteolysis when DAPT was applied at the same time with GM 6001 (data not shown) was not detectable. For future studies, it is suggested to search again in detail for very small processed fragments after a potential cut by  $\gamma$ -secretase. Probably, yet another protease is responsible for an intracellular cut close to the membrane.

Moreover, it has been reported in the literature that TrkA is involved in shedding, with a high sensitivity to metalloprotease inhibitors and with CaM as a regulator of this processing event. This process is independent of CaM–substrate interaction (Diaz-Rodriguez *et al.*, 2000). First, Diaz-Rodriguez *et al.* (2000) have shown that CaM inhibitors trigger the re-

lease of several cell-bound fragments and of a soluble TrkA fragment. Later, CaM has been shown to directly interact with the C terminus of TrkA. Beyond that, CaM co-precipitation studies demonstrated that endogenous TrkB and TrkC receptors are also associated with CaM. In addition, CaM inhibition induced the generation of an intracellular tyrosine phosphorylated 41-kDa TrkA fragment that was able to recruit PLC $\gamma$  and Shc adaptor proteins (Llovera *et al.*, 2004). However, in this study, cleavage of TrkB was not induced by the CaM inhibitor CGS9343B (CGS), and CGS did not have an effect on TrkB shedding (see 5.10). Yet, shedding not only plays a role for TrkB but also for NCAM. Kalus (2005) investigated the NCAM shedding that is inhibited by GM 6001 (110-kDa soluble NCAM) in *in vitro* proteolysis assays. These results provide evidence that proteolytic processing and shedding might probably regulate the interaction between the two molecules. According to the hypothesis of an intracellular binding, proteolytic processing at intracellular sites of Trk was investigated (5.10).

Surprisingly, proteolytic processing of intracellular Trk fragments did not take place under dephosphorylation-inhibiting (P+) conditions, neither in the supernatant nor in the membrane pellet, as verified by using the panTrk antibody. In contrast, under lysis conditions inhibiting tyrosine kinase phosphorylation (P-), the intracellular soluble and the intracellular membrane-bound 80-kDa Trk fragment were generated, but none of them was inhibited by GM 6001. These results imply that the inhibition of tyrosine kinase phosphorylation may be a prerequisite for the subsequent proteolytic processing of the intracellular Trk fragment. This result is in contrast to the one of Llovera *et al.* (2004) who described a tyrosine-autophosphorylated 41-kDa TrkA fragment from the ID of the protein.

In summary, it is concluded that an interaction between full-length TrkB and NCAM180-ID requires conditions in which dephosphorylation is inhibited, because in that case Trk-ID does not undergo any proteolytic processing events. One explanation could be that when tyrosine kinase phosphorylation is inhibited, more full-length Trk is processed instead of binding to NCAM180. The questions that arise from this study are: How is the proteolytic processing of NCAM and Trk regulated when downstream adapter proteins are phosphorylated and how are signaling cascades influenced by this?

Recently, a completely different processing pathway termed 'regulated ubiquitin/proteasome-dependent processing' (RUP) has been described (Hoppe *et al.*, 2000; Pickart, 2001; Klimschewski, 2003). Since the responsible protease involved in the proteolytic processing of Trk-ID was not identified, the question was addressed whether full-length Trk and NCAM undergo RUP resulting in the generation of processed 80-kDa pro-

tein fragments. To investigate whether the detected NCAM and Trk fragments were indeed the products of ubiquitin-dependent proteolysis, specific proteasome inhibitors were tested in *in vitro* proteolysis assays. Although the ubiquitination of membrane receptors (Levkowitz *et al.*, 1998; Kerkhof *et al.*, 2001) and receptor tyrosine kinases has been recognized to be important for appropriate receptor trafficking and degradation (Hicke and Dunn, 2003), not much was known about the ubiquitination of TrkB until a very recent study. Makkerh *et al.* (2005) have shown that TrkB receptors are involved in an intense BDNF-induced poly-ubiquitination. This process seems to depend on activation of the endogenous TrkB activity and is greatly decreased in the presence of the co-receptor p75<sup>NTR</sup> (Makkerh *et al.*, 2005).

In this study, however, the detection of ubiquitinated Trk or TrkB in a co-immunoprecipitation assay was not successful. An explanation could be that in adult brain the abundance of p75<sup>NTR</sup> would interfere with ubiquitination of Trk. In contrast, Makkerh *et al.* (2005) have chosen cortical neurons from E16 mice which express abundant TrkB but little p75<sup>NTR</sup> (Bhakar *et al.*, 2003).

Multiple investigations have provided evidence that p75<sup>NTR</sup> and Trks are characterized by intense cross-talk (Huang and Reichardt, 2003; Chao, 2003; Gascon *et al.*, 2005). On the one hand, expression of p75<sup>NTR</sup> can enhance the affinity of the Trks to their respective ligands (Horton *et al.*, 1997; Chao, 2003). On the other hand, Trks are in turn capable of silencing p75<sup>NTR</sup> signaling (Barrett *et al.*, 1998). For instance, sequential activation of the p75<sup>NTR</sup> and TrkB receptors has been shown to be responsible for the dendritic development of neuronal progenitor cells (Gascon *et al.*, 2005). In order to get a more complete picture of the regulatory and functional role of the proven interaction between TrkB and NCAM180, it is therefore suggested to include p75<sup>NTR</sup> in future studies.

In the present study, however, it was shown that NCAM seems to be ubiquitinated, which was not investigated before (see 5.12, Fig. 26). When the regular P+ or P- lysis conditions were used, NCAM was not precipitated by the monoclonal mouse anti-ubiquitin antibody. In contrast, when the proteasome inhibitors MG132 and MG262 were added to the lysis buffer, it was possible to detect ubiquitin conjugated to full-length NCAM180, implicating the involvement of NCAM in ubiquitination or RUP. However, no ubiquitin-labeled NCAM180 fragments were observable. This is probably due to the lower total amount of available fragment and the high turnover rate of deconjugation of ubiquitin from the target proteins by de-ubiquitinating enzymes. Together, these data suggest that NCAM180 is likely to be involved in ubiquitin-dependent proteolysis.

In *in vitro* proteolysis assays, the effect of proteasome inhibitors on Trk and NCAM processing was investigated. There was no difference between P+ and P- lysis conditions when the membrane pellet was analyzed for the generation of the NCAM fragment, which was slightly inhibited by the proteasome inhibitor MG262 (see 5.11, Fig. 25). The increased amount of the soluble 80-kDa Trk fragment was inhibited by the proteasome inhibitor MG132. Yet, the amount of membrane-associated Trk fragment was increased in the presence of the proteasome inhibitor MG262, whereas a significantly lower amount of this fragment was yielded in the presence of MG132. It remains to be investigated further why the proteasome inhibitors have inhibitory as well as enhancing effects on the generation of the processed fragments.

Rape and Jentsch (2004) have proposed a new model for RUP: After ubiquitination of the substrate, which is catalyzed by the ubiquitin-activating enzyme (E1), the ubiquitin-conjugating enzyme (E2), and the ubiquitin ligase (E3), processing is induced by translocation of flexible domains into the proteasome. These flexible parts can be located at the N- or C-terminal ends of the proteins or within internal protein loops. Degradation runs towards both ends of the polypeptide chain; however, this process stops when tightly folded protein domains are reached by the proteasome. The proteasome selects specific protein segments for degradation that are free of barriers; in contrast, the folded domains (and sequences beyond this domain) are left intact. The above-said model was established for transcription factors (*e.g.* the mammalian NF- $\kappa$ B family and the yeast proteins SPT23 and MGA2). Transcription factors are processed following dimerization of the processing substrate with a second molecule which serves as a processing template. Indeed, complexes of processed and unprocessed precursors have been described for both NF- $\kappa$ B1/2 and SPT23/MGA2 *in vivo* (for review see Rape and Jentsch, 2004). So far, neither NCAM nor Trk have been known for their involvement in RUP. This model might, however, explain why certain expected released fragments were not detectable (see 5.10). Probably, full-length NCAM or Trk are partially degraded into small peptides according to the classical ubiquitination, but other parts might undergo proteolytic processing in order to yield protein fragments with various biological functions. From this study, we conclude that after binding of NCAM180 and TrkB to each other, dimerization of both molecules takes place, followed by proteolytic processing. As both the NCAM and the Trk fragments have a molecular weight of 80 kDa, dimerization with each other has to be involved since NCAM180-ID has a molecular weight of 39 kDa and TrkB-ID has 41 kDa.

Both the ubiquitin-proteasome system (UPS) and the ubiquitin-like modifier systems (UBLs) such as SUMO seem to influence each other, but how exactly is poorly understood (Jentsch und Pyrowolakis, 2000). For instance, SUMO seems to act as an antagonist to ubiquitin or functions as regulator in protein–protein interactions. It is very likely that SUMO enhances the stability or mediates the subcellular location of proteins (for review see Melchior, 2000; Müller *et al.*, 2001). Since both NCAM180-ID and TrkB-ID contain several SUMOlation sites (motifs with high probability) according to a SUMOplot Prediction (see 4.5), future investigation of the SUMOlation of NCAM and TrkB is also suggested.

In addition, co-immunoprecipitation studies under the P+ lysis conditions have confirmed an interaction between TrkB and full-length NCAM180 in the ‘natural environment’ of the cell membrane within the brain. Also, the 80-kDa NCAM fragment has been shown to be associated with this complex (see 5.7). However, it was impossible to demonstrate any direct physical interaction of TrkB and NCAM by co-capping experiments (see 5.8). It is very likely that these experiments failed due to conformational changes of the two proteins that resulted in masking of the antibody epitopes.

## 6.2 Functional analysis of the NCAM180–TrkB interaction

In this study, the functional importance of this newly described binding between the two proteins NCAM180 and TrkB was further characterized by investigating the effect of BDNF on NCAM-dependent neurite outgrowth. The appropriate outgrowth of axons and dendrites, *i.e.* neurite formation, has an immense importance for the regeneration process after injuries in the nervous system. During this remodeling process, multiple soluble or substrate-bound guidance molecules influence the growth cone, which consists of actin microfilaments and microtubules during growth (Mueller, 1999). It is widely accepted that multiple interactions of CAMs such as NCAM (Cunningham *et al.*, 1987; Doherty *et al.*, 1990; Diestel *et al.*, 2004) as well as neurotrophic factors like BDNF with its corresponding receptor TrkB (Cohen *et al.*, 1994; Williams *et al.*, 2005) govern neurite outgrowth on the neuronal cell surface. To answer the question whether the interaction between NCAM and TrkB is involved in NCAM-dependent neurite outgrowth, a cerebellar microexplant culture system was chosen. BDNF stimulation inhibited the NCAM-induced neurite outgrowth as compared to the unaffected positive control, laminin. This inhibition of NCAM-induced neurite outgrowth was highly significant. Although promotion of neurite outgrowth is a well-known activity of neurotrophins (Kuffler, 1994; Lundborg *et al.*, 1994), inhibitory

effects of neurotrophins on neurite growth have also been described (Griffin and Letourneau, 1980). Furthermore, the involvement of  $\alpha$ -2,8-linked PSA on NCAM-dependent neurite outgrowth after BDNF stimulation was documented by using the PSA-specific Endo-N enzyme, which splits PSA chains from NCAM. The inhibitory influence of BDNF was slightly reduced after Endo-N treatment (see 5.14, Fig. 29). Loss of PSA seems to lead to less inhibition of NCAM-dependent neurite outgrowth after BDNF stimulation. To exclude effects by endogenous BDNF, neurite outgrowth assays were performed in the presence of K252a, which specifically inhibits Trk tyrosine kinase activity when used at low concentrations (Tapley *et al.*, 1992; Segal *et al.*, 1995). Blockage of endogenous BDNF resulted in a minor but still significant inhibitory effect of BDNF on NCAM-dependent neurite outgrowth. The analysis of the neurite outgrowth assays confirmed the hypothesis of a functional interplay between NCAM and TrkB. Homophilic interaction takes place between NCAM molecules (Walmod *et al.*, 2004) and leads to the stimulation of neurite outgrowth based on the activation of two pathways: Heterophilic interaction (between NCAM and FGFR) and activation of the FGFR first triggers the PLC $\gamma$ -mediated pathway and then the Ras–MAPK pathway *via* activation of Fyn and FAK after preferential binding to NCAM140 (Beggs *et al.*, 1997; Povlsen *et al.*, 2003). Recently, PI3K also has been implicated in the NCAM-mediated signaling (Ditlevsen *et al.*, 2003). To illuminate the functional role of the intracellular domains of both NCAM isoforms on neurite outgrowth, NCAM140-ID and NCAM180-ID (including the TMD) were chosen for overexpression studies in PC12 cells. When NCAM140-ID was overexpressed, NCAM-mediated neurite outgrowth was decreased because NCAM140-ID seems to compete with endogenous NCAM140 for Fyn and FAK, the activators of the Ras–MAPK pathway. This is in contrast to the overexpressed NCAM180-ID which stimulated neurite outgrowth but normally increased stabilization and cell adhesion due to a competition between cytoskeletal proteins (*e.g.* spectrin) and endogenous NCAM180 (Büttner *et al.*, 2004). Based on the results of Büttner *et al.* (2004), a hypothetical model was developed to explain the inhibitory effect of BDNF on NCAM-mediated neurite outgrowth (see 5.14, Fig. 29). Receptor tyrosine kinases such as TrkB use signaling pathways similar to those utilized by NCAM, including common interaction partners such as the non-receptor tyrosine kinase Fyn (Beggs *et al.*, 1997; Iwasaki *et al.*, 1998). Fyn has been shown to be associated with TrkB-ID. This interaction is dependent on autophosphorylation of TrkB and on BDNF induction (Iwasaki *et al.*, 1998). It is suggested that after BDNF stimulation Fyn binds to autophosphorylated

TrkB. Thereby, TrkB competes with NCAM140 for Fyn, which consequently might cause less activation of the Ras–MAPK pathway and reduced neurite outgrowth.

Some transmembrane proteins that are involved in signal transduction events undergo RIP. Their released intracellular fragments have been shown to migrate to the nucleus as transcriptional regulators (Hoppe *et al.*, 2001; Kanning *et al.*, 2003; Brown *et al.*, 2003; Selkoe and Kopan, 2003; Zampieri *et al.*, 2005). Preliminary data from this work provides some evidence that the final destiny of the processed NCAM fragment might be also the nucleus, implicating a potential role in alteration of transcription: A weak but detectable intracellular NCAM fragment was found in the precipitate of the nuclear extract from NCAM<sup>+/+</sup> mice (see 5.13, Fig. 27). However, this preliminary result has to be confirmed not only with co-immunoprecipitation assays but also with another method. Such a process has already been reported for another CAM: L1 undergoes RIP and the L1 fragment was detected in the nucleus after transport from the plasma membrane (Kalus, 2005).

After identification of TrkB as a potential binding partner for NCAM-ID using phage display analysis, sequence alignments revealed that a peptide sequence in NCAM-ID showed homology to a peptide sequence in the inwardly rectifying K<sup>+</sup>-channels of the Kir3 family (see 5.1 and 5.2). NCAM regulates the trafficking of the neuron-specific Kir3 heterodimer subunits to the cell surface by as yet unknown mechanisms (Delling *et al.*, 2002). Activated TrkB determines the open-state of the Kir channels by phosphorylation: Stimulation of TrkB results in tyrosine phosphorylation of the Kir3.4 but not the Kir3.2 subunit and leads to an inhibition of the basal activity of this channel (Wischmeyer *et al.*, 1998; Rogalski *et al.*, 2000; Ippolito *et al.*, 2002). In this study, cross-linking experiments have shown an association between the Kir3.3 channel, NCAM and TrkB (5.5). Therefore, it is hypothesized that TrkB competes with Kir3.3 for NCAM-ID. TrkB increases the Kir3.3 but not the Kir3.2 or Kir3.4 currents, which are reduced by NCAM180 (in collaboration with Dr. Erhard Wischmeyer, Universität Würzburg, Germany, unpublished data). Thus, both NCAM and TrkB seem to share a common mechanism of regulation of ionic homeostasis that determines the excitability of neurons.

In summary, although the exact regulation mechanisms of the NCAM–TrkB binding based on proteolytic processing remain to be elucidated, this study showed for the first time an interaction between NCAM and TrkB. Furthermore, first insights into the functional impact of this interaction were provided.

## 7 Summary

For quite some time now, it has been hypothesized that the two molecules NCAM and TrkB interact with each other extracellularly *via* PSA-NCAM and BDNF (Charles *et al.*, 2000; Muller *et al.*, 2000; Vutskits *et al.*, 2001).

In contrast, the hypothesis we set out to prove in this study proposes an intracellular interaction between NCAM and TrkB. First, observations from a phage display analysis provided evidence that TrkB may be considered as a potential binding partner of NCAM180: A peptide in TrkB-ID was identified that bound to a peptide in NCAM180-ID. The major aim of this work was to characterize the potential binding between NCAM180-ID and TrkB-ID including a potential functional relevance. For this purpose, biochemical cross-linking, co-immunoprecipitation assays and binding studies were performed. ELISA experiments revealed that NCAM180-ID bound to TrkB-ID, or to the TrkB peptide discovered in the phage display analysis as containing the putative NCAM180-ID binding site. In the ID of the 180-kDa NCAM isoform, a peptide motif that binds to a peptide sequence in the tyrosine kinase domain of TrkB was identified. This peptide motif in NCAM180 shows sequence similarities with the C terminus of the Kir3.3 isoform, but not with the other three isoforms of this potassium channel. Epitope mapping showed that the binding site within NCAM is located in an overlapping region between the NCAM exon 18 and the C terminus of NCAM180-ID and NCAM140-ID. To show a binding between full-length TrkB and NCAM180-ID *via* biochemical cross-linking, not only the phosphorylation conditions but also the presence of certain protease inhibitors such as the matrix metalloprotease inhibitor GM 6001 and the  $\gamma$ -secretase inhibitor DAPT in the lysis buffer was shown to be necessary. Taken together, these results implicate that the interaction requires conditions in which phosphorylation is enhanced (*via* inhibition of dephosphorylation) without the necessity of having TrkB itself phosphorylated. The cross-linking experiments did not only show a direct interaction between full-length TrkB (TK+ TrkB) and NCAM180-ID but also with an 80-kDa Trk fragment. Beyond that, the truncated isoform (TK- TrkB) was also isolated with NCAM180-ID and TrkB. In addition, co-immunoprecipitation studies under the same lysis conditions have confirmed an interaction between TrkB and full-length NCAM180 in the 'natural environment' of the cell membrane within the brain. In addition, proteasome inhibitors have effects on the intracellular proteolytic processing of both NCAM-ID and Trk-ID. NCAM180 has been shown to be

ubiquitinated and probably involved in ubiquitin-dependent proteolysis. The matrix metalloprotease inhibitor GM 6001 could be proven to inhibit TrkB ectodomain shedding.

A functional interrelationship between TrkB and NCAM-mediated cell interactions was highlighted in experiments in which BDNF inhibited NCAM-induced and -specific neurite outgrowth of cerebellar microexplant cultures.

In summary, although the exact regulation mechanisms of the NCAM–TrkB binding based on proteolytic processing remain to be elucidated, this study showed for the first time an interaction between NCAM and TrkB. The main focus of this study was based on the hypothesis that a cross-talk exists between TrkB and NCAM with the potential of causing convergence and divergence of downstream signaling cascades in various ways.

---

Vor geraumer Zeit wurde die Hypothese aufgestellt, dass die beiden Moleküle NCAM und TrkB über PSA-NCAM und BDNF extrazellulär miteinander interagieren (Charles *et al.*, 2000; Muller *et al.*, 2000; Vutskits *et al.*, 2001).

Im Gegensatz dazu haben wir mit dieser Studie die Hypothese einer intrazellulären Interaktion zwischen NCAM und TrkB verfolgt. Zuerst lieferten Beobachtungen aus einer Phagen-Display-Analyse Hinweise darauf, dass TrkB als potenzieller Bindungspartner für NCAM180 in Frage kommt: Es wurde ein Peptid in der intrazellulären Domäne von TrkB (TrkB-ID) identifiziert, das an ein Peptid innerhalb der intrazellulären Domäne von NCAM180 (NCAM180-ID) bindet. Hauptziel dieser Arbeit war, die potenzielle Bindung zwischen NCAM180-ID und TrkB-ID einschließlich ihrer funktionellen Relevanz zu charakterisieren. Aus diesem Grund wurden biochemische Crosslinking-Versuche, Koimmunpräzipitationen und Bindungsstudien durchgeführt. ELISA-Experimente zeigten deutlich, dass NCAM180-ID an TrkB-ID bindet, oder an das TrkB-Peptid, das die mögliche NCAM180-ID-Bindungsstelle enthält und im Rahmen der Phagen-Display-Analyse entdeckt wurde. In der ID der 180-kDa NCAM-Isoform wurde ein Peptidbindungsmotiv identifiziert, das eine Peptidsequenz in der Tyrosinkinase-Domäne von TrkB bindet. Dieses Peptidbindungsmotiv in NCAM180 zeigt nur mit dem C-Terminus der Kir3.3-Isoform Sequenzähnlichkeiten und nicht mit den anderen drei Isoformen dieses Kaliumkanals. Epitop-Mapping machte deutlich, dass die sich die Bindungsstelle innerhalb von NCAM in einer überlappenden Region zwischen NCAM-Exon18 und dem C-Terminus von NCAM180-ID und NCAM140-ID befindet. Um nun mittels biochemischen Crosslink-

ings eine Bindung zwischen TrkB (in voller Länge) und NCAM180-ID nachzuweisen, war neben bestimmten Phosphorylierungsbedingungen auch die Anwesenheit von bestimmten Protease-Inhibitoren wie zum Beispiel dem Matrix-Metalloprotease-Inhibitor GM 6001 und dem  $\gamma$ -Sekretase-Inhibitor DAPT im Lysepuffer von entscheidender Bedeutung. Zusammenfassend implizieren diese Ergebnisse, dass die Interaktion Bedingungen erfordert, in denen die Phosphorylierung begünstigt wird (durch Hemmung der Dephosphorylierung), ohne dass TrkB selbst phosphoryliert sein muss. Die Crosslinking-Versuche bewiesen nicht nur eine direkte Interaktion zwischen vollständigem TrkB (TK+ TrkB) und NCAM180-ID, sondern auch zwischen NCAM180-ID und einem 80-kDa Trk-Fragment. Darüber hinaus wurde auch noch die verkürzte Isoform (TK- TrkB) mit NCAM180-ID und TrkB isoliert. Des Weiteren konnte die Bindung zwischen TrkB und vollständigem NCAM180 im Gehirn in der 'natürlichen Umgebung' der Zellmembran mittels Koimmunpräzipitation unter den gleichen Lysebedingungen nachgewiesen werden. Zusätzlich konnte gezeigt werden, dass Proteasom-Inhibitoren auf die intrazelluläre proteolytische Prozessierung von sowohl NCAM-ID als auch Trk-ID einwirken. Es wurde nachgewiesen, dass NCAM180 ubiquitiniert wird und möglicherweise in die Ubiquitin-abhängige Proteolyse involviert ist. Für TrkB konnte erstmals der Nachweis für das Ektodomän-Shedding, das sich durch den Matrix-Metalloprotease-Inhibitor GM 6001 inhibieren ließ, geliefert werden.

Eine funktionelle Beziehung zwischen TrkB- und NCAM-abhängigen Zellinteraktionen wurde durch Experimente an Kleinhirnmikroexplantkulturen dargelegt, in denen BDNF spezifisch das durch NCAM ausgelöste Neuritenwachstum hemmt.

Zusammenfassend kann gesagt werden, dass im Rahmen dieser Studie erstmals eine Bindung zwischen NCAM und TrkB mit funktioneller Bedeutung nachgewiesen werden konnte. Der genaue Regulationsmechanismus der NCAM–TrkB-Bindung basierend auf proteolytischer Prozessierung muss jedoch noch aufgeklärt werden. Das Hauptaugenmerk dieser Studie basierte auf der Hypothese, dass TrkB und NCAM über ein intensives Kommunikationsnetz miteinander interagieren, das möglicherweise auf unterschiedliche Weise Signaltransduktionskaskaden zusammenführt und auseinander driften lässt.

## 8 Literature

Allendoerfer, K. L., Cabelli, R. J., Escandon, E., Kaplan, D. R., Nikolics, K., and Shatz, C. J. (1994). Regulation of neurotrophin receptors during the maturation of the mammalian visual system. *J. Neurosci.* 14(3 Pt 2): 1795-811.

Amaral, D. G. (2000). The anatomical organization of the central nervous system. In: *Principles of neural science. 4<sup>th</sup> edition*. Kandel, E. R., Schwartz, J. H., and Jessell, T. M. (Ed.), McGraw-Hill Companies, Inc., New York, pp. 317-336.

Auld, D. S., Kornecook, T. J., Bastianetto, S., and Quirion, R. (2002). Alzheimer's disease and the basal forebrain cholinergic system: relations to beta-amyloid peptides, cognition, and treatment strategies. *Prog. Neurobiol.* 68(3): 209-45.

Ausrubel, F. M. (1996). *Current Protocols in Molecular Biology*. (Brooklyn, New York: Greene Publishing Associates, Inc.).

Balkowiec, A., Kunze, D., and Katz, D. (2000). Brain-derived neurotrophic factor acutely inhibits AMPA-mediated currents in developing sensory relay neurons. *J. Neurosci.* 20(5): 1904-11.

Banfield, M. J., Naylor, R. L., Robertson, A. G., Allen, S. J., Dawbarn, D., and Brady, R. L. (2001). Specificity in Trk receptor: neurotrophin interactions: the crystal structure of TrkB-d5 in complex with neurotrophin-4/5. *Structure (Camb)*. 9(12): 1191-9.

Barbacid, M., Lamballe, F., Pulido, D., and Klein, R. (1991). The trk family of tyrosine protein kinase receptors. *Biochim. Biophys. Acta.* 1072(2-3): 115-27.

Barbacid, M. (1994). The Trk family of neurotrophin receptors. *J. Neurobiol.* 25(11): 1386-403.

Barde, Y.-A. (1989) Trophic factors and neuronal survival. *Neuron* 2: 1525-1534.

Barrett, G. L., Georgiou, A., Reid, K., Bartlett, P. F., and Leung, D. (1998). Rescue of dorsal root sensory neurons by nerve growth factor and neurotrophin-3, but not brain-derived neurotrophic factor or neurotrophin-4, is dependent on the level of the p75 neurotrophin receptor. *Neuroscience* 85: 1321-1328.

Barker, P., Barbee, G., Misko, T. P., and Shooter, E. (1994). The low affinity neurotrophin receptor, p75LNTR, is palmitoylated by thioester formation through cysteine 279. *J. Biol. Chem.* 269(48): 30645-50.

Becker, C. G., Artola, A., Gerardy-Schahn, R., Becker, T., Welzl, H., and Schachner, M. (1996). The polysialic acid modification of the neural cell adhesion molecule is involved in spatial learning and hippocampal long-term potentiation. *J. Neurosci. Res.* 45: 143-152.

- Beggs, H. E., Baragona, S. C., Hemperly, J. J., and Maness, P. F. (1997). NCAM140 interacts with the focal adhesion kinase p125(fak) and the SRC-related tyrosine kinase p59(fyn). *J. Biol. Chem.* 272: 8310-8319.
- Bhakar A. L., Howell J. L., Paul C. E., Salehi A. H., Becker E. B., Said F., Bonni A., and Barker P. A. (2003). Apoptosis induced by p75NTR overexpression requires Jun kinase-dependent phosphorylation of Bad. *J. Neurosci.* 23: 11373-11381.
- Bibel, M., and Barde, Y.-A. (2000). Neurotrophins: key regulators of cell fate and cell shape in the vertebrate nervous system. *Genes Dev.* 14(23): 919-37.
- Bix, G. J., and Clark, G. D. (1998). Platelet-activating factor receptor stimulation disrupts neuronal migration in vitro. *J. Neurosci.* 18: 307-318.
- Blum, R., and Konnerth, A. (2005). Neurotrophin-mediated rapid signaling in the central nervous system: mechanisms and functions. *Physiology (Bethesda)* 20: 70-8.
- Blobel, C. P. (1997). Metalloprotease-disintegrins: links to cell adhesion and cleavage of TNF alpha and Notch. *Cell* 90: 589-592.
- Blobel, C. P. (2000). Remarkable roles of proteolysis on and beyond the cell surface. *Curr. Opin. Cell Biol.* 12: 606-612.
- Brewer G. J., Torricelli J. R., Evege E. K., and Price P. J. (1993). Optimized survival of hippocampal neurons in B27-supplemented Neurobasal, a new serum-free medium combination. *J. Neurosci. Res.* 35: 567-576.
- Burnette, W. N. (1981). "Western blotting": electrophoretic transfer of proteins from sodium dodecyl sulfate-polyacrylamide gels to unmodified nitrocellulose and radiographic detection with antibody and radioiodinated protein A. *Anal. Biochem.* 112(2): 195-203.
- Büttner, B., Reutter, W., and Horstkorte, R. (2004). Cytoplasmic domain of NCAM 180 reduces NCAM-mediated neurite outgrowth. *J. Neurosci. Res.* 75(6): 854-60.
- Brackenbury, R., Thiery, J. P., Rutishauser, U., and Edelman, G. M. (1977). Adhesion among neural cells of the chick embryo. I. An immunological assay for molecules involved in cell-cell binding. *J. Biol. Chem.* 252: 6835-6840.
- Brown, M. S., Ye, J., Rawson, R. B., and Goldstein, J. L. (2000). Regulated intramembrane proteolysis: a control mechanism conserved from bacteria to humans. *Cell* 100: 391-398.
- Brummendorf, T., Lemmon, V. (2001). Immunoglobulin superfamily receptors: cis-interactions, intracellular adapters and alternative splicing regulate adhesion. *Curr. Opin. Cell Biol.* 13(5): 611-8.
- Cabrera, N., Diaz-Rodriguez, E., Becker, E., Martin-Zanca, D., and Pandiella, A. (1996). TrkA receptor ectodomain cleavage generates a tyrosine-phosphorylated cell-associated fragment. *J Cell Biol.* 132 (3): 427-436.

- Chao, M. V. (1992). Neurotrophin receptors: A window into neuronal differentiation. *Neuron* 9: 583-593.
- Chao, M. V., and Hempstead, B. L. (1995). p75 and Trk: A two-receptor system. *Trends Neurosci.* 18: 321-326.
- Chao, M. V. (2003). Neurotrophins and their receptors: a convergence point for many signalling pathways. *Nat. Rev. Neurosci.* 4(4): 299-309.
- Charles, P., Hernandez, M. P., Stankoff, B., Aigrot, M. S., Colin C., Rougon, G., Zalc, B., and Lubetzki, C. (2000). Negative regulation of central nervous system myelination by polysialylated-neural cell adhesion molecule. *PNAS.* 97(13): 7585-7590.
- Ciechanover, A. (1994). The ubiquitin-proteasome proteolytic pathway. *Cell* 79: 13-21.
- Close, B. E., and Colley, K. J. (1998). In vivo autopolysialylation and localization of the polysialyltransferases PST and STX. *J. Biol. Chem.* 273(51): 34586-93.
- Cohen, A., Bray, G., and Aguayo, A. (1994). Neurotrophin4/5 (NT4/5) increases adult rat retinal ganglion cell survival and neurite outgrowth in vitro. *J Neurobiol.* 25: 953-959.
- Cole, G. J., and Glaser, L. (1986). A heparin-binding domain from N-CAM is involved in neural cell- substratum adhesion. *J. Cell Biol.* 102: 403-412.
- Cole, G. J., Loewy, A., Cross, N. V., Akeson, R., and Glaser, L. (1986a). Topographic localization of the heparin-binding domain of the neural cell adhesion molecule N-CAM. *J. Cell Biol.* 103: 1739-1744.
- Connor, B., Young, D., Lawlor, P., Gai, W., Waldvogel, H., Faull, R. L., and Dragunow, M. (1996). Trk receptor alterations in Alzheimer's disease. *Brain Res Mol Brain Res.* 42(1): 1-17.
- Cotman, C. W., Hailer, N. P., Pfister, K. K., Soltesz, I., and Schachner, M. (1998). Cell adhesion molecules in neural plasticity and pathology: similar mechanisms, distinct organizations? *Prog. Neurobiol.* 55: 659-669.
- Coulson, E. J., Reid, K., Baca, M., Shipham, K. A., Hulett, S. M., Kilpatrick, T. J., and Bartlett, P. F. (2000). Chopper, a new death domain of the p75 neurotrophin receptor that mediates rapid neuronal cell death. *J. Biol. Chem.* 275(39): 30537-45.
- Cremer, H., Lange, R., Christoph, A., Plomann, M., Vopper, G., Roes, J., Brown, R., Baldwin, S., Kraemer, P., and Scheff, S. (1994). Inactivation of the N-CAM gene in mice results in size reduction of the olfactory bulb and deficits in spatial learning. *Nature* 367: 455-459.
- Cremer, H., Chazal, G., Goriadis, C., and Represa, A. (1997). NCAM is essential for axonal growth and fasciculation in the hippocampus. *Mol. Cell Neurosci.* 8: 323-335.

Crossin, K. L., and Krushel, L. A. (2000). Cellular signaling by neural cell adhesion molecules of the immunoglobulin superfamily. *Dev. Dyn.* 218: 260-279.

Cunningham, B. A., Hemperly, J. J., Murray, B. A., Prediger, E. A., Brackenbury, R., and Edelman, G. A. (1987). Neural cell adhesion molecule: structure, immunoglobulin-like domains, cell surface modulation, and alternative RNA splicing. *Science* 236(4803): 799-806.

Das, M., and Fox, C., F. (1979). Chemical cross-linking in biology. *Annu. Rev. Biophys. Bioeng.* 8: 165-93.

Davies, A. M., Thoenen, H., and Barde Y.-A. (1986). The Response of Chick Sensory Neurons to Brain-Derived Neurotrophic Factor. *J. Neuroscience* 6(7): 1897-1904.

Davies, A. M. (1994). The role of neurotrophins during successive stages of sensory neuron development. *Prog. Growth Factor Res.* 5(3): 263-89.

Delling, M., Wischmeyer, E., Dityatev, A., Sytnyk, V., Veh, R., Karschin, A., and Schachner, M. (2002). The neural cell adhesion molecule regulates cell-surface delivery of G-protein-activated inwardly rectifying potassium channels via lipid rafts. *J. Neurosci.* 22(16): 7154-64.

Diaz-Rodriguez, E., Cabrera, N., Esparis-Ogando, A., Montero, J. C., and Pandiella, A. (1999). Cleavage of the TrkA neurotrophin receptor by multiple metalloproteases generates signalling-competent truncated forms. *Eur. J. Neurosci.* 11(4): 1421-30.

Diaz-Rodriguez, E., Esparis-Ogando, A., Montero, J. C., Yuste L., and Pandiella, A. (2000). Stimulation of cleavage of membrane proteins by calmodulin inhibitors. *Biochem. J.* 346 Pt 2: 359-67.

Diaz-Rodriguez, E., Montero, J. C., Esparis-Ogando, A., Yuste L., and Pandiella, A. (2002). Extracellular signal-regulated kinase phosphorylates tumor necrosis factor alpha-converting enzyme at threonine 735: a potential role in regulated shedding. *Mol. Biol. Cell.* 13(6): 2031-44.

Diehl, J. A., Cheng, M., Roussel, M. F., and Sherr, C. J. (1998). Glycogen synthase kinase-3 $\beta$  regulates cyclin D1 proteolysis and subcellular localization. *Genes Dev.* 12: 3499-3511.

Diehl, J. A., Zindy, F., and Sherr, C. J. (1997). Inhibition of cyclin D1 phosphorylation on threonine-286 prevents its rapid degradation via the ubiquitin-proteasome pathway. *Genes Dev.* 11: 957-972.

Diestel, S., Laurini, C., Traub, O., and Schmitz, B. (2004). Tyrosine 734 of NCAM180 interferes with FGF receptor-dependent signaling implicated in neurite growth. *Biochem. Biophys. Res. Commun.* 322(1): 186-96.

- Dityatev, A., Dityatev, G., and Schachner, M. (2000). Synaptic strength as a function of post- versus presynaptic expression of the neural cell adhesion molecule NCAM. *Neuron*. 26(1): 207-17.
- Ditlevsen, D. K., Køhler, L. B., Pedersen, M. V., Risell, M., Kolkova, K., Meyer, M., Berezin, V., and Bock, E. (2003). The role of phosphatidylinositol 3-kinase in neural cell adhesion molecule-mediated neuronal differentiation and survival. *J. Neurochem.* 84: 546–556.
- Dijkhuizen, P. A., and Ghosh, A. (2005). BDNF regulates primary dendrite formation in cortical neurons via the PI3-Kinase and MAP kinase signaling pathways. *J. Neurobiol.* 62(2): 278-88.
- Dodd, J., Morton, S. B., Karagogeos, D., Yamamoto, M., and Jessell, T. M. (1988). Spatial regulation of axonal glycoprotein expression on subsets of embryonic spinal neurons. *Neuron* 1: 105-116.
- Doherty, P., Fruns, M., Seaton, P., Dickson, G., Barton, C. H., Sears, T. A., and Walsh, F. S. (1990). A threshold effect of the major isoforms of NCAM on neurite outgrowth. *Nature* 343: 464-466.
- Doherty, P., and Walsh, F. S. (1992). Cell adhesion molecules, second messengers and axonal growth. *Curr. Opin. Neurobiol.* 2: 595-601.
- Doherty, P., Williams, G., and Williams, E. J. (2000). CAMs and axonal growth: a critical evaluation of the role of calcium and the MAPK cascade. *Mol. Cell Neurosci.* 16(4): 283-95.
- Doherty, F. J., Dawson, S., and Mayer, R. J. (2002). The ubiquitin-proteasome pathway of intracellular proteolysis. *Essays Biochem.* 38: 51-63.
- Durlinger, A. L. L., Gruijters, M. J. G., Kramer, P., Karels, B., Kumar, T. R., Matzuk, M. M., Rose, U. M., De Jong, F. H., Uillenbroek, J. T. J., Grootegoed, J. A., and Themmen, A. P. N. (2001). Anti-Müllerian hormone attenuates the effects of FSH on follicle development in the mouse ovary. *Endocrinology.* 142(11): 4891–4899.
- Edelman, G. M., Cunningham, B. A., Gall, W. E., Gottlieb, P. D., Rutishauser, U., and Waxdal, M. J. (1969). The covalent structure of an entire gammaG immunoglobulin molecule. *PNAS.* 63: 78-85.
- Egeblad, M., and Werb, Z. (2002). New functions for the matrix metalloproteinases in cancer progression. *Nat. Rev. Cancer.* 2: 161–74.
- Enenkel, C., Lehmann, A., and Kloetzel, P. M. (1999). GFP-labelling of 26S proteasomes in living yeast: insight into proteasomal functions at the nuclear envelope/rough ER. *Mol. Biol. Rep.* 26: 131-5.

- Esposito, D., Patel, P., Stephens, R. M., Perez, P., Chao, M. V., Kaplan, D. R., and Hempstead, B. L. (2001). The cytoplasmic and transmembrane domains of the p75 and Trk A receptors regulate high affinity binding to nerve growth factor. *J. Biol. Chem.* 276: 32687–32695.
- Fields, R. D., and Itoh, K. (1996). Neural cell adhesion molecules in activity-dependent development and synaptic plasticity. *Trends Neurosci.* 19: 473-480.
- Finkbeiner, S., Tavazoie, S. F., Maloratsky, A., Jacobs, K. M., Harris, K. M., and Greenberg, M. E. (1997) CREB: a major mediator of neuronal neurotrophin responses. *Neuron* 19(5): 1031-47.
- Fischer, G., Kunemund, V., and Schachner, M. (1986). Neurite outgrowth patterns in cerebellar microexplant cultures are affected by antibodies to the cell surface glycoprotein L1. *J. Neurosci.* 6: 605-612.
- Foley, A. G., Hartz, B. P., Gallagher, H. C., Rønn, L. C. B., Berezin, V., Bock E., and Regan C. M. (2000). A synthetic peptide ligand of neural cell adhesion molecule (NCAM) IgI Domain prevents NCAM internalisation and disrupts passive avoidance learning. *J. Neurochem.* 74 (6): 2607-2613.
- Fryer, H. J., and Hockfield, S. (1996). The role of polysialic acid and other carbohydrate polymers in neural structural plasticity. *Curr. Opin. Neurobiol.* 6: 113-118.
- Gennarini, G., Hirn, M., Deagostini-Bazin, H., and Goridis, C. (1984). Studies on the transmembrane disposition of the neural cell adhesion molecule N-CAM: a monoclonal antibody recognizing a cytoplasmic domain and evidence for the presence of phosphoserine residues. *Eur. J. Biochem.* 142 (1): 57-64.
- Gennarini, G., Hirn, M., Deagostini-Bazin, H., and Goridis, C. (1984). Studies on the transmembrane disposition of the neural cell adhesion molecule N-CAM. The use of liposome-inserted radioiodinated N-CAM to study its transbilayer orientation. *Eur. J. Biochem.* 142(1): 65-73.
- Grosse, G., Eulitz, D., Thiele, T., Pahner, I., Schroter, S., Takamori, S., Grosse, J., Wickman, K., Tapp, R., Veh, R. W., Ottersen, O. P., and Ahnert-Hilger, G. (2003). Axonal sorting of Kir3.3 defines a GABA-containing neuron in the CA3 region of rodent hippocampus. *Mol. Cell. Neurosci.* 24(3): 709-24.
- Haniu, M., Talvenheimo, J., Le, J., Katta, V., Welcher, A., and Rohde, M. F. (1995). Extracellular domain of neurotrophin receptor trkB: Disulfide structure, N-glycosylation sites, and ligand binding. *Arch. Biochem. Biophys.* 322(1): 256-64.
- Haniu, M., Montestrucque, S., Bures, E. J., Talvenheimo J., Toso, R., Lewis-Sandy, S., Welcher, A. A., and Rohde, M. F. (1997). Interactions between Brain-derived Neurotrophic Factor and the TRKB Receptor. *J. Biol. Chem.* 272(40): 25296–25303.

- Hantzopoulos, P., Suri, C., Glass, D., Goldfarb, M., and Yancopoulos, G. (1994). The low affinity NGF receptor, p75, can collaborate with each of the Trks to potentiate functional responses to the neurotrophins. *Neuron*. 13(1): 187-201.
- Hawley-Nelson, P., Ciccarone, V., Gebeyehu, G., Jesse, J., and Felger, P. (1993). *FOCUS* 15:78.
- Hempstead, B. L., Rabin, S. J., Kaplan, L., Reid, S., Parada, L. F., and Kaplan, D. R. (1992). Overexpression of the trk tyrosine kinase rapidly accelerates nerve growth factor-induced differentiation. *Neuron*. 9: 883-896.
- Hershko, A., and Ciechanover, A. (1998). The ubiquitin system. *Annu. Rev. Biochem.* 67: 425-79.
- Hicke, L., and Dunn, R. (2003). Regulation of membrane protein transport by ubiquitin and ubiquitin-binding proteins. *Annu. Rev. Cell Dev. Biol.* 19: 141-172.
- Hillenbrand, R., Molthagen, M., Montag, D., and Schachner, M. (1999). The close homologue of the neural adhesion molecule L1 (CHL1): patterns of expression and promotion of neurite outgrowth by heterophilic interactions. *Eur. J. Neurosci.* 11(3): 813-26.
- Hinsby, A. M., Berezin, V., and Bock, E. (2004). Molecular mechanisms of NCAM function. *Front. Biosci.* 9: 2227-44.
- Hoppe, T., Rape, M., and Jentsch, S. (2001). Membrane-bound transcription factors: regulated release by RIP or RUP. *Curr. Opin. Cell Biol.* 13: 344-348.
- Hoffman, K. B., Larson, J., Bahr, B. A., and Lynch, G. (1998a). Activation of NMDA receptors stimulates extracellular proteolysis of cell adhesion molecules in hippocampus. *Brain Res.* 811: 152-155.
- Hoffman, K. B., Martinez, J., and Lynch, G. (1998b). Proteolysis of cell adhesion molecules by serine proteases: a role in long term potentiation? *Brain Res.* 811: 29-33.
- Hoffman, S., Sorkin, B. C., White, P. C., Brackenbury, R., Mailhammer, R., Rutishauser, U., Cunningham, B. A., and Edelman, G. M. (1982). Chemical characterization of a neural cell adhesion molecule purified from embryonic brain membranes. *J. Biol. Chem.* 257: 7720-7729.
- Hoffman, S., and Edelman, G. M. (1983). Kinetics of homophilic binding by embryonic and adult forms of the neural cell adhesion molecule. *PNAS.* 80: 5762-5766.
- Horstkorte R., Schachner M., Magyar J. P., Vorherr T., and Schmitz B. (1993). The fourth immunoglobulin-like domain of NCAM contains a carbohydrate recognition domain for oligomannosidic glycans implicated in association with L1 and neurite outgrowth. *J. Cell Biol.* 121: 1409-1421.

- Horton, A., Laramée, G., Wyatt, S., Shih, A., Winslow, J., and Davies, A. M. (1997). NGF binding to p75 enhances the sensitivity of sensory and sympathetic neurons to NGF at different stages of development. *Mol. Cell Neurosci.* 10: 162–172.
- Huang, E. J., and Reichardt, L. F. (2003). Trk receptors: roles in neuronal signal transduction. *Annu Rev Biochem.* 72: 609–42.
- Hurst, G. B., Lankford, T. K., and Kennel, S. J. (2004). Mass spectrometric detection of affinity purified crosslinked peptides. *J. Am. Soc. Mass Spectrom.* 15(6): 832–9.
- Huttner, W. B., Schiebler, W., Greengard, P., and De Camilli, P. (1983). Synapsin I (protein D), a nerve terminal-specific phosphoprotein. III. Its association with synaptic vesicles studied in a highly purified synaptic vesicle preparation. *J. Cell Biol.* 96: 1374–1388.
- Huyer, G., Liu, S., Kelly, J., Moffat, J., Payette, P., Kennedy, B., Tsapralis, G., Gresser, J. M., and Ramachandran, C. (1997). Mechanism of inhibition of protein-tyrosine phosphatases by vanadate and pervanadate. *J. Biol. Chem.* 272(2): 843–851.
- Hynes, R. O. (1992). Integrins: versatility, modulation, and signaling in cell adhesion. *Cell.* 69: 11–25.
- Ignelzi, M., Miller, D., Soriano, P., and Maness, P. (1994). Impaired neurite outgrowth of src-minus cerebellar neurons on the cell adhesion molecule Ll. *Neuron.* 12: 873–884.
- Ippolito, D. L., Temkin, P. A., Rogalski, S. L., and Chavkin, C. (2002). N-terminal tyrosine residues within the potassium channel Kir3 modulate GTPase activity of Galphai. *J. Biol. Chem.* 277(36): 32692–6.
- Iwasaki, Y., Nishiyama, H., Suzuki, K., and Koizumi, S. (1997). Sequential cis/trans autophosphorylation in TrkB tyrosine kinase. *Biochemistry.* 36(9): 2694–700.
- Iwasaki, Y., Gay, B., Wada, K., and Koizumi, S. (1998). Association of the Src family tyrosine kinase Fyn with TrkB. *J. Neurochemistry.* 71: 106–111.
- Jensen, O. N., Podtelejnikov, A. V., and Mann, M. (1997). Identification of the components of simple protein mixtures by high- accuracy peptide mass mapping and database searching. *Anal. Chem.* 69: 4741–4750.
- Jentsch, S., and Pyrowolakis, G. (2000). Ubiquitin and its kin: how close are the family ties? *Trends Cell Biol.* 10: 335–42.
- Jing, S., Tapley, P., and Barbacid, M. M. (1992). Nerve growth factor mediates signal transduction through trk homodimer receptors. *Neuron.* 9: 1067–1079.
- Jørgensen, O. S., and Bock, E. (1974). Brain specific synaptosomal membrane proteins demonstrated by crossed immunoelectrophoresis. *J. Neurochem.* 23(4): 879–80.

Jørgensen, O. S. (1995). Neural cell adhesion molecule (NCAM) as a quantitative marker in synaptic remodeling. *Neurochem. Res.* 20: 533-547.

Jung, K. M., Tan, S., Landman, N., Petrova, K., Murray, S., Lewis, R., Kim, P. K., Kim, D. S., Ryu, S. H., Chao, M. V., and Kim, T.-W. (2003). Regulated intramembrane proteolysis of the p75 neurotrophin receptor modulates its association with the TrkA Receptor. *J. Biol. Chem.* 278(43): 42161–42169.

Kalus, I. (2005). Untersuchungen zu der Entstehung und der Bedeutung löslicher Fragmente der neuronalen Zelladhäsionsmoleküle L1 und NCAM im Zentralen Nervensystem der Maus. (Dissertation: Institut für Biosynthese Neuraler Strukturen, ZMNH, Universität Hamburg/ Institut für Anatomie und Zellbiologie der Philipps-Universität Marburg, Germany).

Kalus, I., Schnegelsberg, B., Seidah, N. G., Kleene, R., and Schachner, M. (2003). The proprotein convertase PC5A and a metalloprotease are involved in the proteolytic processing of the neural adhesion molecule L1. *J. Biol. Chem.* 278(12): 10381-8.

Kanning, K. C., Hudson, M., Amieux, P. S., Wiley, J. C., Bothwell, M., and Schecterson, L. C. (2003). Proteolytic processing of the p75 neurotrophin receptor and two homologs generates C-terminal fragments with signaling capability. *J. Neurosci.* 23(13): 5425-5436.

Kaplan, D. R., Hempstead, B. L., Martin-Zanca, D., Chao, M. V., and Parada, L. F. (1991a). The *trk* proto-oncogene product: a signal transducing receptor for nerve growth factor. *Science.* 252: 558–561.

Kaplan, D. R., Martin-Zanca, D., and Parada, L. F. (1991b). Tyrosine phosphorylation and tyrosine kinase activity of the *trk* proto-oncogene product induced by NGF. *Nature* 350: 158-160.

Kaplan, D. R., and Miller, F. D. (2000). Neurotrophin signal transduction in the nervous system. *Curr. Opin. Neurobiol.* 10(3): 381-91.

Kaplan, D. R., and Stephens, R. M. (1994). Neurotrophin signal transduction by the Trk receptor. *J. Neurobiol.* 25: 1404–1417.

Keilhauer, G., Faissner, A., and Schachner, M. (1985). Differential inhibition of neurone-neurone, neurone-astrocyte and astrocyte-astrocyte adhesion by L1, L2 and N-CAM antibodies. *Nature.* 316: 728-730.

Kiss, J. Z., and Muller, D. (2001). Contribution of the neural cell adhesion molecule to neuronal and synaptic plasticity. *Rev Neurosci.* 12(4): 297-310.

Kleene, R., Yang, H., Kutsche, M., and Schachner, M. (2001). The neural recognition molecule L1 is a sialic acid-binding lectin for CD24, which induces promotion and inhibition of neurite outgrowth. *J. Biol. Chem.* 276(24): 21656–21663.

Klein, R., Parada, L. F., Coulier, F., and Barbacid, M. (1989). *trk B*, a novel tyrosine protein kinase receptor expressed during mouse neural development. *EMBO J.* 8: 3701-3709.

Klein, R., Martin-Zanca, D., Barbacid, M., and Parada, L. F. (1990). Expression of the tyrosine kinase receptor gene *trk B* is confined to the murine embryonic and adult nervous system. *Development.* 109: 845-850.

Klein R., Nanduri V., Jing S., Lamballe F., Tapley P., Bryant S., Cordon-Cardo C., Jones K. R., Reichardt L. F., and Barbacid M. (1991a). The *trk B* tyrosine protein kinase is a receptor for brain-derived neurotrophic factor and neurotrophin-3. *Cell.* 66: 395-403.

Klein R., Nanduri V., Jing S., and Barbacid M. (1991b). The *trkB* tyrosine protein kinase is a receptor for brain-derived neurotrophic factor and neurotrophin-3. *Cell.* 1991 Jul 26;66(2):395-403.

Knusel, B., Winslow, J. W., Rosenthal, A., Burton, L. E., Seid, D. P., Nikolics, K., and Hefti, F. (1991). Promotion of central cholinergic and dopaminergic neuron differentiation by brain-derived neurotrophic factor but not neurotrophin-3. *PNAS.* 88: 961-965.

Kolkova, K., Novitskaya, V., Pedersen, N., Berezin, V., and Bock, E. (2000). Neural cell adhesion molecule-stimulated neurite outgrowth depends on activation of protein kinase C and the Rasmitogen-activated protein kinase pathway. *J. Neurosci.* 20: 2238-2246.

Krushel, L. A., Cunningham, B. A., Edelman, G. M., and Crossin, K. L. (1999). NF-kappaB activity is induced by neural cell adhesion molecule binding to neurons and astrocytes. *J. Biol. Chem.* 274: 2432-2439.

Kruttgen, A., Saxena, S., Evangelopoulos, M. E., and Weis, J. (2003). Neurotrophins and neurodegenerative diseases: receptors stuck in traffic? *J. Neuropathol. Exp. Neurol.* 62(4): 340-50.

Lamballe, F., Klein, R., and Barbacid, M. (1991). *TrkC*, a new member of the *trk* family of tyrosine protein kinases, is a receptor for neurotrophin-3. *Cell.* 66(5): 967-79.

Laney, J. D., and Hochstrasser, M. (1999). Substrate targeting in the ubiquitin system. *Cell.* 97: 427-30.

Lee, F. S. and Chao, M. V. (2001). Activation of *Trk* neurotrophin receptors in the absence of neurotrophins. *PNAS.* 98(6): 3555-60.

Lee, R., Kermani, P., Teng, K. K., and Hempstead, B. L. (2001). Regulation of cell survival by secreted proneurotrophins. *Science.* 294(5548): 1945-8.

Lewin, G. R., and Barde, Y.-A. (1996). Physiology of neurotrophins. *Annu. Rev. Neurosci.* 19: 289-317.

Levi-Montalcini, R., and Angeletti, P. U. (1968). Nerve growth factor. *Physiol. Rev.* 48: 534-569.

- Levkowitz, G., Waterman, H., Zamir, E., Kam, Z., Oved, S., Langdon, W. Y., Beguinot, L., Geiger, B., and Yarden, Y. (1998). c-Cbl/Sli-1 regulates endocytic sorting and ubiquitination of the epidermal growth factor receptor. *Genes Dev.* 12(23): 3663-74.
- Li H. S., Xu X. Z., and Montell C. (1999). Activation of a TRPC3-dependent cation current through the neurotrophin BDNF. *Neuron.* 24(1): 261-73.
- Lindholm, D., Dechant, G., Heisenberg, C. P., and Thoenen, H. (1993). Brain-derived neurotrophic factor is a survival factor for cultured rat cerebellar granule neurons and protects them against glutamate-induced neurotoxicity. *Eur. J. Neurosci.* 5: 1455-1464.
- Lindholm, D., Hamner, S., and Zirrgiebel, U. (1997). Neurotrophins and cerebellar development. *Persp. Dev. Neurol.* 5(1): 83-94.
- Little, E. B., Edelman, G. M., and Cunningham, B. A. (1998). Palmitoylation of the cytoplasmic domain of the neural cell adhesion molecule N-CAM serves as an anchor to cellular membranes. *Cell Adhes. Commun.* 6: 415-430.
- Llovera, M., De Pablo, Y., Egea, J., Encinas, M., Peiro, S., Martin-Zanca, D., Rocamora, N. and Comella, J. X. (2004). Trk is a calmodulin-binding protein: Implications for receptor processing. *J. Neurochem.* 88:422-433.
- Lochter, A., Vaughan, L., Kaplony, A., Prochiantz, A., Schachner, M., and Faissner, A. (1991). J1/tenascin in substrate-bound and soluble form displays contrary effects on neurite outgrowth. *J. Cell Biol.* 113: 1159-1171.
- Lysetskiy, M., Foldy, C., and Soltesz, I. (2005). Long- and short-term plasticity at mossy fiber synapses on mossy cells in the rat dentate gyrus. *Hippocampus.* 15(6): 691-6.
- Makkerh, J. P., Ceni, C., Auld, D. S., Vaillancourt, F., and Barker, P. A. (2005). p75 neurotrophin receptor reduces ligand-induced Trk receptor ubiquitination and delays Trk receptor internalization and degradation. *EMBO Rep.* 2005 Aug 19; [Epub ahead of print]
- Mallett, S., and Barclay, A. N. (1991). A new superfamily of cell surface proteins related to the nerve growth factor receptor. *Immunol. Today.* 12: 220-223.
- Martin-Zanca, D., Barbacid, M., and Parada, L. F. (1990). Expression of the trk proto-oncogene is restricted to the sensory cranial and spinal ganglia of neural crest origin in mouse development. *Genes Dev.* 4(5): 683-94.
- Martin-Zanca, D., Hughes, S. H., and Barbacid, M. (1986). A human oncogene formed by the fusion of truncated tropomyosin and protein tyrosine kinase sequences. *Nature.* 319(6056): 743-8.
- Marini, A. M., Rabin, S. J., Lipsky, R. H., and Mocchetti, I. (1998). Activity-dependent release of brain-derived neurotrophic factor underlies the neuroprotective effect of N-methyl-D-aspartate. *J. Biol. Chem.* 273(45): 29394-9.

- Massa, S. M., Xie, Y., and Longo, F. M. (2003). Alzheimer's therapeutics: neurotrophin domain small molecule mimetics. *J. Mol. Neurosci.* 20(3): 323-6.
- McAllister, A. K., Katz, L. C., and Lo, D. C. (1999). Neurotrophins and synaptic plasticity. *Annu. Rev. Neurosci.* 22: 295-318.
- McQuibban, G. A., Gong, J. H., Wong, J. P., Wallace, J. L., Clark-Lewis, I., and Overall, C. M. (2002). Matrix metalloproteinase processing of monocyte chemoattractant proteins generates CC chemokine receptor antagonists with anti-inflammatory properties *in vivo*. *Blood.* 100: 1160-7.
- Melchior, F. (2000). SUMO--nonclassical ubiquitin. *Annu. Rev. Cell Dev. Biol.* 16: 591-626.
- Middlemas, D. S., Lindberg, R. A., and Hunter, T. (1991). trkB, a neural receptor protein-tyrosine kinase: evidence for a full-length and two truncated receptors. *Mol. Cell Biol.* 11(1): 143-53.
- Minichiello, L., Calella, A. M., Medina, D. L., Bonhoeffer, T., Klein, R., and Korte, M. (2002). Mechanism of TrkB-mediated hippocampal long-term potentiation. *Neuron.* 36(1): 121-37.
- Minichiello, L., and Klein, R. (1996). TrkB and TrkC neurotrophin receptors cooperate in promoting survival of hippocampal and cerebellar granule neurons. *Genes Dev.* 10(22): 2849-58.
- Minichiello, L., Korte, M., Wolfer, D., Kuhn, R., Unsicker, K., Cestari, V., Rossi-Arnaud, C., Lipp, H. P., Bonhoeffer, T., and Klein, R. (1999). Essential role for TrkB receptors in hippocampus-mediated learning. *Neuron.* 24: 401-414.
- Mowla, S. J., Farhadi, H. F., Pareek, S., Atwal, J. K., Morris, S J., Seidah, N. G., and Murphy R. A. (2001). Biosynthesis and post-translational processing of the precursor to brain-derived neurotrophic factor. *J. Biol. Chem.* 276(16): 12660-6.
- Mueller, B. K. (1999). Growth cone guidance: first steps towards a deeper understanding. *Annu. Rev. Neurosci.* 22: 351-88.
- Müller, S., Hoegge, C., Pyrowolakis, G., and Jentsch, S. (2001). SUMO, ubiquitin's mysterious cousin. *Nat. Rev. Mol. Cell Biol.* 2(3): 202-10.
- Muller, D., Wang, C., Skibo, G., Toni, N., Calaora, V., Cremer, H., Rougon, G., and Kiss, J. Z. (1996). PSA-NCAM is required for activity-induced synaptic plasticity. *Neuron.* 17(3): 413-22.
- Muller, D., Djebbara-Hannas, Z., Jourdain, P., Vutskits, L., Durbec, P., Rougon, G., and Kiss, J. Z. (2000). Brain-derived neurotrophic factor restores long-term potentiation in polysialic acid-neural cell adhesion molecule-deficient hippocampus. *PNAS.* 97(8): 4315-4320.

Naruse, S., Thinakaran, G., Luo, J. J., Kusiak, J. W., Tomita, T., Iwatsubo, T., Qian, X., Ginty, D. D., Price, D. L., Borchelt, D. R., Wong, P. C., and Sisodia, S. S. (1998). Effects of PS1 deficiency on membrane protein trafficking in neurons. *Neuron*. 21(5): 1213-21.

Niethammer, P., Delling, M., Sytnyk, V., Dityatev, A., and Schachner, M. (2002). Co-signaling of NCAM via lipid rafts and the FGF receptor is required for neuriteogenesis. *J. Cell Biol.* 157(3): 521-32.

Nybroe, O., Albrechtsen, M., Dahlin, J., Linnemann, D., Lyles, J. M., Moller, C. J., and Bock, E. (1985). Biosynthesis of the neural cell adhesion molecule: characterization of polypeptide C. *J. Cell Biol.* 101: 2310-2315.

Obermeier, A., Lammers, R., Wiesmuller, K., Jung, G., Schlessinger, J., and Ullrich, A. (1993). Identification of Trk binding sites for SHC and phosphatidylinositol 3'-kinase and formation of a multimeric signaling complex. *J. Biol. Chem.* 268: 22963-22966.

Obermeier, A., Bradshaw, R. A., Seedorf, K., Choidas, A., Schlessinger, J., and Ullrich, A. (1994). Tyrosine 785 is a major determinant of Trk--substrate interaction. *EMBO J.* 13: 1585-1590.

Olsen, M., Krog, L., Edvardsen, K., Skovgaard, L. T., and Bock, E. (1993) Intact transmembrane isoforms of the neural cell adhesion molecule are released from the plasma membrane. *J. Biochem.* 295(Pt 3): 833-840.

Orr, H. T., Lancet, D., Robb, R. J., Lopez de Castro, J. A., and Strominger, J. L. (1979). The heavy chain of human histocompatibility antigen HLA-B7 contains an immunoglobulin-like region. *Nature*. 282: 266-270.

Palombella, V. J., Rando, O. J., Goldberg, A. L., and Maniatis, T. (1994). The ubiquitin-proteasome pathway is required for processing the NF- $\kappa$ B1 precursor protein and the activation of NF- $\kappa$ B. *Cell*. 78: 773-785.

Paratcha, G., Ledda, F., and Ibanez, C. F. (2003). The neural cell adhesion molecule NCAM is an alternative signaling receptor for GDNF family ligands. *Cell*. 113(7): 867-79.

Patterson, S., Abel, T., Deuel, T., Martin, K., Rose, J., and Kandel, E. (1996). Recombinant BDNF rescues deficits in basal synaptic transmission and hippocampal LTP in BDNF knockout mice. *Neuron*. 16: 1137-1145.

Persohn, E., Pollerberg, G. E., and Schachner, M. (1989). Immunoelectron-microscopic localization of the 180 kD component of the neural cell adhesion molecule N-CAM in post-synaptic membranes. *J. Comp Neurol.* 288: 92-100.

Peschon, J. J., Slack, J. L., Reddy, P., Stocking, K. L., Sunnarborg, S. W., Lee, D. C., Russell, W. E., Castner, B. J., Johnson, R. S., Fitzner, J. N., Boyce, R. W., Nelson, N., Kozlosky, C. J., Wolfson, M. F., Rauch, C. T., Cerretti, D. P., Paxton, R. J., March, C. J., and Black, R. A. (1997). An essential role for ectodomain shedding in mammalian development. *Science*. 282: 1281-1284.

- Philo J. S., Talvenheimo J., Wen J., Rosenfeld R., Welcher A., and Arakawa T. (1994). Interactions of neurotrophin-3 (NT-3), brain-derived neurotrophic factor (BDNF), and the NT-3.BDNF heterodimer with the extracellular domains of the TrkB and TrkC receptors. *J. Biol. Chem.* 269: 27840-27846.
- Pickart, C. M. (1997). Targeting of substrates to the 26S proteasome. *Faseb J.* 11: 1055-66.
- Pickart, C. M. (2000). Ubiquitin in chains. *Trends Biochem. Sci.* 25: 544-8.
- Pollerberg, E. G., Burridge, K., Krebs, K. E., Goodman, S. R., and Schachner, M. (1987). The 180-kD component of the neural cell adhesion molecule N-CAM is involved in a cell-cell contacts and cytoskeleton-membrane interactions. *Cell Tissue Res.* 250(1): 227-36.
- Pollerberg, E. G., Sadoul, R., Goridis, C., and Schachner, M. (1985). Selective expression of the 180-kD component of the neural cell adhesion molecule N-CAM during development. *J. Cell Biol.* 101: 1921-1929.
- Povlsen, G. K., Ditlevsen, D. K., Berezin, V., and Bock, E. (2003). Intracellular signaling by the neural cell adhesion molecule. *Neurochem. Res.* 28(1): 127-41.
- Poltorak, M., Khoja, I., Hemperly, J. J., Williams, J. R., el Mallakh, R., and Freed, W. J. (1995). Disturbances in cell recognition molecules (N-CAM and L1 antigen) in the CSF of patients with schizophrenia. *Exp. Neurol.* 131: 266-272.
- Poo, M. M. (2001). Neurotrophins as synaptic modulators. *Nat. Rev. Neurosci.* 2(1):24-32.
- Postigo, A., Calella, A. M., Fritsch, B., Knipper, M., Katz, D., Eilers, A., Schimmang, T., Lewin, G. R., Klein, R., and Minichiello, L. (2002). Distinct requirements for TrkB and TrkC signaling in target innervation by sensory neurons. *Genes Dev.* 16: 633-645.
- Primakoff, P., and Myles, D. G. (2000). The ADAM gene family: surface proteins with adhesion and protease activity. *Trends Genet.* 16(2): 83-87.
- Probstmeier, R., Kuhn, K., and Schachner, M. (1989). Binding properties of the neural cell adhesion molecule to different components of the extracellular matrix. *J. Neurochem.* 53(6): 1794-801.
- Rabacchi, S. A, Kruk, B., Hamilton, J., Carney, C., Hoffman, J. R., Meyer, S. L., Springer, J. E., and Baird, D. H. (1999). BDNF and NT4/5 promote survival and neurite outgrowth of pontocerebellar mossy fiber neurons. *J. Neurobiol.* 40(2): 254-69.
- Rajagopal, R., Chen, Z. Y., Lee, F. S., and Chao, M. V. (2004). Transactivation of Trk neurotrophin receptors by G-protein-coupled receptor ligands occurs on intracellular membranes. *J. Neurosci.* 24(30): 6650-8.
- Rape, M., and Jentsch, S. (2004). Productive RUpture: activation of transcription factors by proteasomal processing. *Biochim. Biophys. Acta.* 1695: 209-213.

- Regan, C. M. and Fox, G. B. (1995). Polysialylation as a regulator of neural plasticity in rodent learning and aging. *Neurochem. Res.* 20: 593-598.
- Rathjen, F. G., and Schachner, M. (1984). Immunocytological and biochemical characterization of a new neuronal cell surface component (L1 antigen) which is involved in cell adhesion. *EMBO J.* 3: 1-10.
- Reichardt, L. F. and Tomaselli, K. J. (1991). Extracellular matrix molecules and their receptors: functions in neural development. *Annu.Rev.Neurosci.* 14: 531-570.
- Rentzos, M., Michalopoulou, M., Nikolaou, C., Cambouri, C., Rombos A., Dimitrakopoulos, A., Kapaki, E., and Vassilopoulos, D. (2005). The role of soluble intercellular adhesion molecules in neurodegenerative disorders. *J. Neurol. Sci.* 228(2): 129-35.
- Rico, B., Xu, B. and Reichardt, L. F. (2002). TrkB receptor signaling is required for establishment of GABAergic synapses in the cerebellum. *Nature neuroscience.* 5(3): 225-233.
- Rifkin, D. B., Mazziere R., Munger J. S., Moguera, I., Song, J. (1999). Proteolytic control of growth factor availability. *APMIS.* 107(1): 80-5.
- Rogalski, S. L., Appleyard, S. M., Pattillo, A., Terman, G. W., and Chavkin, C. (2000). TrkB activation by brain-derived neurotrophic factor inhibits the G protein-gated inward rectifier Kir3 by tyrosine phosphorylation of the channel. *J. Biol. Chem.* 275: 25082-25088.
- Rong, Y., Lu, X., Bernard, A., Khrestchatisky, M., and Baudry, M. (2001). Tyrosine phosphorylation of ionotropic glutamate receptors by Fyn or Src differentially modulates their susceptibility to calpain and enhances their binding to spectrin and PSD-95. *J. Neurochem.* 79(2): 382-90.
- Ronn, L. C., Hartz, B. P., and Bock, E. (1998). The neural cell adhesion molecule (NCAM) in development and plasticity of the nervous system. *Exp. Gerontol.* 33(7-8): 853-64.
- Ross, C. A. and Pickart, C. M. (2004). The ubiquitin-proteasome pathway in Parkinson's disease and other neurodegenerative diseases. *Trends Cell Biol.* 14(12): 703-11.
- Rothbard, J. B., Brackenbury, R., Cunningham, B. A., and Edelman, G. M. (1982). Differences in the carbohydrate structures of neural cell-adhesion molecules from adult and embryonic chicken brains. *J. Biol. Chem.* 257: 11064-11069.
- Roux, P. P., Bhakar, A. L., Kennedy, T. E., and Barker, P. A. (2001). The p75 neurotrophin receptor activates Akt (protein kinase B) through a phosphatidylinositol 3-kinase-dependent pathway. *J. Biol. Chem.* 276(25): 23097-104.
- Roux, P. P., and Barker, P. A. (2002). Neurotrophin signaling through the p75 neurotrophin receptor. *Prog. Neurobiol.* 67(3): 203-33.

- Russell, S. J., Steger, K. A., und Johnston, S. A. (1999). Subcellular localization, stoichiometry, and protein levels of 26 S proteasome subunits in yeast. *J. Biol. Chem.* 274: 21943-52.
- Rutishauser, U. (1990). Neural cell adhesion molecule as a regulator of cell-cell interactions. *Adv. Exp. Med. Biol.* 265: 179-183.
- Santhoshkumar, P., and Sharma K. K. (2002). Identification of a region in alcohol dehydrogenase that binds to alpha-crystallin during chaperone action. *Biochim. Biophys. Acta.* 1598(1-2): 115-21.
- Schachner, M., and Martini, R. (1995). Glycans and the modulation of neural-recognition molecule function. *Trends Neurosci.* 18: 183-191.
- Schechterson, L., Kanning, K., Hudson, M., and Bothwell, M. (2002). The neurotrophin receptor p75 is cleaved by regulated intramembraneous proteolysis. *Soc. Neurosci. Abstr.* 27, 822.10.
- Schmid, R. S., Graff, R. D., Schaller, M. D., Chen, S., Schachner, M., Hemperly, J. J., and Maness, P. F. (1999) NCAM stimulates the Ras-MAPK pathway and CREB phosphorylation in neuronal cells. *J. Neurobiol.* 38: 542-558.
- Schlondorff, J., and Blobel, C. P. (1999). Metalloprotease-disintegrins: modular proteins capable of promoting cell-cell interactions and triggering signals by protein-ectodomain shedding. *J. Cell Sci.* 112 (Pt 21): 3603-3617.
- Schnegelsberg, B. (2001). *In vitro* Untersuchungen zur posttranslationalen Prozessierung der Zelladhäsionsmoleküle L1 und CHL1 (Dissertation durchgeführt am Institut für Biosynthese Neuraler Strukturen, ZMNH, Universität Hamburg).
- Schneider, R., and Schweiger, M. (1991). A novel modular mosaic of cell adhesion motifs in the extracellular domains of the neurogenic trk and trkB tyrosine kinase receptors. *Oncogene.* 6(10): 1807-11.
- Schuch, U., Lohse, M. J., and Schachner, M. (1989). Neural cell adhesion molecules influence second messenger systems. *Neuron.* 3: 13-20.
- Segal, R., Pomeroy, S., and Stiles, C. (1995). Axonal growth and fasciculation linked to differential expression of BDNF and NT3 receptors in developing cerebellar granule cells. *J. Neurosci.* 15: 4970-4981.
- Segal, R., Bhattacharyya, A., Rua, L., Alberta, J., Stephens, R., Kaplan, D., and Stiles, C. (1996). Differential utilization of Trk autophosphorylation sites. *J. Biol. Chem.* 271(33): 20175-81.
- Seidah, N. G., and Chretien, M. (1999). Proprotein and prohormone convertases: a family of subtilases generating diverse bioactive polypeptides. *Brain Res.* 848: 45-62.

- Selkoe, D., and Kopan, R. (2003). Notch and Presenilin: regulated intramembrane proteolysis links development and degeneration. *Annu. Rev. Neurosci.* 26: 565-97.
- Shevchenko, A., Wilm, M., Vorm, O., and Mann, M. (1996). Mass spectrometric sequencing of proteins silver-stained polyacrylamide gels. *Anal. Chem.* 68(5): 850-858.
- Shih, P., Evans, K., Schifferli, K., Ciccarone, V., Lichaa, F., Masoud, M., Lan, J., and Hawley-Nelson P. (1997). *FOCUS* 19:52.
- Shimada, A., Mason, C. A., and Morrison, M. E. (1998). TrkB signaling modulates spine density and morphology independent of dendrite structure in cultured neonatal Purkinje cells. *J. Neurosci.* 18(21): 8559-70.
- Shooter, E. M. (2001). Early days of the nerve growth factor proteins. *Annu. Rev. Neurosci.* 24: 601-29.
- Stephens, R., Loeb, D., Copeland, T., Pawson, T., Greene, L., and Kaplan, D. (1994). Trk receptors use redundant signal transduction pathways involving SHC and PLC-gamma 1 to mediate NGF responses. *Neuron.* 12(3): 691-705.
- Stork, O., Welzl, H., Cremer, H., and Schachner, M. (1997). Increased intermale aggression and neuroendocrine response in mice deficient for the neural cell adhesion molecule (NCAM). *Eur. J. Neurosci.* 9: 1117-1125.
- Stork, O., Welzl, H., Wotjak, C. T., Hoyer, D., Delling, M., Cremer, H., and Schachner, M. (1999). Anxiety and increased 5-HT1A receptor response in NCAM null mutant mice. *J. Neurobiol.* 40: 343-355.
- Takeichi, M. (1991). Cadherin cell adhesion receptors as a morphogenetic regulator. *Science.* 251: 1451-1455.
- Tapley, P., Lamballe, F., and Barbacid, M. (1992). K252a is a selective inhibitor of the tyrosine protein kinase activity of the trk family of oncogenes and neurotrophin receptors. *Oncogene.* 7(2): 371-81.
- Thoenen, H. (1995). Neurotrophins and neuronal plasticity. *Science.* 270(5236): 593-8.
- Tomasiewicz, H., Ono, K., Yee, D., Thompson, C., Goridis, C., Rutishauser, U., and Magnuson, T. (1993). Genetic deletion of a neural cell adhesion molecule variant (N-CAM-180) produces distinct defects in the central nervous system. *Neuron.* 11: 1163-1174.
- Towbin, H., Staehelin, T., and Gordon, J. (1979). Electrophoretic transfer of proteins from polyacrylamide gels to nitrocellulose sheets: procedure and some applications. *PNAS.* 76: 4350-4354.
- Ultsch, M. H., Wiesmann, C., Simmons, L. C., Heinrich, J., Yang, M., Reilly, D., Bass, S. H., de Vos, A. M. (1999). Crystal structures of the neurotrophin-binding domain of TrkA, TrkB and TrkC. *J. Mol. Biol.* 290(1): 149-59.

- Van Kerkhof, P., Alves Dos Santos, C. M., Sachse, M., Klumperman, J., Bu, G., and Strous, G. J. (2001). Proteasome inhibitors block a late step in lysosomal transport of selected membrane but not soluble proteins. *Mol. Biol. Cell.* 12(8): 2556-66.
- Vawter, M. P., Cannon-Spoor, H. E., Hemperly, J., Hyde, T. M., Van der Putten, D. M., Kleinman, J. E., and Freed, W. J. (1998). Abnormal expression of cell recognition molecules in schizophrenia. *Exp. Neurol.* 149: 424-432.
- Verdi, J., Birren, S., Ibanez, C., Persson, H., Kaplan, D., Benedetti, M., Chao, M., and Anderson D (1994) p75LNGFR regulates Trk signal transduction and NGF-induced neuronal differentiation in MAH cells. *Neuron.* 12: 733-745.
- Vutskits, L., Djebbara-Hannas, Z., Zhang, H., Paccaud, J.-P., Durbec, P., Rougon, G., Muller, D., and Kiss, J. Z. (2001). PSA-NCAM modulates BDNF-dependent survival and differentiation of cortical neurons. *Eur. J. Neurosci.* 13(7): 1391-1402.
- Vyssotski, A. L., Dell'Omo, G., Poletaeva, I. I., Vyssotsk, D. L., Minichiello, L., Klein, R., Wolfer, D. P., and Lipp, H. P. (2002). Long-term monitoring of hippocampus-dependent behavior in naturalistic settings: mutant mice lacking neurotrophin receptor TrkB in the forebrain show spatial learning but impaired behavioral flexibility. *Hippocampus.* 12(1): 27-38.
- Walmod, P. S., Kolkova, K., Berezin, V., and Bock, E. (2004). Zippers make signals: NCAM-mediated molecular interactions and signal transduction. *Neurochem. Res.* 29(11): 2015-35.
- Werb, Z., and Yan, Y. (1998). A cellular striptease act. *Science.* 282: 1279-1280.
- Williams, A. F., and Barclay, A. N. (1988). The immunoglobulin superfamily--domains for cell surface recognition. *Annu. Rev. Immunol.* 6: 381-405.
- Williams, E. J., Furness, J., Walsh, F. S., and Doherty, P. (1994a). Activation of the FGF receptor underlies neurite outgrowth stimulated by L1, N-CAM, and N-cadherin. *Neuron.* 13: 583-594.
- Williams, E. J., Walsh, F. S., and Doherty, P. (1994b). The production of arachidonic acid can account for calcium channel activation in the second messenger pathway underlying neurite outgrowth stimulated by NCAM, N-cadherin, and L1. *J. Neurochem.* 62: 1231-1234.
- Williams, E. J., Mittal, B., Walsh, F. S., and Doherty, P. (1995). FGF inhibits neurite outgrowth over monolayers of astrocytes and fibroblasts expressing transfected cell adhesion molecules. *J. Cell Sci.* 108(Pt 11): 3523-3530.
- Williams, G., Williams, E. J., Maison, P., Pangalos, M. N., Walsh, F. S., and Doherty, P. (2005). Overcoming the inhibitors of myelin with a novel neurotrophin strategy. *J. Biol. Chem.* 280(7): 5862-9.

- Williams, R.W., and Herrup, K. (1988). The control of neuron number. *Annu. Rev. Neurosci.* 11: 423-53.
- Windisch, J. M., Auer, B., Marksteiner, R., Lang, M. E., and Schneider, R. (1995). Specific neurotrophin binding to leucine-rich motif peptides of TrkA and TrkB. *FEBS Lett.* 374(1): 125-9.
- Wischmeyer, E., Doring, F., and Karschin, A. (1998). Acute suppression of inwardly rectifying Kir2.1 channels by direct tyrosine kinase phosphorylation. *J. Biol. Chem.* 273: 34063-34068.
- Xiao, Z. C., Taylor, J., Montag, D., Rougon, C., and Schachner, M. (1996). Distinct effects of recombinant tenascin-R domains in neuronal cell functions and identification of the domain interacting with the neuronal recognition molecule F3/11. *Eur. J. Neurosci.* 8(4): 766-82.
- Xu, B., Gottschalk, W., Chow, A., Wilson, R., Schnell, E., Zang, K., Wang, D., Nicoll, R., Lu, B., and Reichardt, L. (2000). The role of brain-derived neurotrophic factor receptors in the mature hippocampus: Modulation of long-term potentiation through a presynaptic mechanism involving TrkB. *J. Neurosci.* 20: 6888-6897.
- Yan, Q., Radeke, M. J., Matheson, C. R., Talvenheimo, J., Welcher, A. A., and Feinstein, S. C. (1997). Immunocytochemical localization of TrkB in the central nervous system of the adult rat. *J. Comp. Neurol.* 382(4): 546-7.
- Yong, V. W., Power, C., Forsyth, P., and Edwards, D. R. (2001). Metalloproteinases in biology and pathology of the nervous system. *Nat. Rev. Neurosci.* 2: 502-511.
- Zampieri, N., Xu, C. F., Chao, M. V. (2005). Cleavage of p75 neurotrophin receptor by alpha-secretase and gamma-secretase requires specific receptor domains. *J. Biol. Chem.* 280(15): 14563-71.

## 9 Appendix

### 9.1 Abbreviations

g g-force (9.81 m/s<sup>2</sup>)  
°C degree Celsius  
aa amino acid  
A adenine  
AA arachidonic acid  
Acc. accession number  
ADAM a disintegrin and a metalloprotease  
Amp ampicillin  
APP amyloid precursor protein  
APS ammonium peroxydisulfate  
ATCC American Type Culture Collection  
ATP adenosine triphosphate  
bp base pair  
BCA bicinchoninic acid disodium salt  
BDNF brain-derived neurotrophic factor  
BME basal medium Eagle's  
BSA bovine serum albumin  
C cytosine  
CaM calmodulin  
CAM cell adhesion molecule  
cDNA complementary deoxyribonucleic acid  
CHL1 close homologue of L1  
CHO Chinese hamster ovary  
CREB cAMP response element-binding  
Da dalton  
DAG diacylglycerol  
DIC differential interference image  
DMEM Dulbecco's modified Eagle medium  
DMSO dimethylsulfoxide  
DNA deoxyribonucleic acid  
DNase deoxyribonuclease  
ECL enhanced chemiluminescence  
*E. coli* *Escherichia coli*  
ED extracellular domain  
EDTA ethylene diamine tetraacetic acid  
ELISA enzyme-linked immunosorbent assay  
ERK extracellular signal-regulated kinase  
FAK focal adhesion kinase  
f. c. final concentration  
FCS fetal calf serum  
FGF fibroblast growth factor  
Fig. figure  
FNIII fibronectin subtype III repeat  
FRS-2 FGF receptor substrate 2  
g gram

G guanosine  
GABA gamma-aminobutyric acid  
GMEM Glasgow-modified Eagle medium  
GPI glycosylphosphatidylinositol  
h human, hour  
HEPES 2-(4-(2-hydroxyethyl)-piperazine)-ethane sulfonic acid  
HBSS Hank's buffered sodium chloride solution  
His6 hexahistidine tag  
HRP horseradish peroxidase  
IB immunoblotting  
ID intracellular domain  
IgG immunoglobulin subclass G  
IP<sub>3</sub> inositol trisphosphate  
IH immunohistochemistry  
IP immunoprecipitation  
IPTG isopropyl-D-thiogalactopyranoside  
JNK Jun N-terminal kinase  
Kana kanamycin  
kb kilo base pair  
Kir K<sup>+</sup> inwardly rectifying channel  
l liter  
LB Luria Bertani  
LTP long-term potentiation  
MAPK mitogen-activated protein kinase  
MEM minimal essential medium  
μ micro (10<sup>-6</sup>)  
m milli (10<sup>-3</sup>)  
MMP matrix metalloprotease  
min minute  
mRNA messenger ribonucleic acid  
n nano (10<sup>-9</sup>)  
NCAM neural cell adhesion molecule  
NGF nerve growth factor  
NT-3 neurotrophin-3  
NT-4 neurotrophin-4  
OD optical density  
p pico (10<sup>-12</sup>)  
p75<sup>NTR</sup> 75 kDa neurotrophin receptor  
PAGE polyacrylamide gel electrophoresis  
PBS phosphate-buffered saline  
PCR polymerase chain reaction  
pfu plaque-forming unit  
PI3K phosphatidylinositol 3-kinase  
PKC protein kinase C  
PLCγ phospholipase Cγ  
PLL poly-L-lysine  
PSA polysialic acid  
psi pounds per square inch  
PST polysialyltransferase  
RIP regulated intramembrane proteolysis  
RUP regulated ubiquitin/proteasome-dependent processing

RNA ribonucleic acid  
 rpm rounds per minute  
 RT room temperature  
 s second  
 SDS sodium dodecyl sulfate  
 SUMO small ubiquitin-related modifier  
 sulfo-SBED sulfosuccinimidyl-2-[6-(biotinamido)-2-(p-azidobenzamido)-hexanoamido]ethyl-  
 1,3-di-thiopropionate  
 T thymine  
 TBS Tris-buffered saline  
 TBST Tween-20 in Tris-buffered saline  
 TE Tris-EDTA  
 TEMED N,N,N',N'-tetraethylene amine  
 TK+ TrkB full-length TrkB  
 TK- TrkB truncated receptors, T1TrkB and T2TrkB  
 TMD transmembrane domain  
 Tris tris-hydroxymethyl aminomethane  
 Trk tropomyosin-related kinase  
 pTrkB phosphorylated TrkB  
 Ub ubiquitin  
 UPS ubiquitin-proteasome system  
 U unit (enzymatic)  
 V volt  
 v/v volume per volume  
 Vol. volume  
 w/v weight per volume  
 X-GAL 5-bromo-4-chloro-3-indolyl- $\beta$ -D-galactopyranoside  
 ZMNH Zentrum für Molekulare Neurobiologie Hamburg

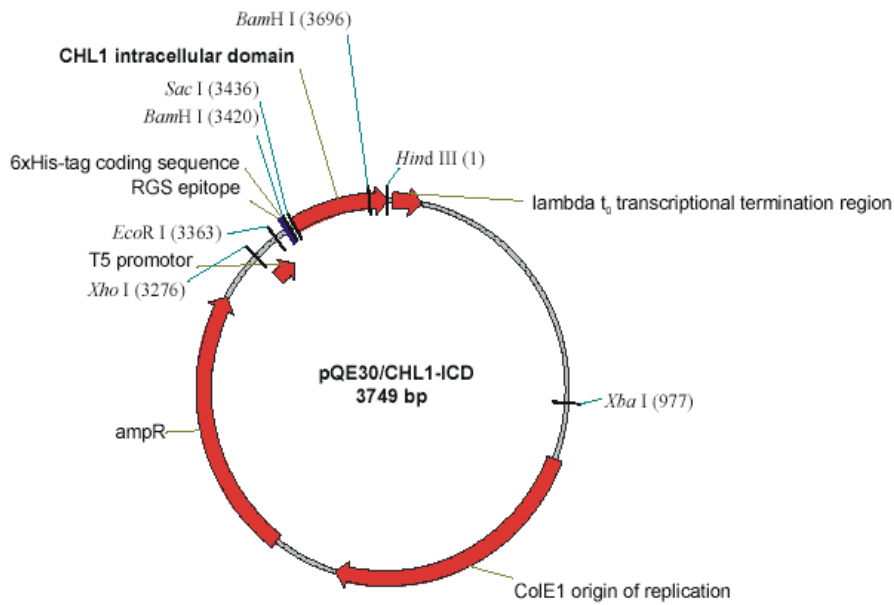
Amino acids were abbreviated using the one-letter code.

## 9.2 Accession numbers

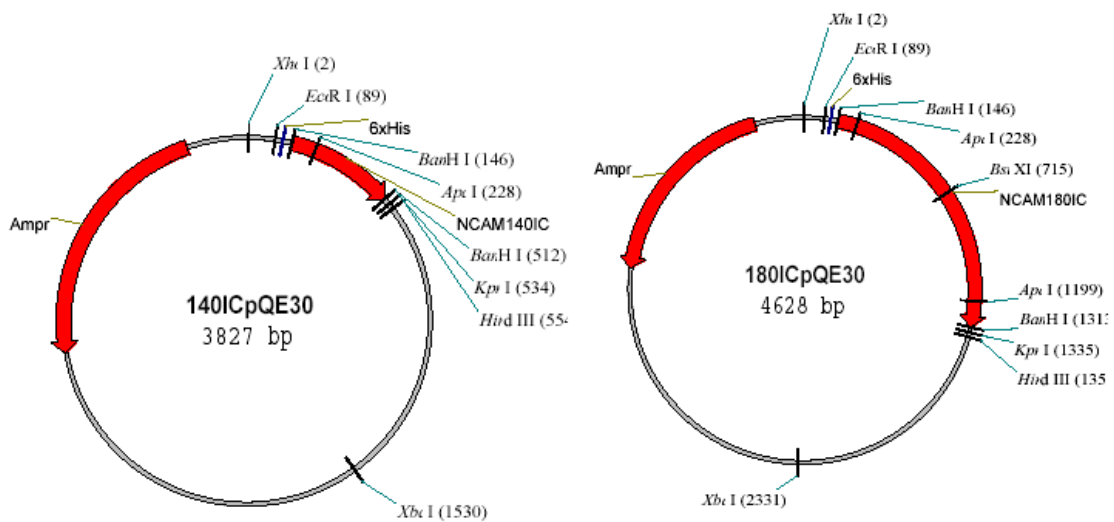
Protein	Organism	Accession No.
NCAM180	rat	not available
NCAM140	rat	X06564
CHL1	mouse	X94310
TrkB	rat	Q63604
NCAM120	mouse	Y00051
Kir3.3	rat	C77929

## 9.3 Plasmids

### 9.3.1 CHL1CpQE30 construct



### 9.3.2 NCAM140IC and NCAM180ICpQE30 constructs



## Curriculum vitae

### Akademischer Werdegang

1977–1981	Grundschule Haiterbach
1981–1990	Otto-Hahn-Gymnasium Nagold
Okt. 1990 bis Sept. 1992	Ausbildung an der Medizinisch Technischen Akademie Esslingen e.V. zur medizinisch-technischen Laboratoriumsassistentin (Note 2,0)
Okt. 1992 bis März 1999	Studium der Ernährungswissenschaften an der Rheinschen Friedrich-Wilhelms-Universität Bonn (Note 1,9)
Jan. 1999	Abgabe der Diplomarbeit Thema: „The effects of choline availability on cell proliferation, cell migration, and apoptosis in fetal rat brain“ (Diplomarbeitenote 1,0)
seit Sept. 2000	Promotion an der Universität Hamburg, Zentrum für Molekulare Neurobiologie, bei Prof. Dr. Melitta Schachner
Okt. 2001 bis Okt. 2003	Aufbaustudium ‚Molekularbiologie‘ an der Universität Hamburg

### Beruflicher Werdegang

März 1994 bis Juli 1995	Teilzeittätigkeit als medizinisch-technische Laboratoriumsassistentin in der Laborgemeinschaft ‚Bonner Ärzte 2‘, Abteilung Serologie
Aug. 1995 bis Okt. 1995	Praktikum bei F. Hoffmann-La Roche AG, Basel, Forschungsabteilung Exploratory Research Analytics, Gruppe Feed/Food-Analytics
Mai 1996 bis Dez. 1996	Studentische Teilzeitkraft am Institut für Ernährungswissenschaft Universität Bonn, Abteilung Pathophysiologie der Ernährung des Menschen, bei Prof. Dr. Klaus Pietrzik
Jan. 1998 bis Sept. 1998	Stipendiatin der Richard-Winter-Stiftung (Stuttgart) für Forschungsaufenthalt in den USA, für Diplomarbeit an der University of North Carolina, Chapel Hill, School of Public Health, Department of Nutrition, bei Prof. Dr. Steven Zeisel

Feb. 1999 bis Juli 2000

Wissenschaftliche Mitarbeiterin an der University of North Carolina, Chapel Hill, School of Public Health, Department of Nutrition, bei Prof. Dr. Steven Zeisel

### **Auszeichnung**

Stipendium für Forschungsaufenthalt in den USA von der Richard-Winter-Stiftung, Stuttgart (1998)

### **Publikationen**

Friedrich, C., Hofmann, P. (1996)

Determination of vitamin D<sub>3</sub> in premixes.

*Interne Publikation bei F. Hoffmann-La Roche AG, Basel, Schweiz*

Albright, C. D., Tsai, A. Y., Friedrich, C. B., Mar, M.-H., Zeisel, S. H. (1999a)

Choline availability alters embryonic development of the hippocampus and septum in the rat.

*Dev. Brain Res.* 113: 13–20

Albright, C. D., Friedrich, C. B., Brown, E. C., Mar, M.-H., Zeisel, S. H. (1999b)

Maternal dietary choline availability alters mitosis, apoptosis and the localization of TOAD-64 protein in the developing hippocampus and septum.

*Dev. Brain Res.* 115: 123–129

Albright, C. D., Mar, M.-H., Friedrich, C. B., Brown, E. C., Zeisel, S. H. (2001)

Maternal dietary choline availability alters the localization of p15<sup>Ink4B</sup> and p27<sup>Kip1</sup> cyclin-dependent kinase inhibitor in the developing fetal rat brain hippocampus.

*Dev. Neurosci.* 23: 100–106

Friedrich, C. B., Kleene, R., Wischmeyer, E., Cassens, C., Schachner, M. (2005)

Functional trimeric complex between the neural cell adhesion molecule NCAM, the neurotrophin receptor TrkB and the neuronal K<sup>+</sup>-channel Kir3.3.

(in preparation)

## **Danksagung**

Frau Professor Melitta Schachner gilt mein herzlicher Dank für die Übertragung des interessanten Doktorarbeitsthemas, die großzügige Unterstützung während der gesamten Doktorarbeitszeit sowie für das begeisterungsvolle Engagement für die Neurobiologische Wissenschaft.

Bei Herrn Professor Konrad Wiese bedanke ich mich für die unbürokratische und überaus nette Bereitschaft zur Betreuung dieser externen Promotion.

Dr. Ralf Kleene danke ich natürlich auch für sein Engagement und seine Unterstützung als Betreuer.

Dank gebührt vor allem auch PD Dr. Erhard Wischmeyer für seine elektrophysiologischen Experimente, die zum besseren Verständnis der TrkB-NCAM Interaktion wesentlich beitragen.

Mein Dank gilt Dr. Michaela Schweitzer für ihre Unterstützung am konfokalen Laserscanning-Mikroskop, Galina Dityatev für die Präparation der hippocampalen Primärneuronen, Peggy Putthoff für die Genotypisierungen, Dr. Markus Delling, Dr. Ingolf Bach, Dr. Alexander Dityatev, Dr. Thomas Tilling, Dr. Carsten Schmid, Dr. Gaby Loers, Dr. Kai-Oliver Wesche und Dr. Andrey Irintchev für ihre Diskussionsbereitschaft, Dr. Ina Kalus für die Einweisung in die Kleinhirnmikroexplantkultur, Frau Dr. Gaby Loers und Frau Dr. Frauke Brendel für die Unterstützung bei der Kleinhirneinzellkultur, Dr. Andrey Irintchev für die Hilfe mit der statistischen Auswertung. Auch den Kollegen der AG Schachner und des ZMNH, die ich nicht namentlich erwähnt habe, danke ich für das ausgesprochen freundliche und inspirierende wissenschaftliche Arbeitsklima.

Vor allem danke ich Dr. Heather P. Ostendorff für die Überprüfung der sprachlichen Korrektheit. Ebenso war das Korrekturlesen von Anja Schrewe, Rhonda Kruithof, Hayes G. Dabney, Thomas Hoffstadt und Marco Fava sehr wertvoll.

Joschka Reuß danke ich für seine exzellente und unschätzbare Unterstützung insbesondere bei der Formatierung.

Meiner ‚Essensgruppe‘ danke ich für die erholsamen schöpferischen Pausen und ganz besonders der E.32-Laborcrew für die lustigen Momente, an die ich mich immer gerne erinnern werde. Weiter danke ich all meinen Freunden, Kletterkollegen und vor allem Ingo für motivierende und heitere Stunden, die mir unvergessen bleiben werden.

Mein tiefster Dank gilt meinen Eltern, Ursula und Nikolaus Friedrich sowie meinem Bruder Christian für ihren festen Glauben an mich und für ihre unschätzbare Förderung meines wissenschaftlichen Bestrebens.